

UNCLASSIFIED

AD NUMBER

AD914362

LIMITATION CHANGES

TO:

Approved for public release; distribution is unlimited.

FROM:

Distribution authorized to U.S. Gov't. agencies only; Test and Evaluation; OCT 1973. Other requests shall be referred to Air Force Weapons Laboratory, Kirtland AFB, NM 87117.

AUTHORITY

AFWL ltr, 30 Apr 1986

THIS PAGE IS UNCLASSIFIED

AD 914 362

AUTHORITY:

AEWL etc.,

30 APR 86



✓
AD 91 436
AFWL-TR-73-111

AFWL-TR-
73-111

**CALCULATION OF VERTICAL
AIRBLAST-INDUCED GROUND MOTIONS
FROM NUCLEAR EXPLOSIONS IN
FRENCHMAN FLAT**

Henry F. Cooper, Jr.

**R&D Associates
Santa Monica, California**

Jimmie L. Bratton

TECHNICAL REPORT NO. AFWL-TR-73-111

October 1973

AIR FORCE WEAPONS LABORATORY

**Air Force Systems Command
Kirtland Air Force Base
New Mexico**

This research was sponsored by the Defense Nuclear Agency under Subtask Y99QAXSB144, Work Unit 03, Work Unit Title, "Phenomenological Study of Ground Motion."

Distribution limited to US Government agencies only because of test and evaluation (Oct 73). Other requests for this document must be referred to AFWL (DEV), Kirtland Air Force Base, NM.

AFWL-TR-73-111

AIR FORCE WEAPONS LABORATORY
Air Force Systems Command
Kirtland Air Force Base
New Mexico 87117

When US Government drawings, specifications, or other data are used for any purpose other than a definitely related Government procurement operation, the Government thereby incurs no responsibility nor any obligation whatsoever, and the fact that the Government may have formulated, furnished, or in any way supplied the said drawings, specifications, or other data, is not to be regarded by implication or otherwise, as in any manner licensing the holder or any other person or corporation, or conveying any rights or permission to manufacture, use, or sell any patented invention that may in any way be related thereto.

DO NOT RETURN THIS COPY. RETAIN OR DESTROY.

AFWL-TR-73-111

CALCULATION OF VERTICAL
AIRBLAST-INDUCED GROUND MOTIONS
FROM NUCLEAR EXPLOSIONS IN
FRENCHMAN FLAT

Henry F. Cooper, Jr.

R&D Associates

Santa Monica, California

Jimmie L. Bratton

TECHNICAL REPORT NO. AFWL-TR-73-111

This research was sponsored by the Defense Nuclear Agency under Subtask Y99QAXSB144, Work Unit 03, Work Unit Title, "Phenomenological Study of Ground Motion.

Distribution limited to US Government agencies only because of test and evaluation (Oct 73). Other requests for this document must be referred to AFWL (DEV), Kirtland Air Force Base, NM.

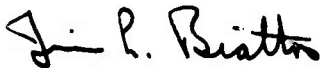
FOREWORD

This report was prepared by the R&D Associates, Santa Monica, California, and by the Air Force Weapons Laboratory. The research was jointly funded by the U.S. Air Force under Contract F29601-72-C-0048 and by the Defense Nuclear Agency under Contract DNA001-72-C-0197. The research was performed under Program Element 11213F, Project 133B1302, Task 13.

Inclusive dates of research were January 1972 through April 1973. The report was submitted 17 August 1973 by the Air Force Weapons Laboratory Project Officer, Mr. Jimmie L. Bratton (DEV).

The authors wish to acknowledge the support of messrs. Robert Thompson and John Levesque of R&D Associates who performed the calculations that were the basis of the analysis reported here.

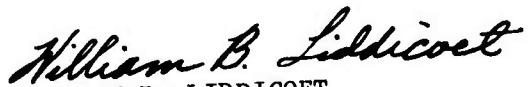
This technical report has been reviewed and is approved.



JIMMIE L. BRATTON
Project Officer



ROY M. GOODWIN
Lt Colonel, USAF
Chief, Facility Survivability
Branch



WILLIAM B. LIDDICOET
Colonel, USAF
Chief, Civil Engineering Research
Division

ABSTRACT

(Distribution Limitation Statement B)

This report discusses vertical airblast-induced ground motions produced by nuclear explosions over a dry soil medium taken to model Frenchman Flat of the Nevada Test Site (NTS). Material properties for use in first principle calculations were synthesized from very limited dynamic laboratory stress-strain data, various soil index characteristics, and seismic data. Parametric calculations with a one-dimensional, plane-strain finite difference code were used to define a "theoretical" simplified model that expresses peak vertical particle velocities and displacements as a function of yield, peak overpressure and depth. Ground motions predicted by this model were then compared to ground motion data from nuclear explosions in Frenchman Flat. In particular, predictions of the simplified model were reasonably consistent with PRISCILLA data which were a primary basis of empirical prediction procedures widely used in the design and analysis of strategic structures during the past ten years. The theoretical model could be altered (where little or no dynamic soil property data exist) to provide even better agreement between calculated and measured ground motions. Conversely, study of qualitative features of the theoretical results provide insight into the basic wave propagation phenomena in Frenchman Flat that could improve the interpretation of the experimental data such that a more consistent comparison between theory and experiment may result.

CONTENTS

<u>Section</u>		<u>Page</u>
I	INTRODUCTION	1
	Key Uncertainties	2
	One-Dimensional Model Uncertainties	2
	Material Properties Uncertainties	4
	Airblast Boundary Condition Uncertainties	5
	Report Outline	5
II	MATERIAL PROPERTIES	7
III	THEORETICAL MODEL FOR VERTICAL GROUND MOTIONS IN FRENCHMAN FLAT	12
	Vertical Ground Motions at the 100 psi Overpressure Range	14
	Model Development for Surface Motions	19
	Attenuation Characteristics	27
	Summary	37
IV	COMPARISONS OF CALCULATION WITH TEST DATA FROM FRENCHMAN FLAT	40
	In-Situ Impedance	40
	Comparison of Simplified Model with PRISCILLA Data	42
	Calculations Using Measured Overpressure Boundary Condition	49
	Peak Overpressure Uncertainties	56
	Summary	62
V	SUGGESTED MODIFICATIONS TO THE MATERIAL PROPERTIES MODEL	67
VI	DISCUSSION AND CONCLUSIONS	71
VII	RECOMMENDATIONS	74
	Appendix Geology and Material Properties for Frenchman Flat	75 95
	References	

ILLUSTRATIONS

<u>Figure</u>		<u>Page</u>
1	Estimated First Arrival Contours from a 37 KT, 700 ft HOB Explosion over Frenchman Flat	3
2	Comparison of Calculated and Measured Overpressure from PRISCILLA (37 KT at 700 ft HOB)	6
3	Theoretical Model for Frenchman Flat	9
4	Stress Strain Curves for Theoretical Model	10
5	Typical Overpressure Waveforms	13
6	Vertical Surface Motion at the 100 psi Overpressure Range	15
7	Comparison of Surface Particle Velocity and Over- pressure Waveforms at the 100 psi Peak Overpressure Range	17
8	Attenuation of Peak Stress, Particle Velocity, and Displacement at 100 psi Range from Near-Surface Airbursts (Calculations for Frenchman Flat)	18
9	Peak Particle Velocity and Displacement at 100 psi Range from Near-Surface Bursts	20
10	Vertical Surface Motion Associated with the Air-Slap at the 10 psi Overpressure Range from Near-Surface Bursts	21
11	Vertical Surface Motions at the 1000 psi Overpressure Range from Near-Surface Bursts	22
12	Peak Surface Particle Velocity and Displacement as a Function of Peak Overpressure	24
13	Peak Surface Particle Displacements as a Function of Yield	25
14	Normalized Surface Displacement as a Function of Yield (d_{1KT} = Surface Displacement from 1 KT)	26
15	Attenuation of Peak Stress, Particle Velocity, and Displacement at 10 psi Range from Near-Surface Airburst (Calculations for Frenchman Flat)	28

ILLUSTRATIONS

<u>Figure</u>		<u>Page</u>
16	Attenuation of Peak Stress, Particle Velocity, and Displacement at 30 psi Range from Near-Surface Airbursts (Calculations for Frenchman Flat)	29
17	Attenuation of Peak Stress, Particle Velocity, and Displacement at 300 psi Range from Near-Surface Airbursts in Frenchman Flat	30
18	Attenuation of Peak Stress, Particle Velocity, and Displacement at 1000 psi Range from Near-Surface Airbursts (Calculations for Frenchman Flat)	31
19	Normalized Peak Particle Velocity and Displacement Attenuation with Depth	33
20	Ratio of Peak Particle Velocity to Peak Overpressure	34
21	Peak Particle Velocity at 30 ft Depth in Frenchman Flat as a Function of Yield	35
22	Normalized Peak Particle Velocity at 30 ft Depth as a Function of Yield (v_{1KT} = Peak Particle Velocity at 30 ft Depth and 1 KT)	36
23	Comparison of Calculated and Measured $\Delta P/v$	41
24	Peak Particle Velocity and Displacement Attenuation for a 37 KT Near-Surface Airburst over Frenchman Flat	43
25	Comparison of Theoretical Model and Near-Surface Ground Motion Data from PRISCILLA	44
26	Comparison of Simplified Model with PRISCILLA Peak Particle Velocity Data	45
27	Comparison of Simplified Model with PRISCILLA Peak Particle Velocity Data	46
28	Comparison of Simplified Model with PRISCILLA Peak Displacement Data	47
29	Comparison of Simplified Model with PRISCILLA Peak Displacement Data	

ILLUSTRATIONS

<u>Figure</u>		<u>Page</u>
30	Best Estimate of Very Near-Surface Vertical Motion Data from PRISCILLA	50
31	Comparison of Calculated Attenuation Rates with Normalized Peak Vertical Motion Data from PRISCILLA	51
32	Vertical Motion Time-of-Arrival Data	52
33	Peak Vertical Particle Velocity Time-of-Arrival	53
34	Comparison of Calculated and Measured Arrival Times for the PRISCILLA Event	54
35	Comparison of Calculated and Measured Arrival Times for the SMALL BOY Event	55
36	Comparison of Overpressure Boundary Condition with PRISCILLA Data	57
37	Comparison of Calculated and Measured Waveforms at 650 ft Range on PRISCILLA	58
38	Comparison of Calculated and Measured Waveforms at 1050 ft Range on PRISCILLA	59
39	Comparison of Peak Vertical Displacements from PRISCILLA with Calculations Using Measured Airblast Overpressure as a Boundary Condition	60
40	Comparison of Relative Displacement Data with Calculated Results Using Measured Overpressure as a Boundary Condition	61
41	Comparison of Theoretical Airblast Results for $W = 37$ KT and PRISCILLA Data	63
42	Comparison of PRISCILLA Data with Ground Motions Predicted Using Brode's Height-of-Burst Overpressure Model	64
43	Suggested Improved Model for Frenchman Flat	68
44	Suggested Alterations to the Low Stress Portion of the Laboratory Uniaxial Stress-Strain Curves	69

ILLUSTRATIONS

<u>Figure</u>		<u>Page</u>
45	Geologic Cross Section	76
46	Aerial Geology	78
47	Seismic Profile	79
48	Soil Composition Data from the Vicinity of FLAT TOP II and III	82
49	Frenchman Flat Soil Composition Data	83
50	Uniaxial Stress-Strain Curves ($z = 0$)	86
51	Uniaxial Stress-Strain Curves ($z = 20$ ft)	87
52	Uniaxial Stress-Strain Curves ($z = 40$ ft)	88
53	Uniaxial Stress-Strain Curves ($z = 70$ ft)	89
54	Static, Uniaxial Strain, Test Results that Suggest Possible Anisotropy in Frenchman Flat	90
55	Normalized Unloading Curves	92
56	Comparison of Loading Curves from the Dynamic Uniaxial Strain Tests	93

TABLES

<u>Table</u>		<u>Page</u>
I	Calculational Matrix for Modeling Vertical Airblast-Induced Ground Motions from Near-Surface Nuclear Explosions at Frenchman Flat	12
II	Prediction Formulae for Near-Surface Vertical Airblast-Induced Ground Motions from Near-Surface Airbursts in Frenchman Flat	38
III	U. S. Geological Survey Seismic Data	80
IV	Best Estimate Seismic Profile	80

SECTION I

INTRODUCTION

In recent years, great emphasis has been placed on the development of first-principle theoretical methods to calculate the ground motions from nuclear explosions. Impressive computing capabilities now exist to perform detailed calculations, but an inadequate understanding of in-situ material properties limit the credibility of quantitative predictions of two-dimensional near-surface ground motions. In fact, major discrepancies between calculated and measured cratering and ground motion phenomena on recent high-explosive experiments are leading to a serious re-examination of all previous assumptions basic to the state-of-the-art theoretical predictive capability (Refs 1, 2). These questions are sufficiently serious that even the most primitive assumptions regarding the calculation of early time vertical airblast-induced ground motions under strongly super-seismic airblast loading conditions must be re-examined and validated.

Our main purpose in this report is to re-examine this issue by considering the vertical ground motions produced by nuclear explosions in Frenchman Flat. Our approach is to:

- Formulate a theoretical model for the mechanical response of the Frenchman Flat soils from the available geologic and material property information;
- Using this model, perform sufficient first principle calculations to estimate the vertical airblast-induced ground motions as a function of yield and peak overpressure;
- Compare the results of these calculations with experimental data to evaluate the validity of the theoretical model;
- Based on any discrepancies between calculations and experiments, suggest improvements to the material property model that may better represent the observed in-situ vertical response of Frenchman Flat.

We note that the first two of the above steps are standard procedure in state-of-the-art attempts to calculate the ground motions at any given site. As is discussed Section II and Appendix A, our knowledge of the soil properties in Frenchman Flat is considerably more limited than at many sites of strategic interest. Nevertheless, sufficient data are available to formulate a reasonable model for the shallow soils and, to the extent that the material property model and calculational procedures applied in this study are representative of the current state-of-the-art. Our third step is an evaluation of the state-of-the-art. As indicated by the fourth step, improvements to the theoretical model will be suggested following our examination of discrepancies between the calculated results and the nuclear test data.

1. Key Uncertainties

A one-dimensional, plane-strain Lagrangian finite-difference code (ref 3) was used to calculate the airblast-induced vertical ground motions, assuming super-seismic airblast loading conditions. The numerical error in peak stresses, particle velocities and displacements from these calculations is estimated to be less than $\pm 10\%$.¹ Thus, any gross failure to accurately predict airblast-induced vertical ground motions from nuclear explosions in Frenchman Flat cannot be attributed to numerical error, but is a failure of the theoretical model, i.e., an incorrect assumption that vertical motions are represented by a one-dimensional model; an inaccurate material property model; and/or an inappropriate assumed airblast overpressure boundary condition. We shall briefly comment on each of these key uncertainties.

a. One-dimensional Model Uncertainties - Figure 1 shows idealized airblast-induced ground shock wave fronts produced by the decelerating blast over-

¹The calculations used 1.5 and 6 inch zones to define the early time near surface particle velocity, and two foot zones were adequate to obtain accurate lower frequency displacements.

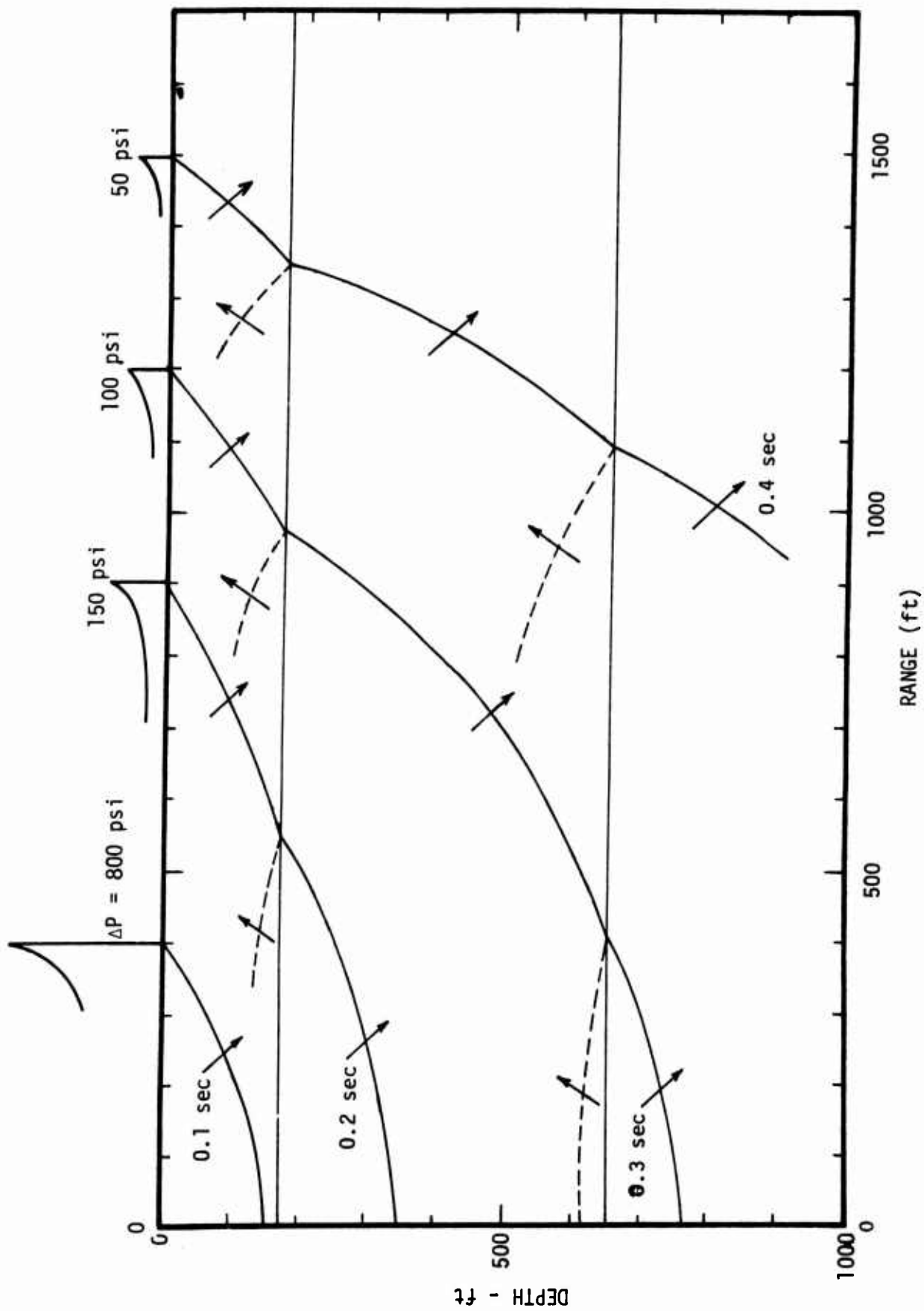


Figure 1. Estimated First Arrival Contours from a 37 KT, 700 ft HOB Explosion over Frenchman Flat

pressure predicted for PRISCILLA, a 37 KT 700 ft height-of-burst detonation in Frenchman Flat (as defined by seismic velocity profiles discussed in Appendix A). Only the effects of major interfaces at 170 and 650 ft depth are included in this schematic. The initial wave-fronts in this strongly super-seismic case are inclined less than about 30 degrees from the earth's surface for ranges less than about 1000 ft (or overpressures greater than about 100 psi). A one-dimensional, plane-strain theoretical model should accurately predict the vertical component of such strongly super-seismic ground motions at shallow depths and early times following passage of the air shock. The one-dimensional model for Frenchman Flat is believed to be valid, at least for times less than a few hundred milliseconds following the airblast arrival at overpressures greater than 50 or 100 psi. (Some comparisons between one- and two-dimensional calculations would suggest that the one-dimensional calculations are valid for predicting vertical motions under even less restrictive conditions.) As indicated in Figure 1, the front of the ground shock wave will have propagated to depths of several hundred feet in such a period of time. Two-dimensional (and even three-dimensional) effects that perturb the motions at large depths and late time will not be considered in the current study. If serious questions persist after attempting to resolve discrepancies between the one-dimensional calculational results and the vertical ground motion test data, then two-dimensional calculations might be performed to better quantify the accuracy of the one-dimensional predictions.

b. Material Properties Uncertainties - The soil properties used in the calculations presented here were derived from inadequate data in the sense that insufficient tests were conducted to define statistically meaningful estimates for the dynamic stress-strain curves of the shallow soils. No dynamic stress-strain data exist for soils deeper than 70 ft in Frenchman Flat. Studies of similar soils suggest that the effective modulus at pressure levels of interest can easily vary by factors of two as a function of local variations within a given general area. The importance of such uncertainties, that can be better assessed via calculations, will be discussed later

in the context of discrepancies between the calculated and measured vertical motions.

c. Airblast Boundary Condition Uncertainties - As has been the case with most calculations of airblast-induced ground motions, we assumed pressure time-histories derived from Brode's idealization for surface or very near surface burst configurations (Ref. 4). The airblast observed on nuclear tests in Frenchman Flat often differed from this idealized boundary condition in qualitative as well as quantitative features. Brode's more recent height-of-burst model (Ref. 5) may be more appropriate for estimating the over-pressure time-histories from many of the nuclear tests in Frenchman Flat, but predictions from even that more correct model sometimes differ from the observed data. For example, Figure 2 shows significant discrepancies between PRISCILLA data and the theoretical prediction for a 37 KT explosions at 700 ft height-of-burst. The effects of these discrepancies, which will be discussed further in later sections, are sometimes more important than soil property uncertainties.

2. Report Outline

Section II describes the soil properties assumed in the calculations to model the vertical ground motions in Frenchman Flat. Section III then discusses the parametric study conducted to develop a simplified theoretical model to predict the vertical ground motions as a function of peak over-pressure and yield. In Section IV, predictions from this simplified model are compared to ground motion data from nuclear tests in Frenchman Flat. Section V discusses possible modifications to the material property model that would improve the consistency between the theoretical calculations and the nuclear test data. Section VI then summarizes the key lessons learned in our study, and Section VII provides recommendations for future work that could clarify certain of the discrepancies and reduce the uncertainties highlighted by our study.

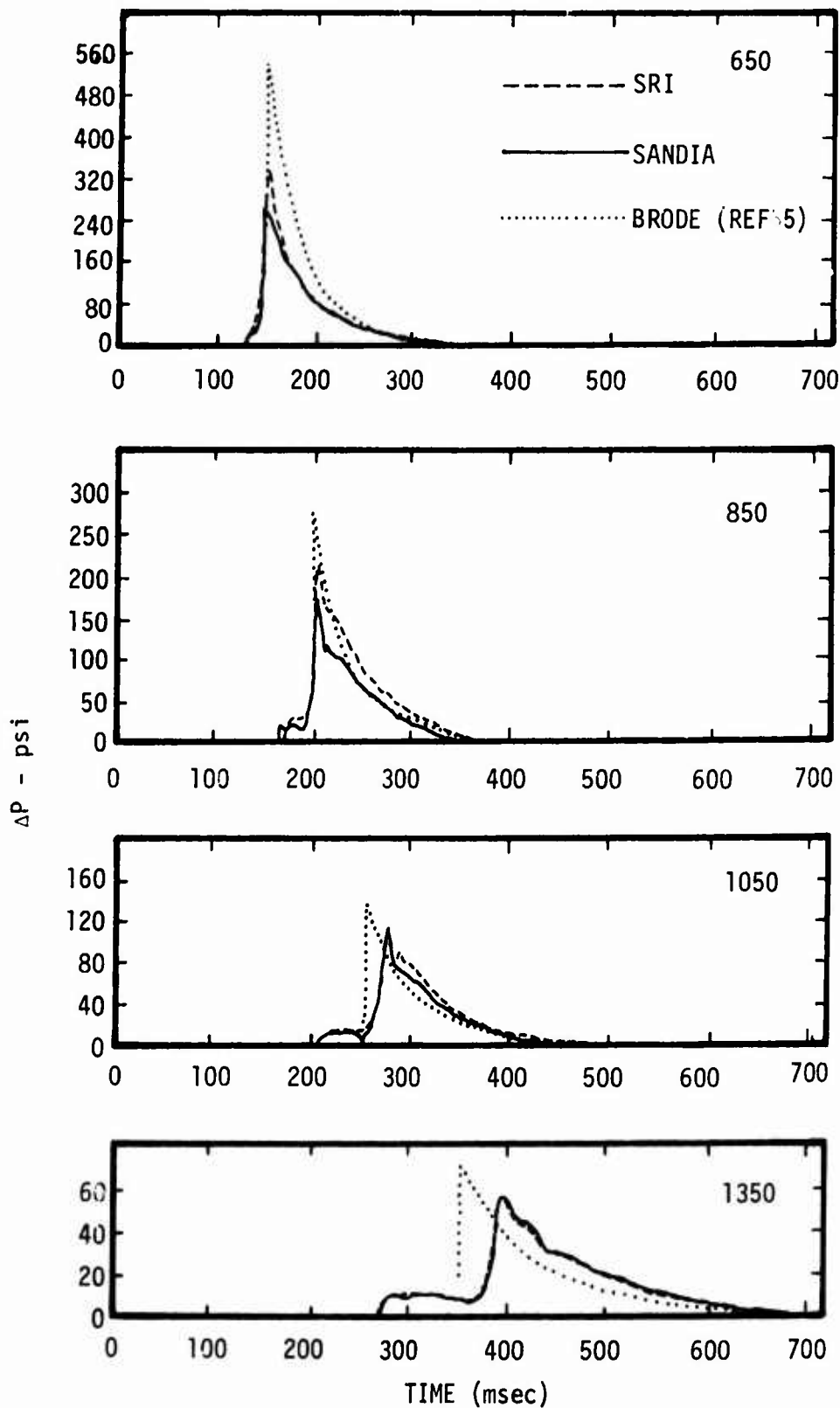


Figure 2. Comparison of Calculated and Measured Overpressure from PRISCILLA (37 KT at 700 ft Height of Burst)

SECTION II

MATERIAL PROPERTIES

This section describes the theoretical model of Frenchman Flat geology and soil response characteristics used in the calculations reported in Section III. This first-cut theoretical model was synthesized from incomplete data from the variety of investigations summarized in Appendix A. Subsequent to Section IV's comparison of calculated ground motion with test data from nuclear explosions in Frenchman Flat, we shall suggest modifications to this theoretical model that might lead to a better representation of the in-situ dynamic soil properties.

Frenchman Flat is at an elevation of about 3080 feet and is surrounded by mountains that rise from 4500 to 6000 feet above sea level. Materials eroded from high areas have been deposited in the low regions forming a large alluvial valley. At the lowest point in this valley, a small shallow lake exists for short periods after unusually large rains. Fine particles deposited by this stagnant water comprise the major constituents of the near surface playa soil.

The soil in the upper 200 feet may be described as being uniform in appearance and composition; and is a hard, friable, tan silt or clayey silt with varying amounts of cementation. Although no sharp interbedding or layers were visually detected during the drilling and sampling at the site, the playa has a stratified nature with thin zones of well-cemented material (caliche beds) in some areas. Such conditions can cause anisotropic stress-strain characteristics because different moduli and strengths exist normal and parallel to the natural bedding planes. As discussed in Appendix A, limited static compression tests in the vertical and horizontal directions on companion samples from the same boring and depth showed a significantly larger (by a factor of 2 or 3) modulus parallel to the bedding planes (in the horizontal direction). Such orthotropic properties are

properties are probably unimportant to the theoretical model for one-dimensional calculations of early-time, vertical motions when the state-of-stress is closely approximated by that associated with uniaxial strain. However, if two-dimensional ground motions are of interest, the effects of such anisotropy must be more seriously considered.

A primary purpose of this study is to compare results from theoretical calculations with vertical ground motions measured on nuclear tests to obtain some measure of the confidence one can place in state-of-the-art calculations of super-seismic airblast-induced ground motions. We eliminated any subjectivity in defining the loading stress-strain curves for the near surface soils in Frenchman Flat by using Davisson's dynamic uniaxial strain test data (ref 6) without alterations; although some adjustment might have been justified on the basis of discussions in Appendix A. The test device used in conducting the dynamic tests could not be unloaded immediately upon reaching peak stress so that in several instances significant creep and reloading took place. In order to synthesize unloading stress-strain curves, the unloading portion of all the tests (ignoring the creep and reloading) were normalized to the peak stress and strain reached on loading. Because the normalized unloading curves for all the available tests were similar, the same normalized unloading curve was assumed to model all layers.

To be reasonably consistent with the seismic data discussed in Appendix A and Davisson's dynamic soil property data available only at 0, 20, 40 and 70 ft depths, we did apply some subjective judgment in defining the five layers shown in Figure 3, with stress-strain characteristics as shown in Figure 4. No stress-strain data are available for the bottom layer. Thus, properties were assumed for a homogeneous layer between 170 and 650 ft such that the loading modulus was consistent with the seismic velocity and the unloading modulus was consistent with the unloading modulus of the shallower soils. A rigid boundary was introduced at 650 ft to represent the interface and provide a reflected compressional wave, consistent with the appropriate physical effects.

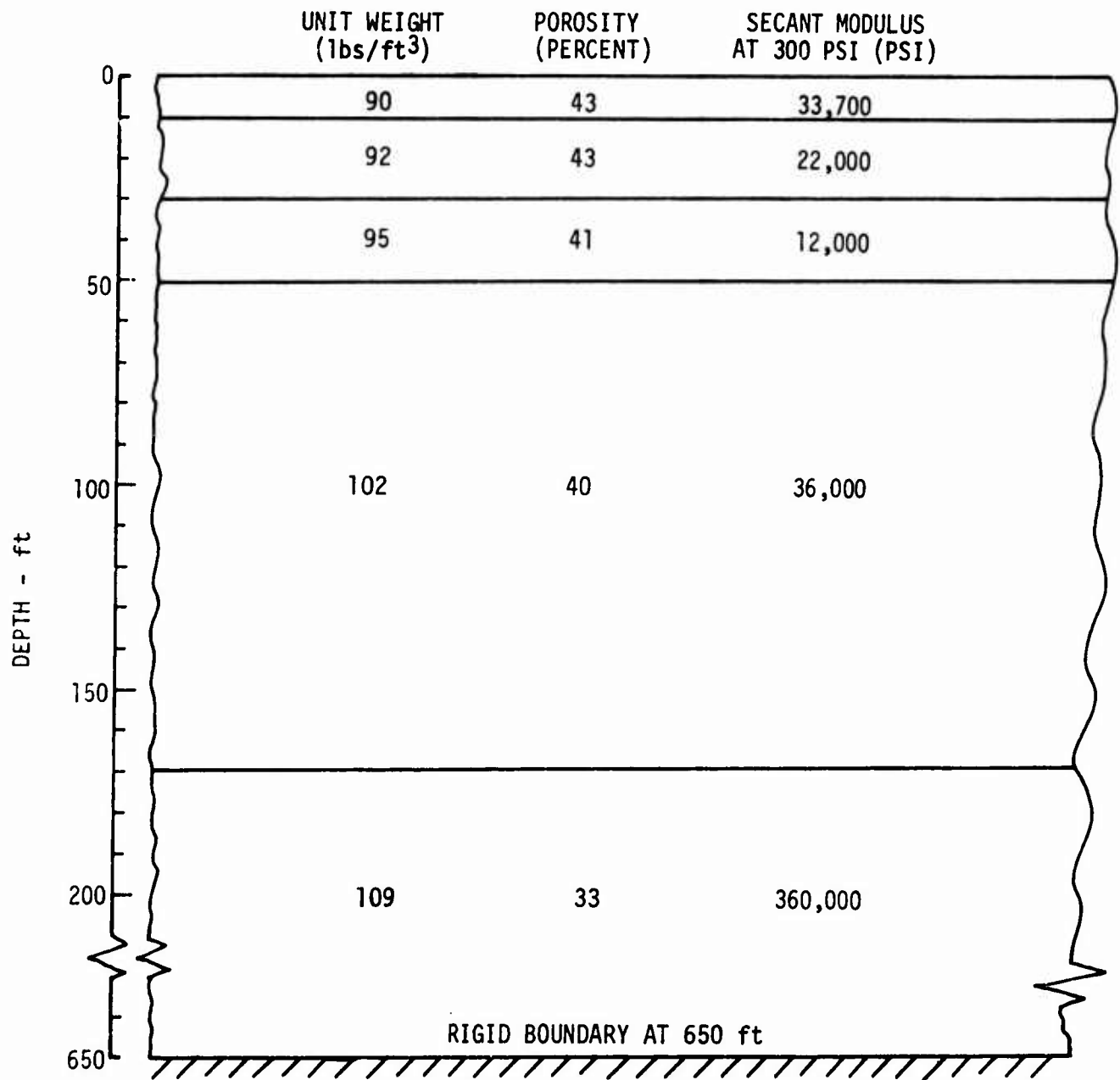


Figure 3. Theoretical Model for Frenchman Flat

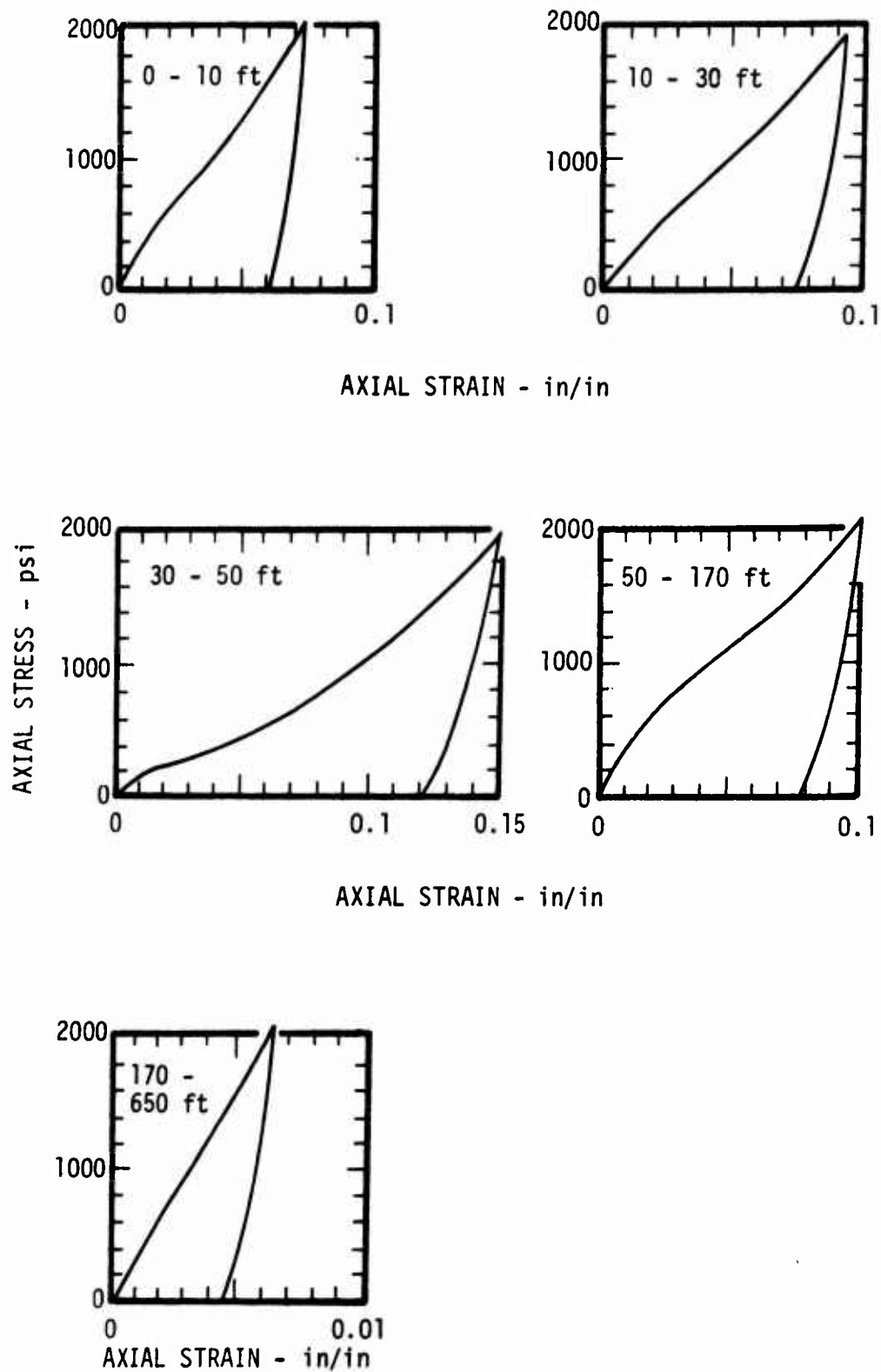


Figure 4. Stress Strain Curves
for Theoretical Model

As will be discussed in the following section, compressional waves reflected from the 170 ft interface cause displacements to peak for yields less than about 100 kt and overpressures greater than about 100 psi. For higher yields and lower overpressures, reflections from the 650 ft interface may be required to reverse the downward motions (see figure 1). For the one-dimensional calculations to be studied here, the detailed properties of these deeper layers may not be important because their primary function is to reflect compressional waves that in turn limit the vertical motions. However, knowledge of the location of the interfaces, and a reasonable representation of the wavespeeds for the intervening media are important in determining the correct arrival time for the reflected waves. In efforts to predict near-surface peak vertical displacements, uncertainties in these key parameters can be important.

In this regard, we emphasize that no dynamic material property data exist for the soils deeper than 70 ft depth, an observation that will be important in our interpretation of discrepancies between calculated and measured peak displacements near the earth's surface. It turns out that the theoretical model defined here underpredicts the initial arrivals of the compressional wave in the soils below about 50-75 ft. Hence, calculated pulse widths are slightly too long. The resolution of such discrepancies will be discussed in more detail in Section V, where we propose modifications to the theoretical model presented here that will provide a more consistent representation of the in-situ response of the deeper soils in Frenchman Flat.

SECTION III

THEORETICAL MODEL FOR VERTICAL GROUND MOTIONS IN FRENCHMAN FLAT

This section interpolates between the results of the 25 one-dimensional calculations indicated in Table I to develop formulae that purport to predict the vertical ground motions caused by near-surface nuclear explosions in Frenchman Flat, as modeled in Section II. As shown in Figure 5, the range of yields and peak overpressures considered in Table I are associated with a significant variation in overpressure waveforms during the first several tenths of a second following the airblast arrival. Increases in explosive yield and decreases in peak overpressure both tend to broaden the overpressure waveform, i.e., to decrease the rate of decay behind the shock front. Perhaps of greater importance, the positive phase at the lower yields is shorter than the time required for the reflection from high impedance layers (Figure 1) that play a role in reversing the downward motion at large yields. Thus, a possible mechanism for free-surface spall exists for low yield explosions when these waves reflected from the 170 ft interface return to the earth's free surface. Such phenomena may be suppressed by the overpressure at high yields. However,

TABLE I

CALCULATIONS MATRIX FOR MODELING VERTICAL
AIRBLAST-INDUCED GROUND MOTIONS FROM NEAR-SURFACE
NUCLEAR EXPLOSIONS AT FRENCHMAN FLAT

Yield (KT)	Peak Overpressure (psi)				
	10	30	100	300	1000
1	x	x	x	x	x
10	x	x	x	x	x
100	x	x	x	x	x
1000	x	x	x	x	x
10000	x	x	x	x	x

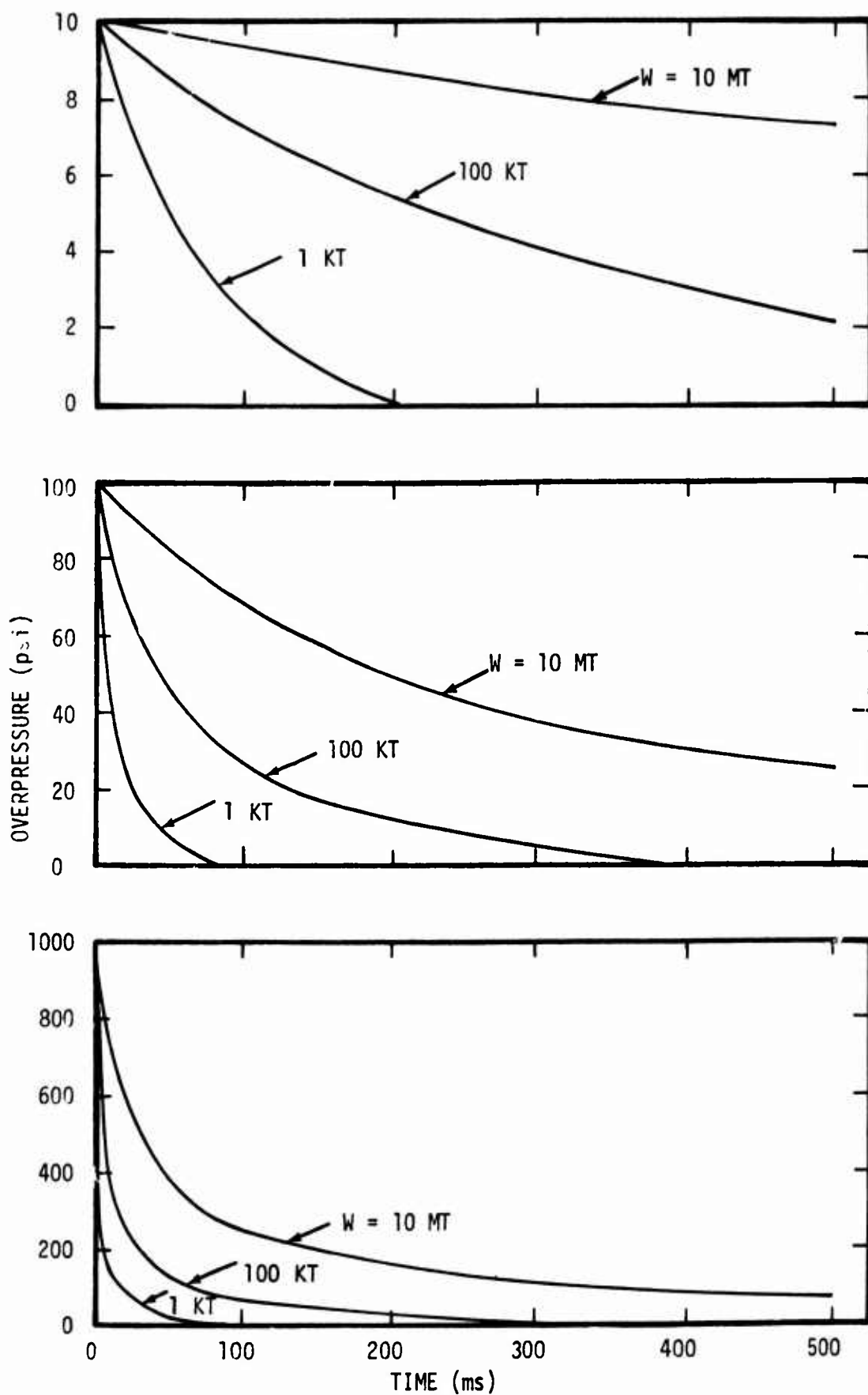


Figure 5. Typical Overpressure Waveforms

reflection from deeper layers, such as the 650 ft interface, might produce similar spalling phenomena at the higher yields.

We shall first discuss the basic phenomena by considering the vertical ground motions calculated for the 100 psi peak overpressure boundary condition and the full range of yields. After identifying the key wave propagation characteristics, we then construct formulae that interpolate between the results of calculations in Table I.

1. Vertical Ground Motions at the 100 psi Overpressure Range

This section discusses the effect of varying the yield on the ground motion amplitudes and waveforms calculated for the 100 psi peak overpressure boundary condition. These results demonstrate most of the key wave propagation features associated with the specific site model. Subsequently, we shall generalize this discussion of the basic phenomenology to also account for variations in overpressure.

Figure 6 shows the effect of varying the explosive yield between 1 kiloton and 10 megatons on the vertical particle velocity and displacement of the earth's surface at the 100 psi overpressure range. Reflections from the more compressible soils between 10 and 50 feet produce a downward acceleration beginning at about 0.01 seconds, and cause the maximum particle velocity for the larger yields. Subsequently, major perturbations in the waveform result from the arrival of the compressional waves reflected from successively stiffer layers at 50, 170 and 650 ft depth. At the lower yields, the reflection from 170 ft is sufficient to reverse the downward particle velocity at about 0.2 seconds. In calculations for these low yield cases, a free surface spall occurs because the positive phase duration of the overpressure is shorter than 0.2 second and consequently only gravity would resist the upward earth motion. Because these calculations did not include the effect of gravity, the upward motion of the free surface is unimpeded; and the calculated spall may be exaggerated.

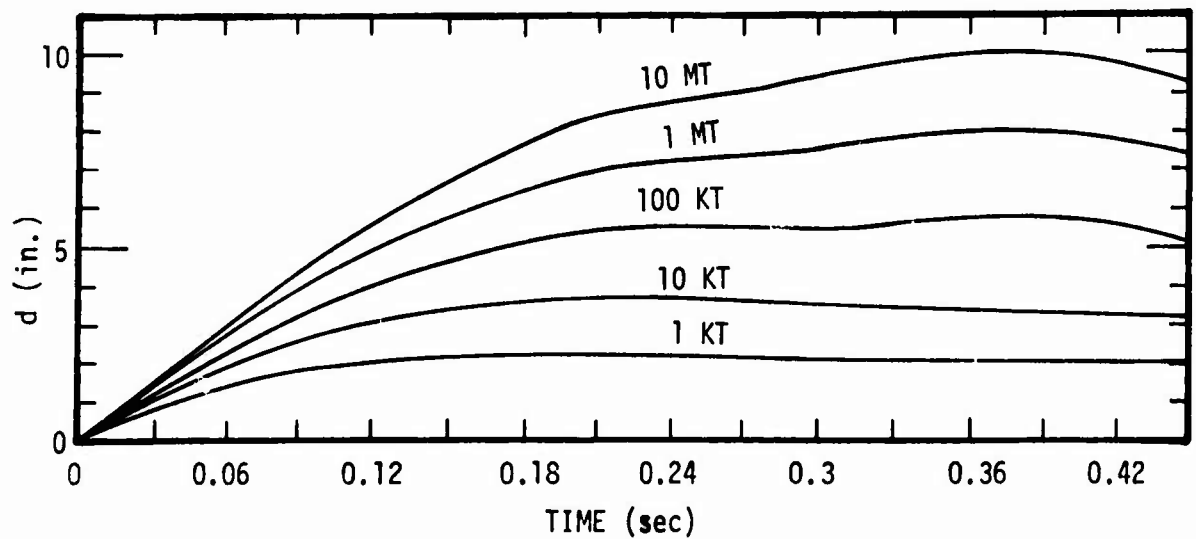
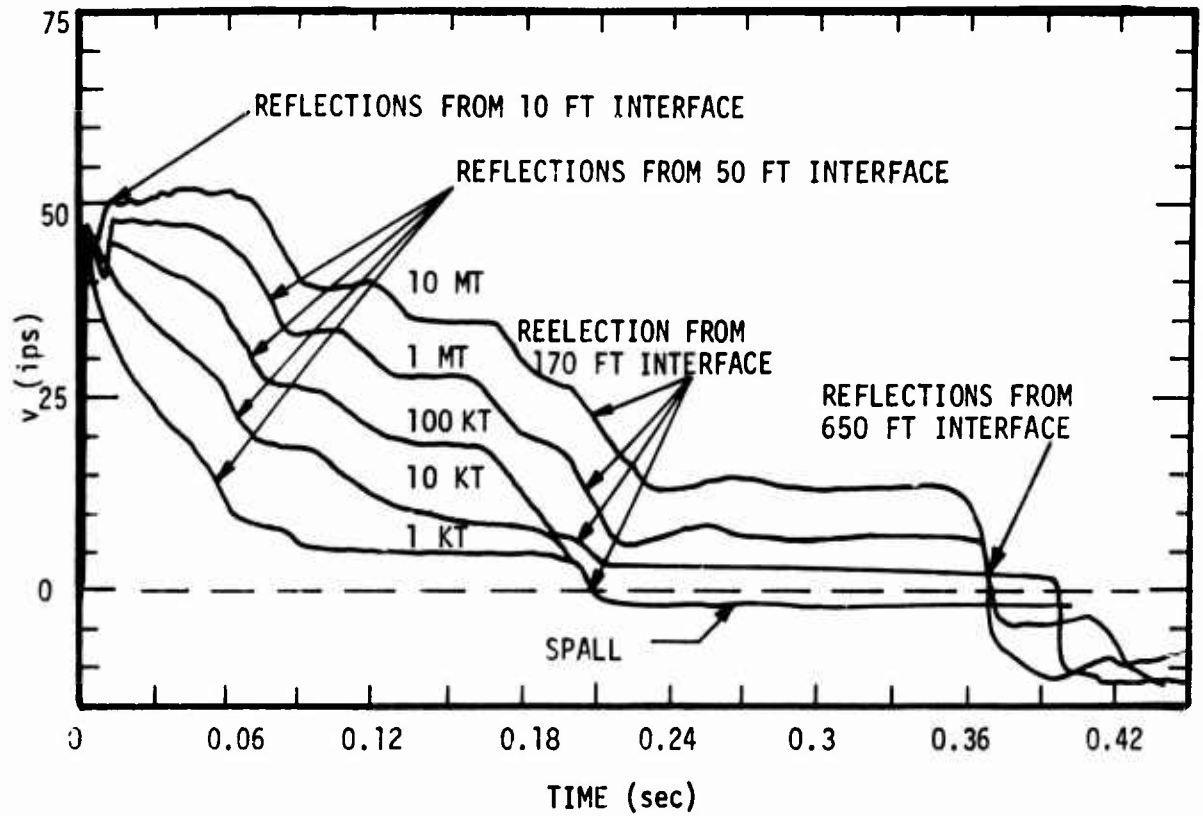


Figure 6. Vertical Surface Motion at the 100 PSI Overpressure Range

Although reflections from the compressible layers between 10 and 50 ft are more apparent for the larger yields, they have a qualitative effect on the particle velocity waveforms for all yields. For example, Figure 7 compares the surface particle velocity waveforms with the overpressure pulse for the 1 kiloton, 100 kiloton, 10 megaton yield cases to emphasize this point. If the impedance and compressibility of the soil were constant or monotonically increasing with depth, then the particle velocity waveforms would be qualitatively similar to the overpressure pulse shape. Because some of the underlying soils are softer than the surface soils in the theoretical model, the particle velocity waveforms fall above (at early times) those that might be expected on the basis of exponentially decaying overpressure waveform.

Following the airblast arrival, the surface particle velocity jump is given by $v = \Delta P / \rho c$ where ΔP is the peak overpressure and ρc is the characteristic impedance of the surface layer (computed from the density (ρ) and effective modulus (ρc^2) at the peak overpressure of interest). In some cases, such as considered here, where a layer of compressible soil underlies a relatively stiff surface layer, the peak particle velocity may not be associated with the initial jump; rather it may occur later. As shown in Figure 6, the effects of such reflections become more pronounced with increasing yield; causing the peak particle velocity at the surface for yields greater than about 100 KT.

Figure 8 shows the calculated near-surface attenuation of peak stress, particle velocity and displacement with depth as a function of the explosive yield. Straight line (exponential decay) fits to the calculated peak displacements are quite good, but peak stress and particle velocity attenuate more rapidly near the surface than at depths greater than about 30 ft.¹

¹Because the purpose of these calculations was to develop a simplified model, the smooth line fits to the data do not necessarily pass through all of the calculated data points. Rather the fits are taken to represent simple functions that are consistent with the calculated data points (usually to within ± 10 percent).

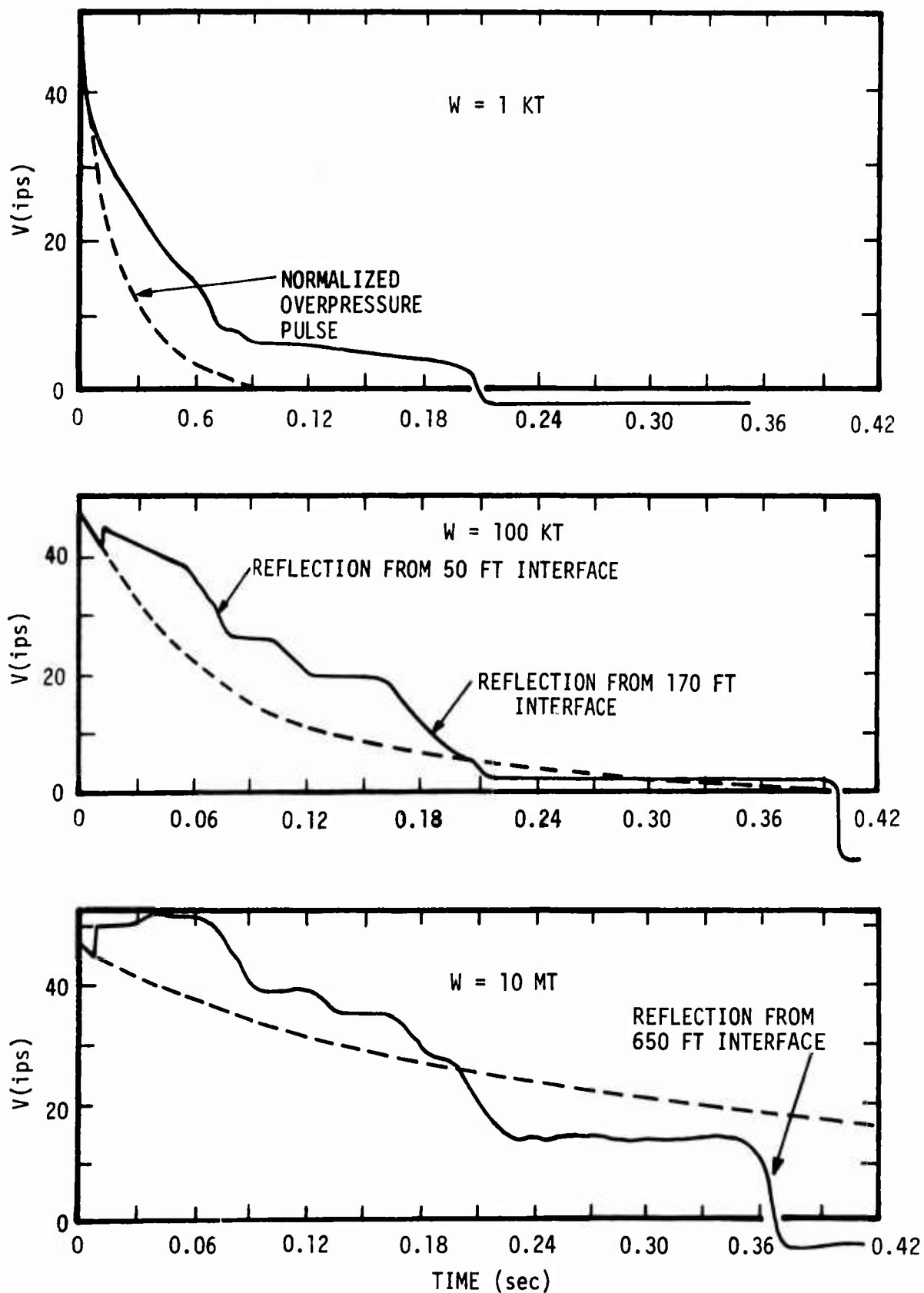


Figure 7. Comparison of Surface Particle Velocity and Overpressure Waveforms at the 100 psi Peak Overpressure Range

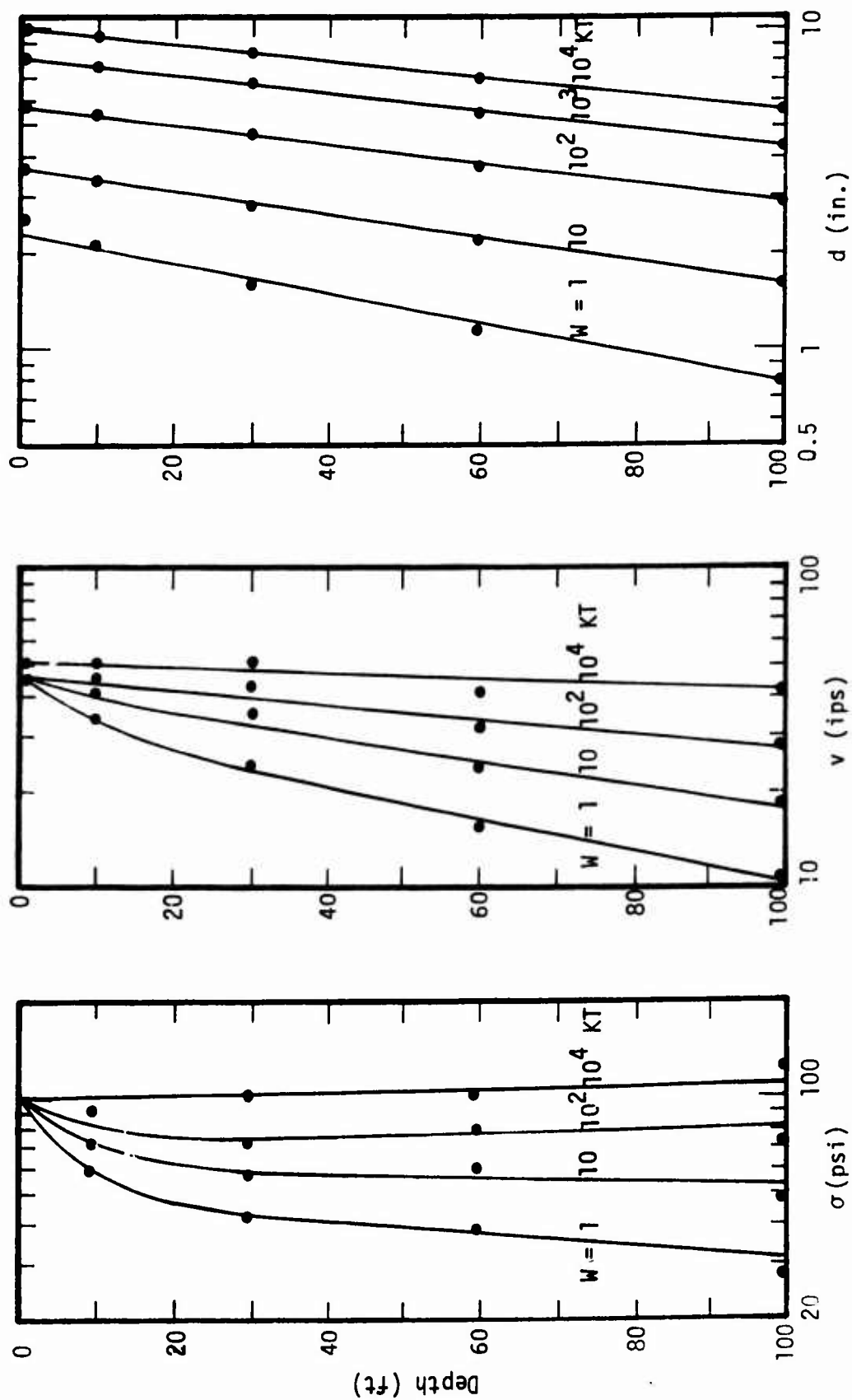


Figure 8. Attenuation of Peak Stress, Particle Velocity, and Displacement at 100 psi Range from Near-Surface Airbursts (Calculations for Frenchman Flat)

Thus, a single straight line fit is an inadequate fit to the peak stress and particle velocity attenuation with depth, except for the larger yields where very little attenuation occurs in the top 30 ft.

Although the rate of attenuation of peak displacement appears to be relatively independent of yield, peak stresses and particle velocities attenuate significantly less rapidly with increasing yield. Figure 9 shows that this effect causes peak particle velocities at a given depth to increase with increasing yield; and the rate of increase with yield increases with increasing depth. The second peak in Figure 6 produces an increase in peak surface velocity with increasing yield for yields greater than about 100 kt. For the higher yields, the surface soils move downward with a maximum velocity equal to the peak velocity of the top of the 30-50 ft layer, i.e., there is little attenuation of the peak particle velocity above 30 ft. The most rapid attenuation occurs in the very compressible soils between 30 and 50 ft.

If there were no geologic layering, then peak vertical displacements would be approximately proportional to the overpressure specific impulse, which in turn scales as $W^{1/3}$ (W is the explosive yield). However, geologic layering perturbs such scaling because stress waves reflected from high impedance (as compared to that of the surface media) deep layers cause the downward displacements to peak at times earlier than predicted on the basis of $W^{1/3}$ scaling. In fact, from Figure 9, peak vertical displacements from the 100 psi peak overpressure at the surface of our model for Frenchman Flat are approximately proportional to $W^{1/6}$ for yields less than about 500 KT. At higher yields, peak displacements from these calculations are even less sensitive to yield, tending toward a $W^{1/12}$ dependence.

2. Model Development for Surface Motions

Much of the previous discussion of basic phenomena in the 100 psi overpressure case can be generalized with slight modifications for other overpressures. For example, Figures 10 and 11 show that qualitative features of the surface motions of the 10 psi and 1000 psi overpressure

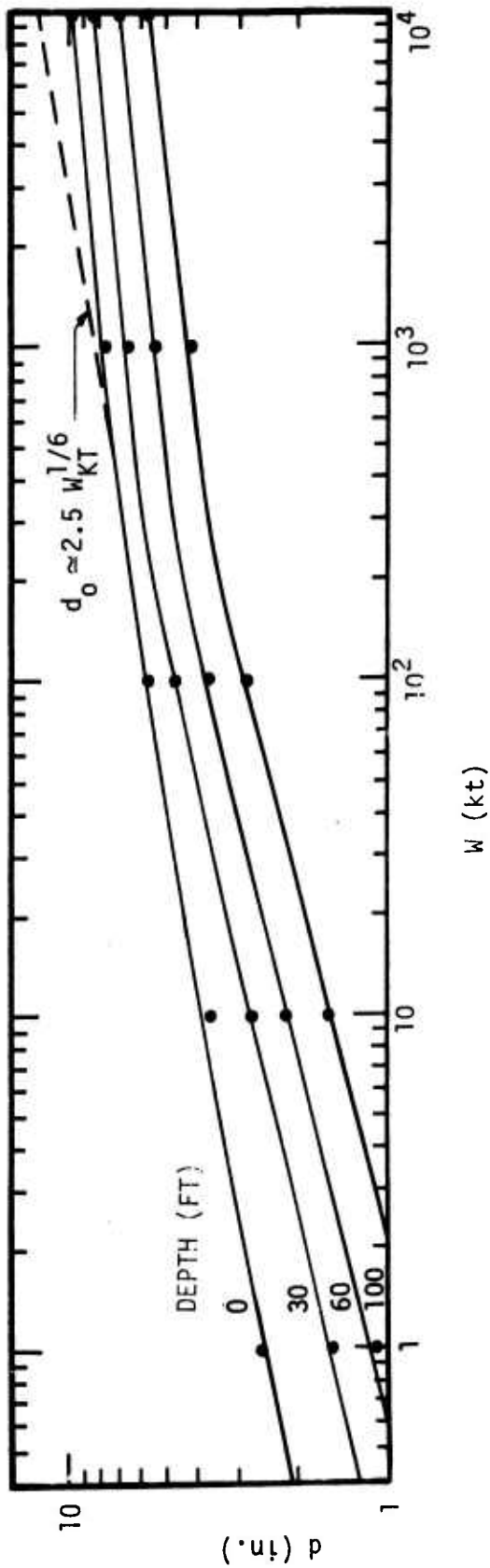
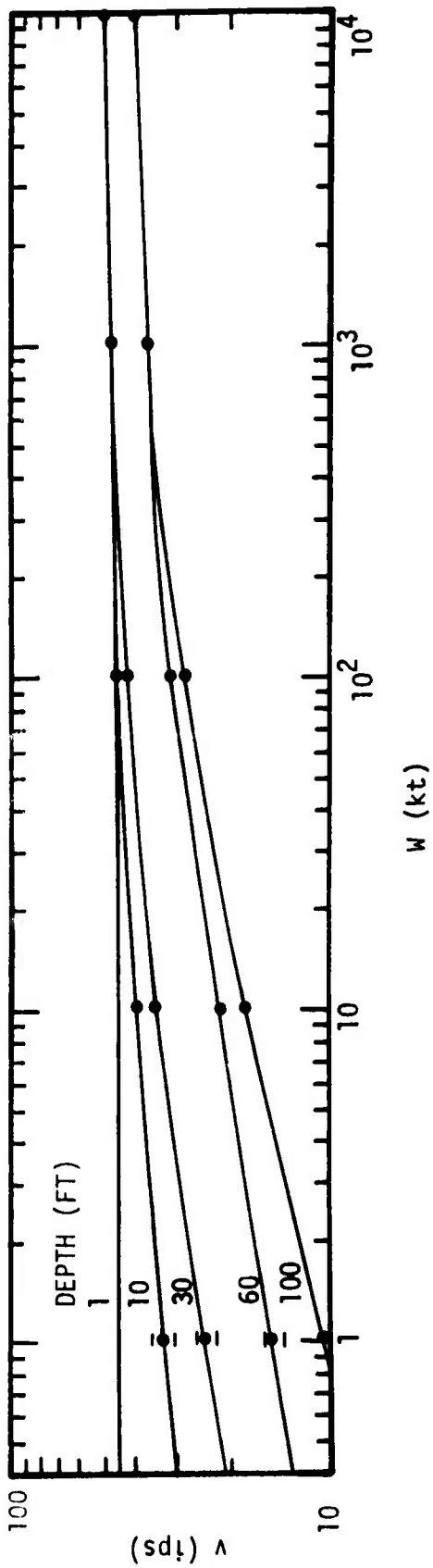


Figure 9. Peak Particle Velocity and Displacement at 100 psi Range from Near Surface Bursts

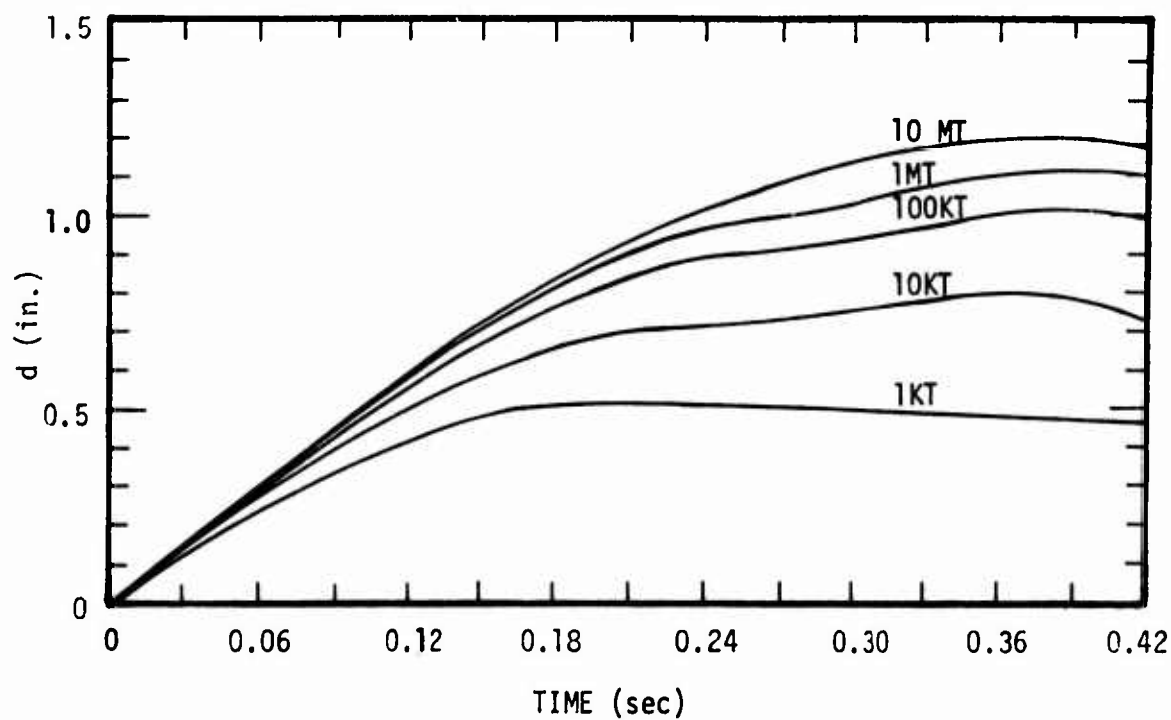
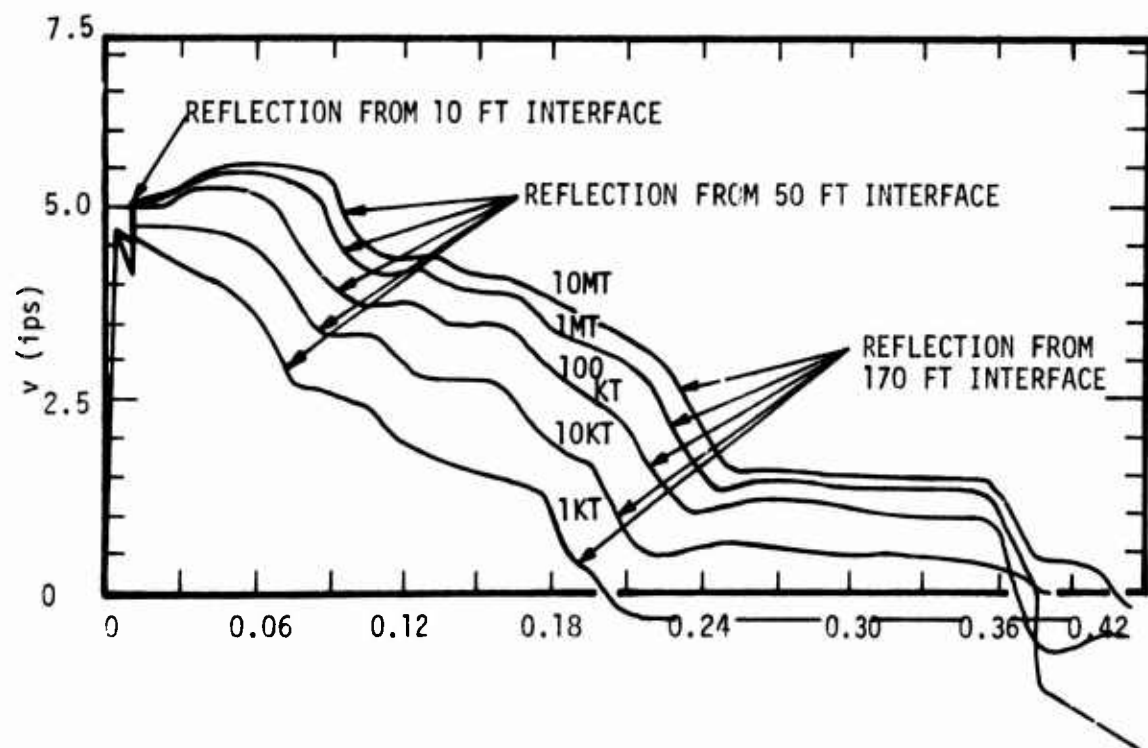


Figure 10. Verticle Surface Motion Associated with the Air-Slap at the 10 psi Overpressure Range from Near-Surface Bursts

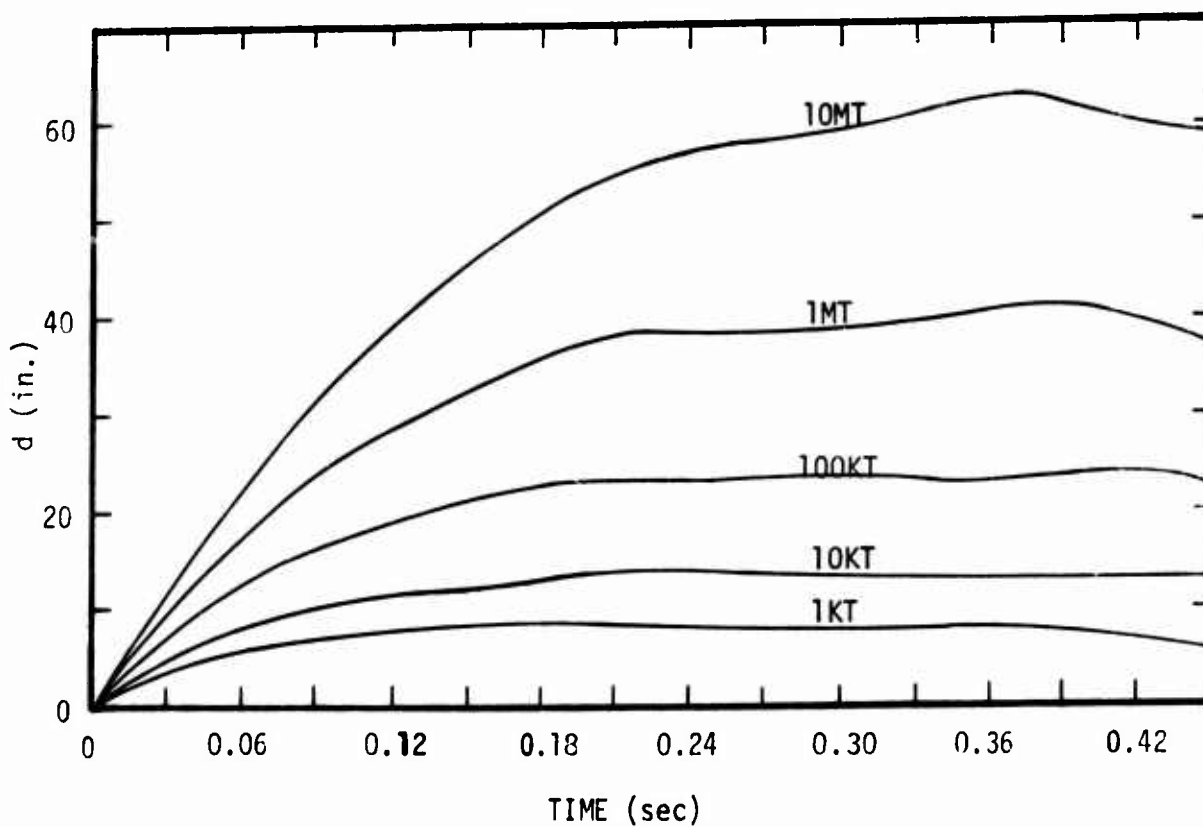
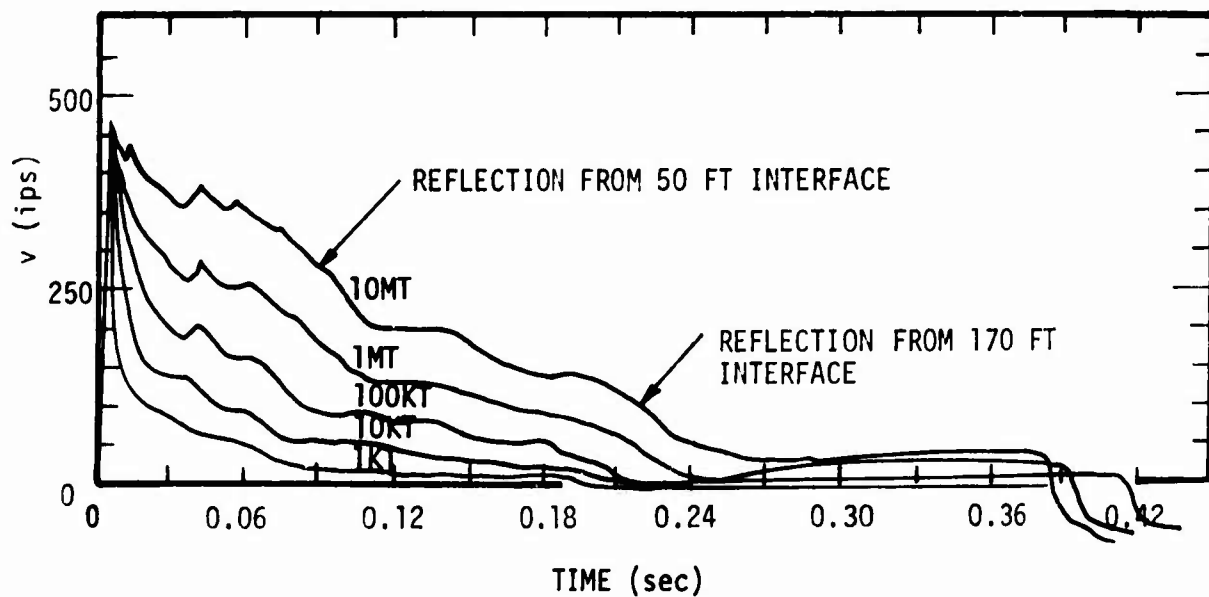


Figure 11. Vertical Surface Motions at the 1000 psi Overpressure Range from Near-Surface Bursts

ranges, are similar to those indicated for 100 psi in Figure 6. At 10 psi, the peak surface particle velocity is caused by reflections from the soil layers between 10 and 50 ft for yields greater than about 1 KT. On the other hand, the initial velocity jump constitutes the peak surface particle velocity for 1000 psi and all yields considered. Between these two overpressure ranges, the peak surface particle velocity is sometimes caused by the initial jump, and sometimes by later reflections depending on the yield. At 100 psi, for example, the initial jump constitutes the peak surface particle velocity for yields less than about 100 KT, but later reflections cause the peak velocity for larger yields. Although different physical phenomena can lead to the peak surface velocity at a given overpressure for different yields, this study suggests a maximum variation of about 20 percent for yields between 1 KT and 10 MT. Figure 12 shows that the calculated peak surface particle velocities are given very closely by

$$v_o \approx 50 \left(\frac{\Delta P}{100 \text{ psi}} \right) \quad \text{IPS.} \quad (1)$$

On the other hand, there is a substantial variation in peak surface displacements at a given overpressure, depending on the yield. These calculations suggest an overpressure dependence for $\Delta P \leq 100$ psi that differs from the overpressure dependence for higher peak pressures. This variation is caused by differences in late time reflection phenomena. For high overpressures (and yields less than about 100 KT), the peak displacements occur when the compressional wave reflected from the 170 ft interface arrives at the earth's surface. (See Figures 6, 10 and 11.) For peak overpressures less than about 100 psi (and yields greater than about 100 KT), the strength of this reflected wave is not sufficient to reverse the motion; and the displacements peak with the arrival of a later compressional wave reflected from the 650 ft interface. The effect of this difference in phenomena is also indicated by the breaks in the solid lines of Figure 13. Also shown in Figures 12 and 13 are a set of dashed straight lines that are within 10 percent of the calculated data.

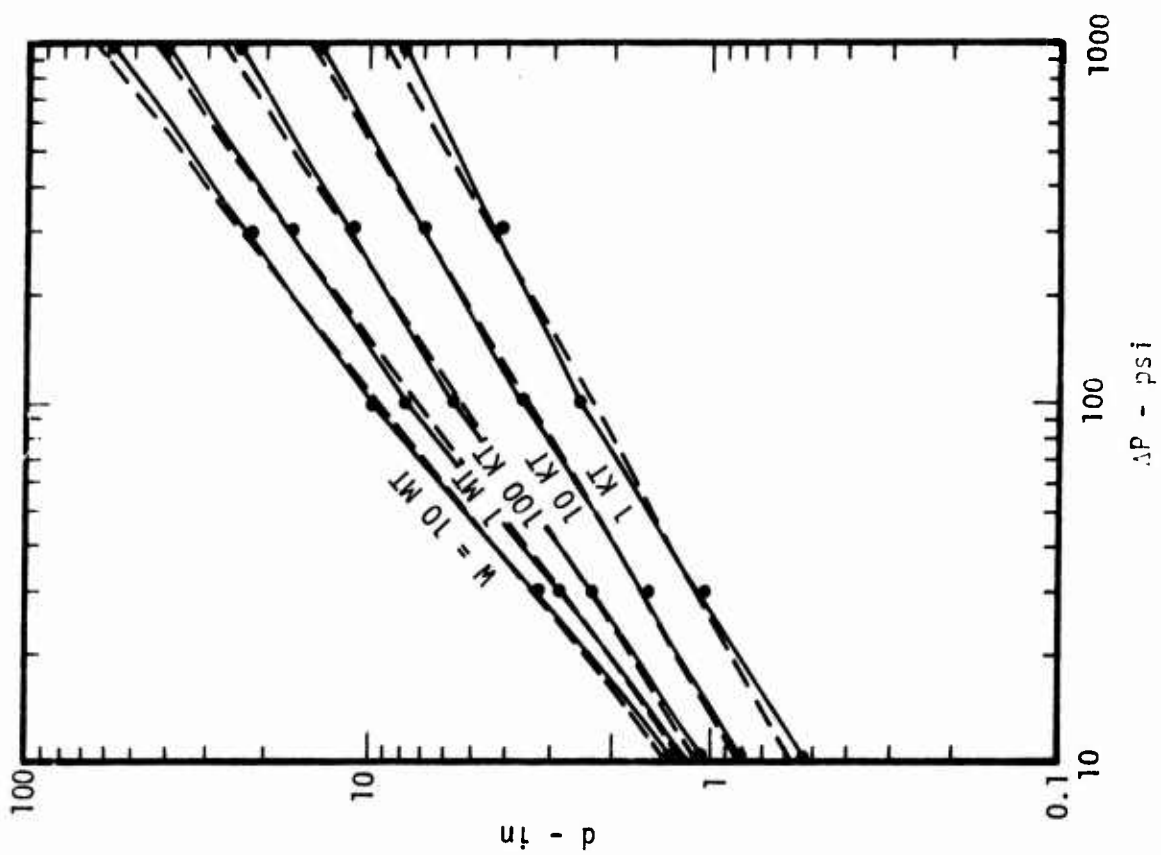
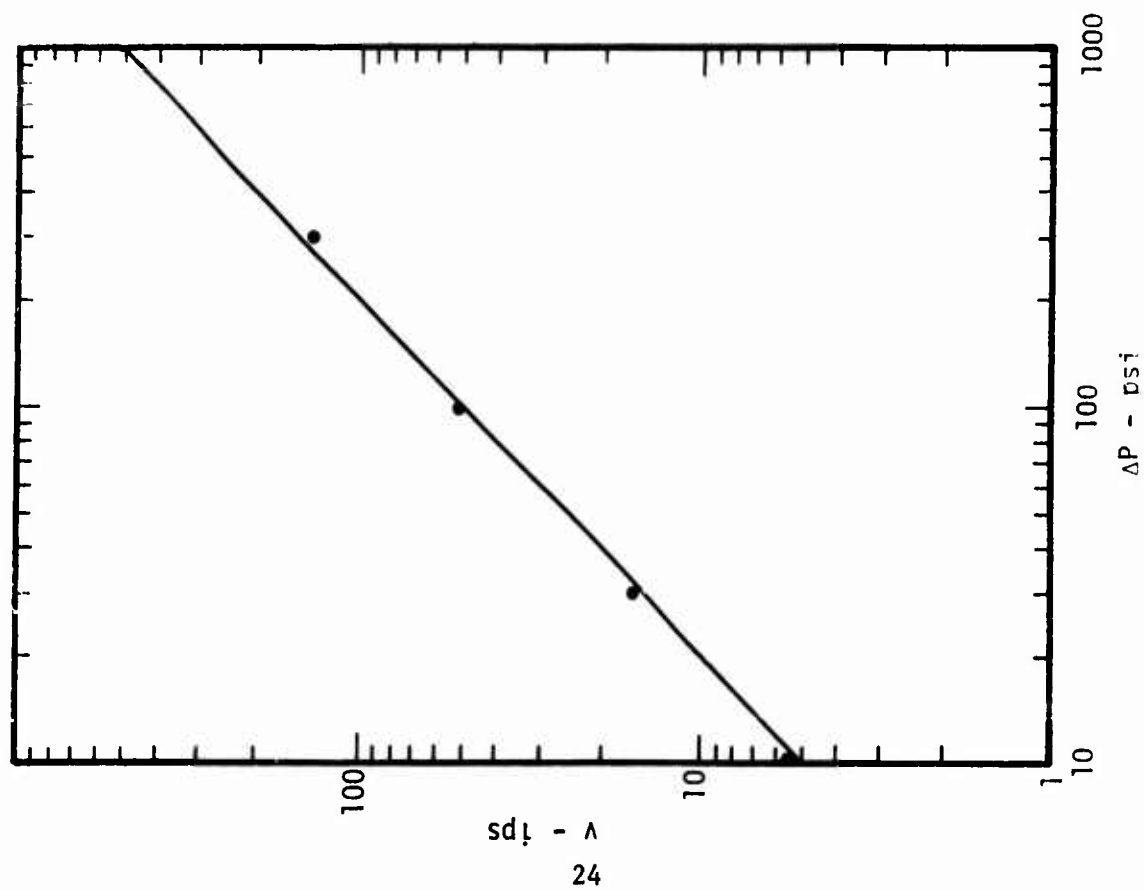


Figure 12. Peak Surface Particle Velocity and Displacement as a Function of Peak Overpressure

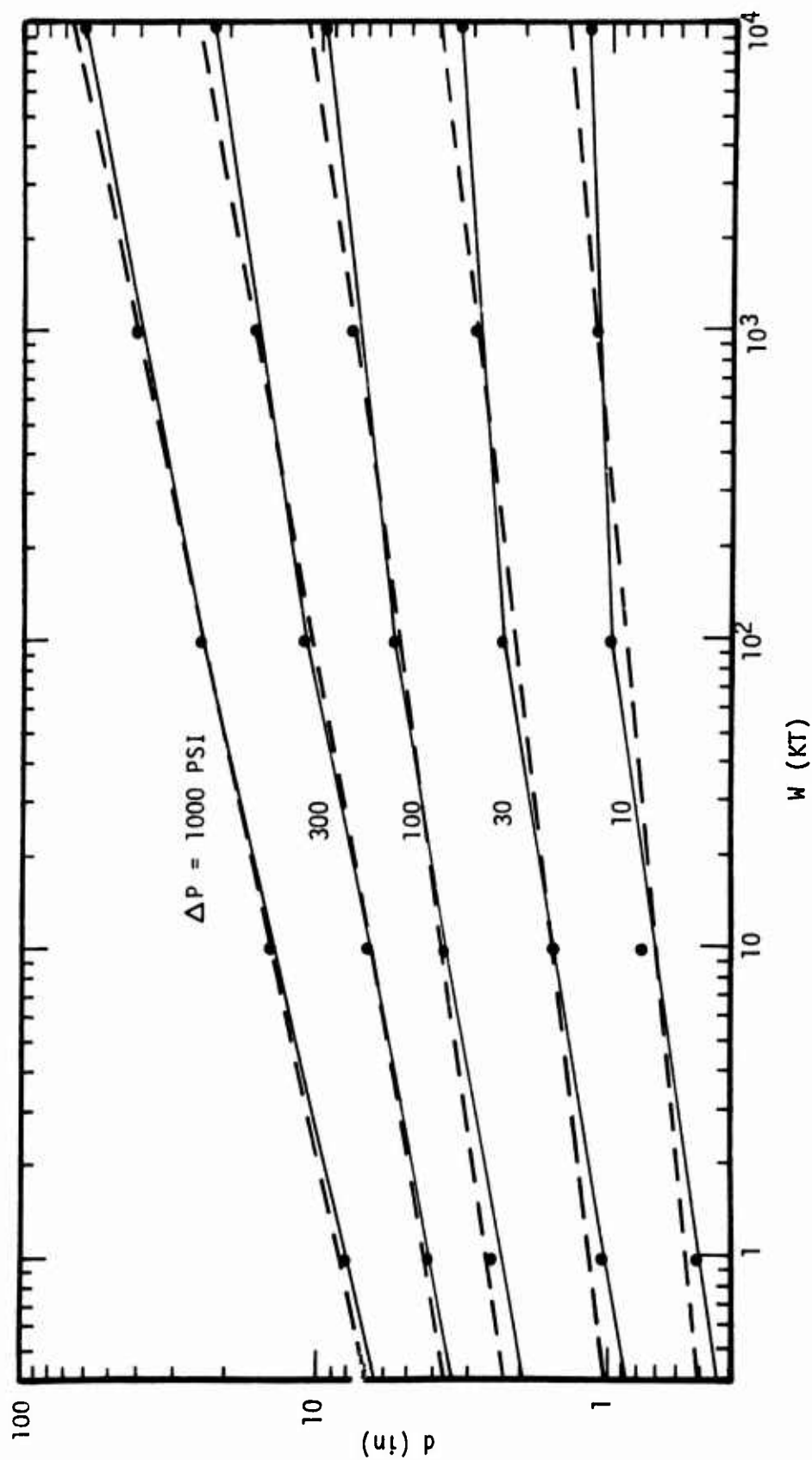


Figure 13. Peak Surface Particle Displacement as a Function of Yield

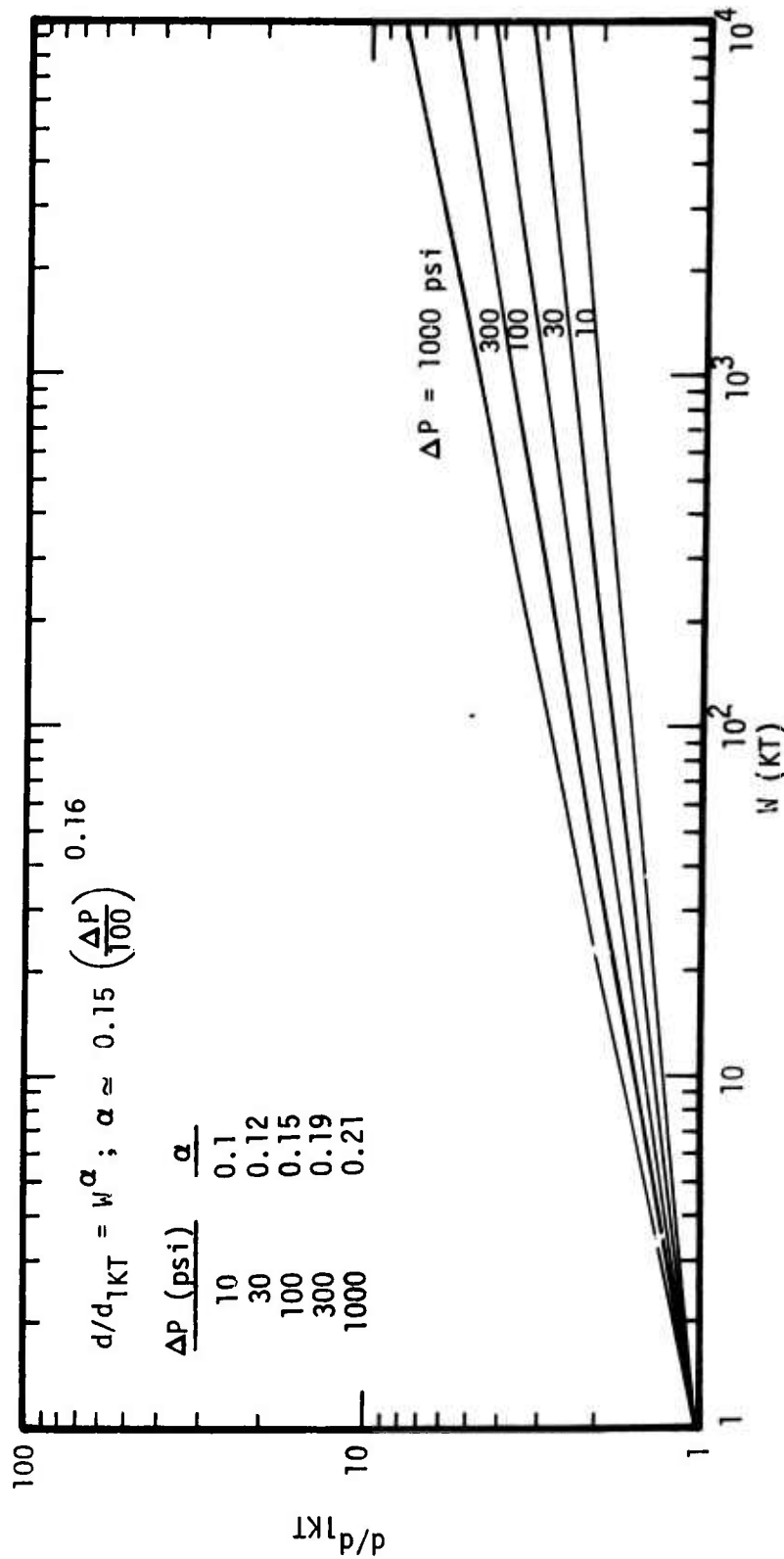


Figure 14. Normalized Surface Displacement as a Function of Yield (d_{1KT} = Surface Displacement from 1KT)

Figure 14 presents these straight line (on log-log paper) approximations for the yield and overpressure dependence in normalized form, i.e., displacements for any overpressure and yield were divided by the peak displacement calculated for that same overpressure and 1 KT. From simple analysis of these plots, it can be shown that the peak surface displacement can be approximated by

$$d_o \approx d_1 \left(\frac{W}{1MT} \right)^\alpha \quad (2)$$

where

$$\alpha \approx 0.15 \left(\frac{\Delta P}{100 \text{ psi}} \right)^{0.16} ; \quad (3)$$

$$d_1 \approx 7 \left(\frac{\Delta P}{100 \text{ psi}} \right)^{0.78} \text{ for } 10 \leq \Delta P \leq 1000 \text{ psi.} \quad (4)$$

3. Attenuation Characteristics

Figures 15 through 18, in conjunction with Figure 8, provide the calculated attenuation of near-surface (0 to 100 ft depth) peak stress, particle velocity, and displacement. These theoretical results show:

a. Displacements attenuate exponentially with depth for all yields and overpressures considered.

b. The attenuation curve for peak particle velocity at overpressures greater than about 100 psi is qualitatively different than the attenuation curve for low overpressures, particularly in the top 30 ft. This qualitative difference is caused by the fact that the peak particle velocity is associated with the initial jump for overpressures greater than about 100 psi (for all depths and yields less than about 1 MT); whereas the reflected waves from the softer layers cause the peak in the top 30 ft for the lower overpressures and all yields considered. In this latter case, essentially no attenuation of peak particle velocities occurs in the top 30 ft.

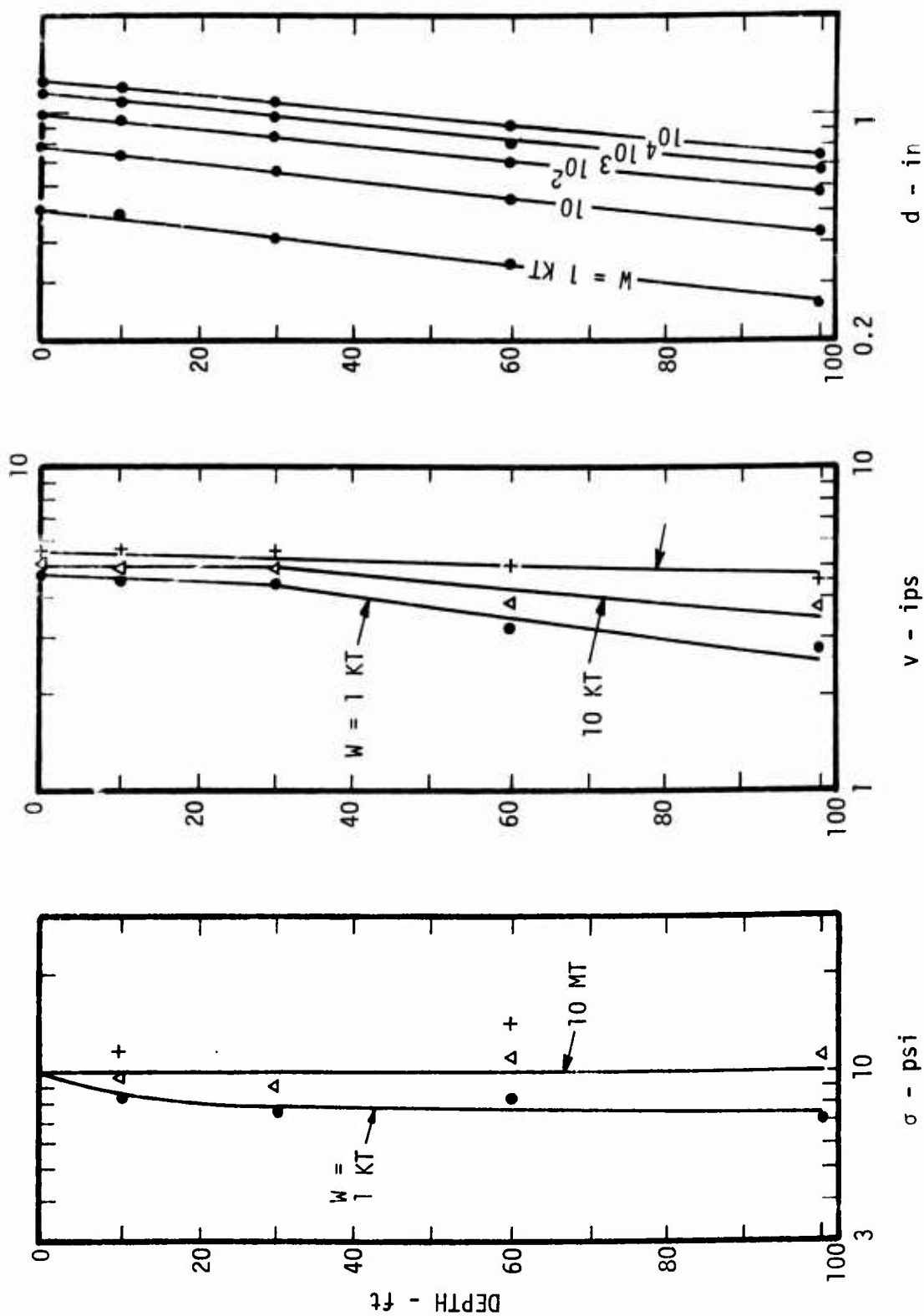


Figure 15. Attenuation of Peak Stress, Particle Velocity, and Displacement at 10 psi Range from Near-Surface Airbursts (Calculations for Frenchman Flat)

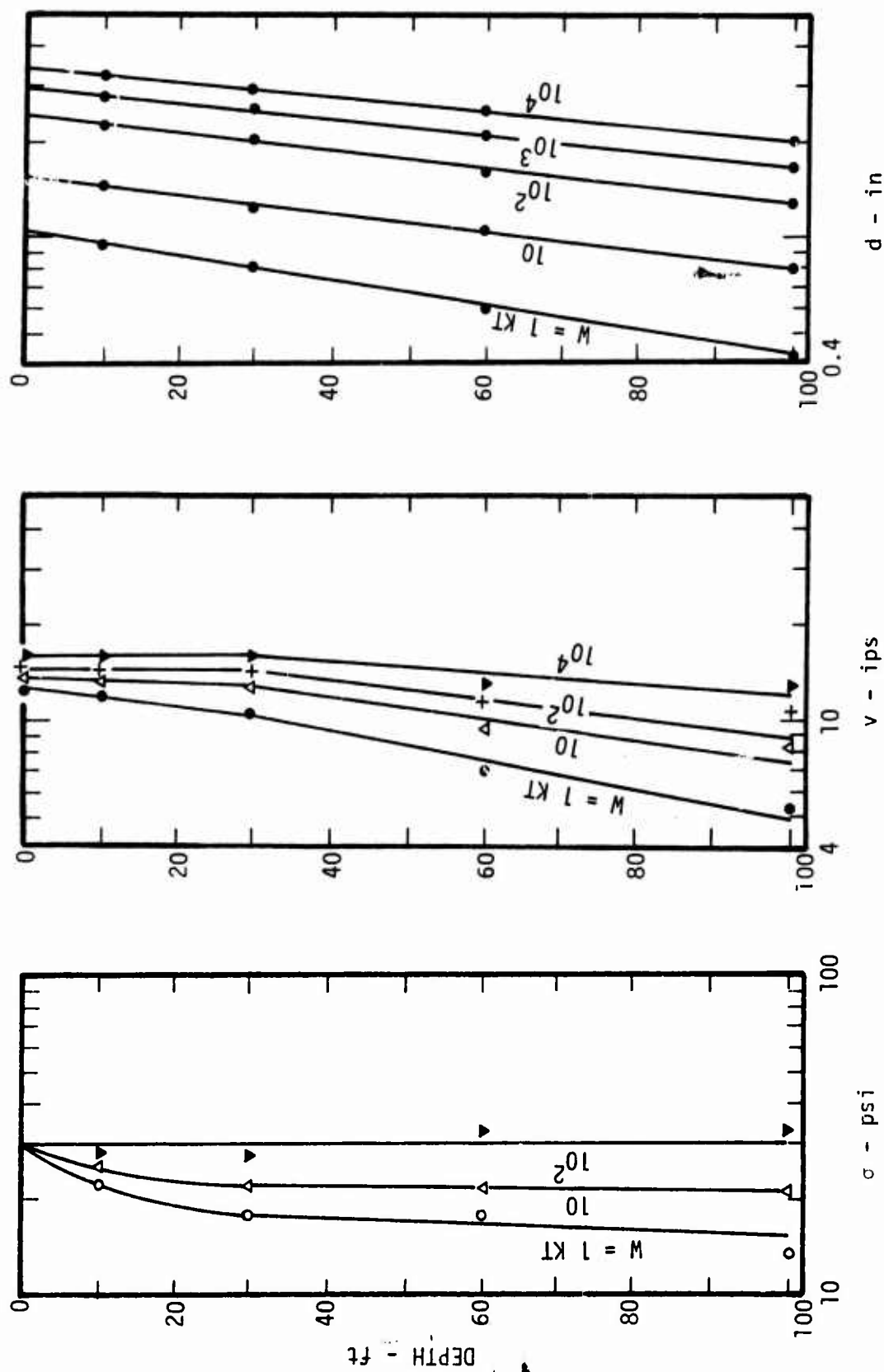


Figure 16. Attenuation of Peak Stress, Particle Velocity, and Displacement at 30 psi Range from Near-Surface Airburst (Calculations for Frenchman Flat)

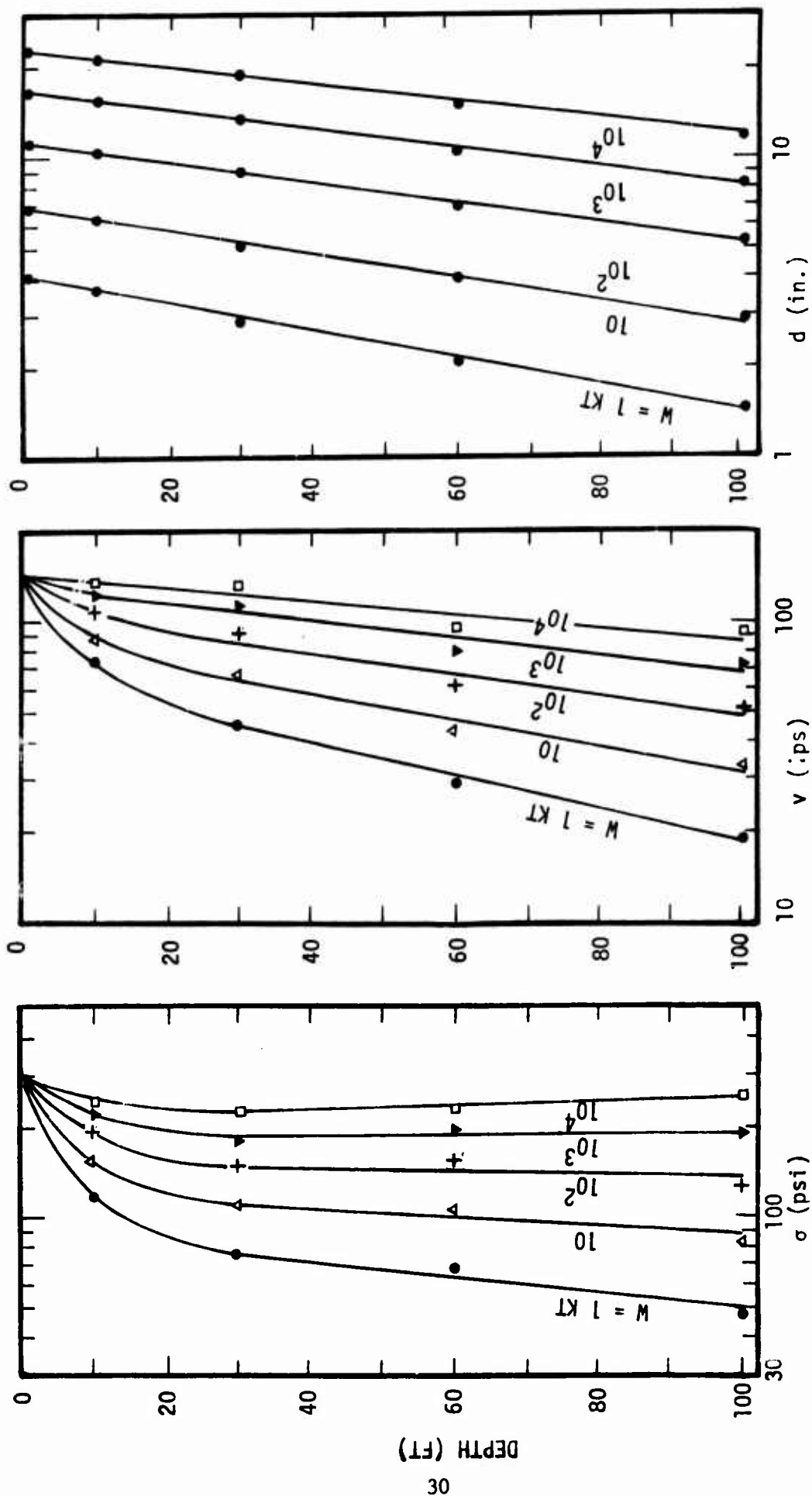


Figure 17. Attenuation of Peak Stress, Particle Velocity, and Displacement at 300 psi Range from Near Surface Airbursts in Frenchman Flat

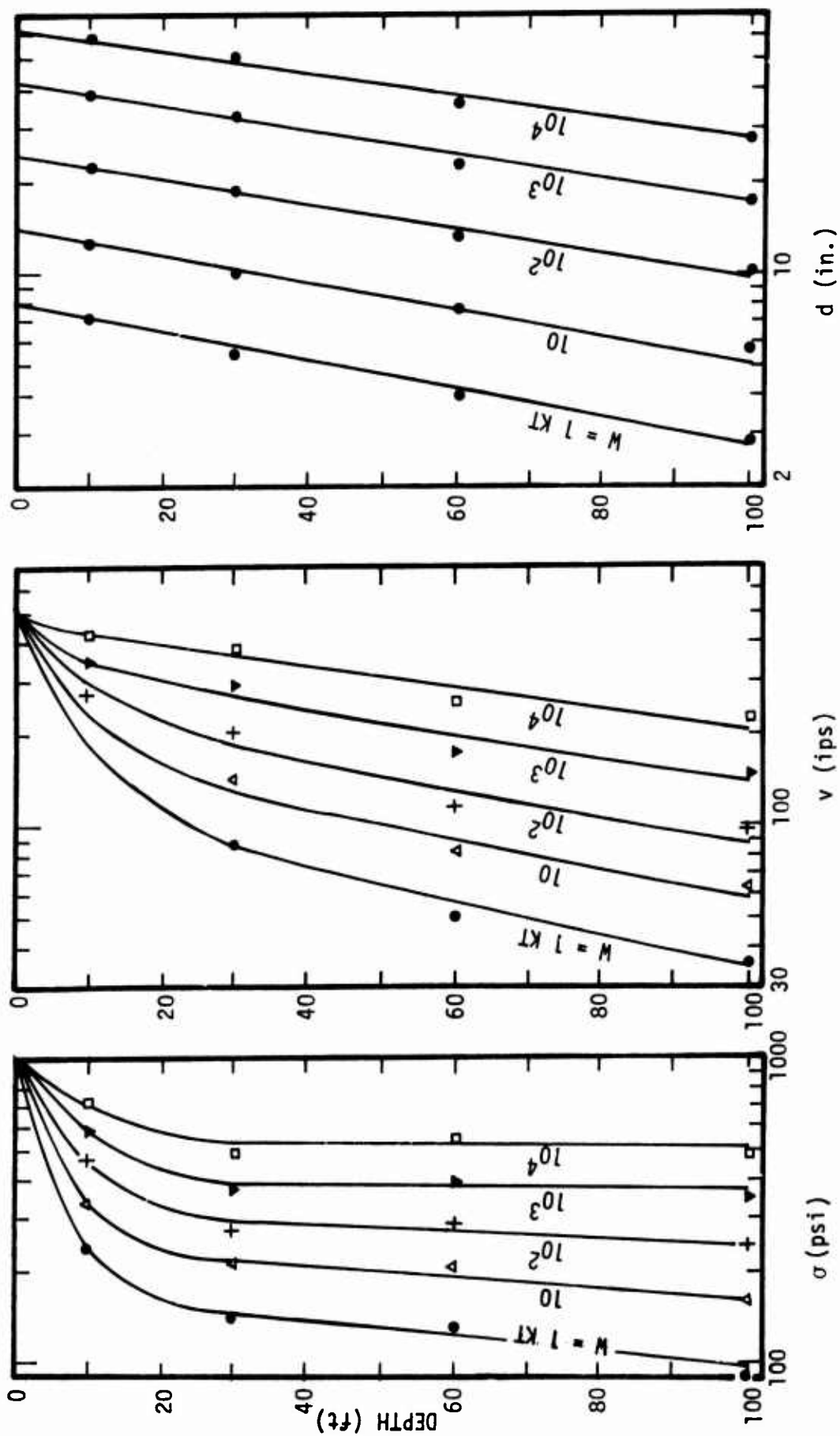


Figure 18. Attenuation of Peak Stress, Particle Velocity, and Displacement at 1000 psi Range from Near-Surface Airbursts (Calculations for Frenchman Flat)

In the former case, considerable attenuation occurs in the upper 30 ft, especially at the higher yields. The attenuation of peak particle velocities below 30 ft can be approximated by an exponential decay.

c. The calculated peak stresses do not attenuate greatly at the lower overpressures. For overpressures of 100 psi and above, significant attenuation occurs in the top 30 ft, depending on the yield. The peak stress between about 30 and 100 ft does not attenuate appreciably except for very low yields; in which case the decay can be reasonably approximated as an exponential decay.

As indicated above, the attenuation of peak displacements between 0 and 100 ft depth and peak particle velocity between 30 and 100 ft depth can be approximated by an exponential decay. Figure 19 shows normalized peak particle velocity and displacement attenuation curves which indicate a slight overpressure dependence. For overpressure between 100 and 1000 psi, these attenuation curves are reasonably approximated by

$$v \approx v_{30} e^{-0.0085(z-30)} \text{ for } 30 \leq z \leq 100 \text{ ft} \quad (5)$$

$$d \approx d_0 e^{-0.0085z} \text{ for } 0 \leq z \leq 100 \text{ ft} \quad (6)$$

where v_{30} = peak particle velocity at 30 ft depth

d_0 = peak displacement at the surface

z = depth (ft)

The above expression for peak particle velocity is primarily applicable for depths between 30 and 100 ft. At shallower depths (and overpressures greater than 100 psi), Eq. 5 significantly underestimates the peak particle velocities shallower than 30 ft depth, especially for low yields and high overpressures. For these shallower depths, Figure 20 provides a useful graphical means of predicting peak particle velocity.

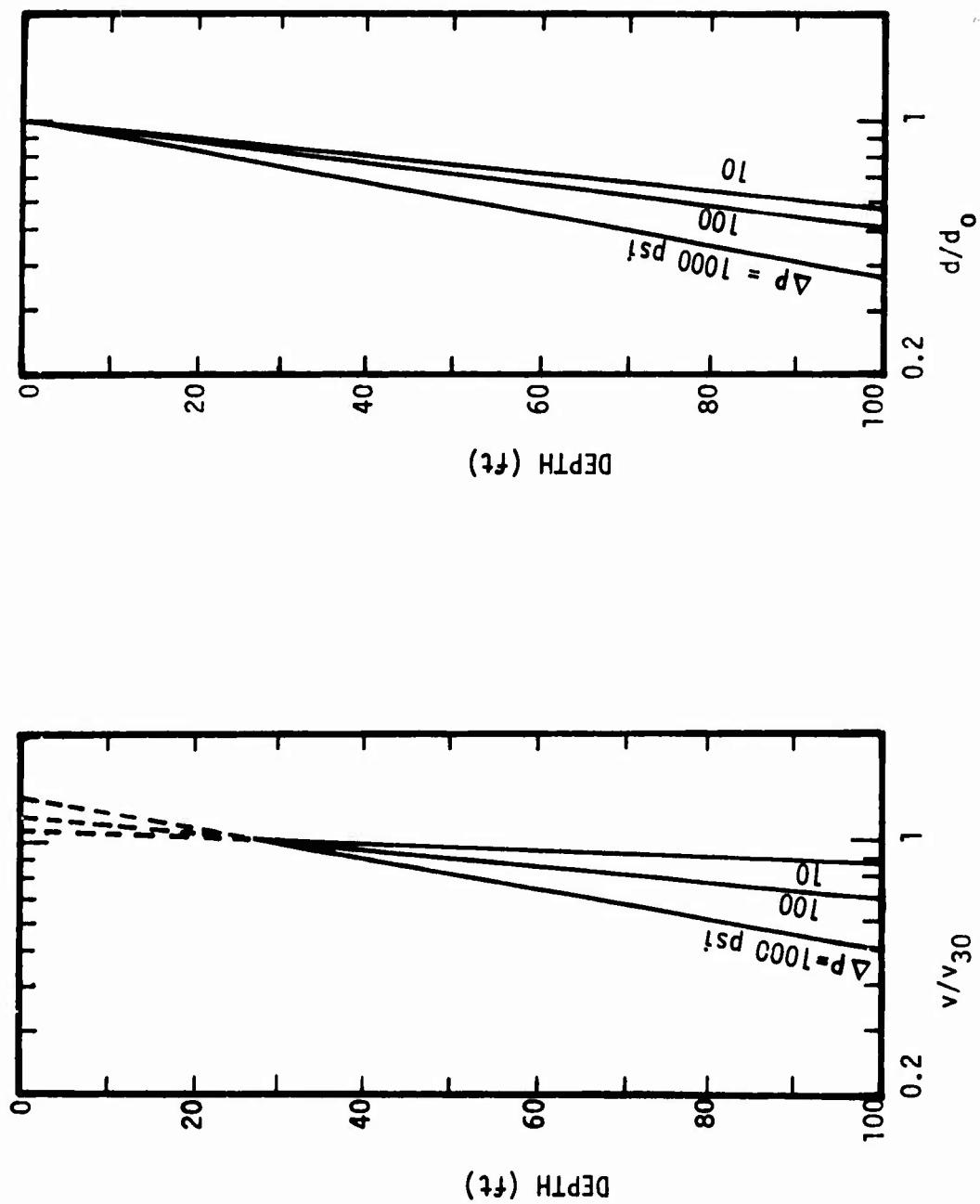


Figure 19. Normalized Peak Particle Velocity and Displacement Attenuation with Depth

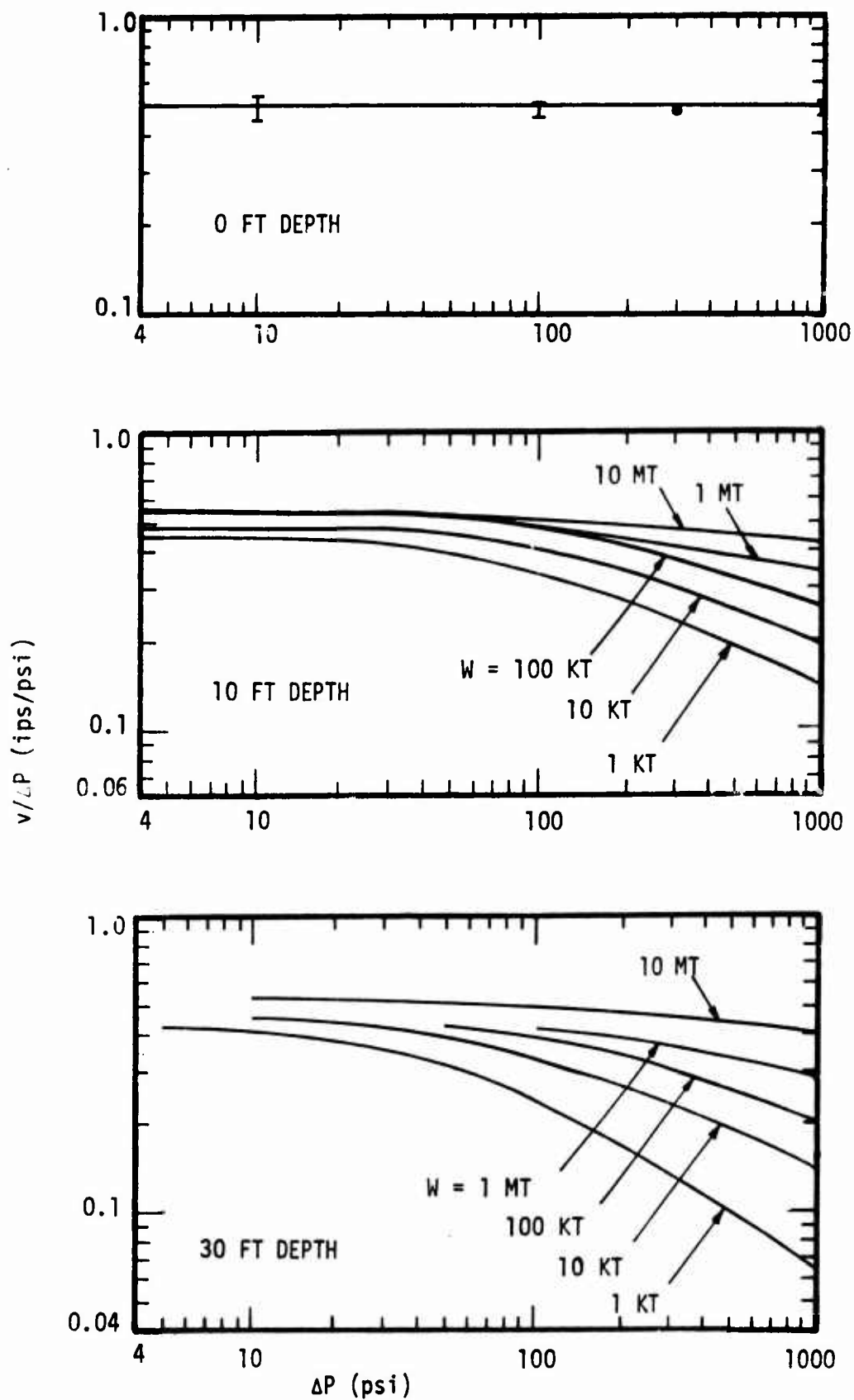


Figure 20. Ratio of Peak Particle Velocity to Peak Overpressure

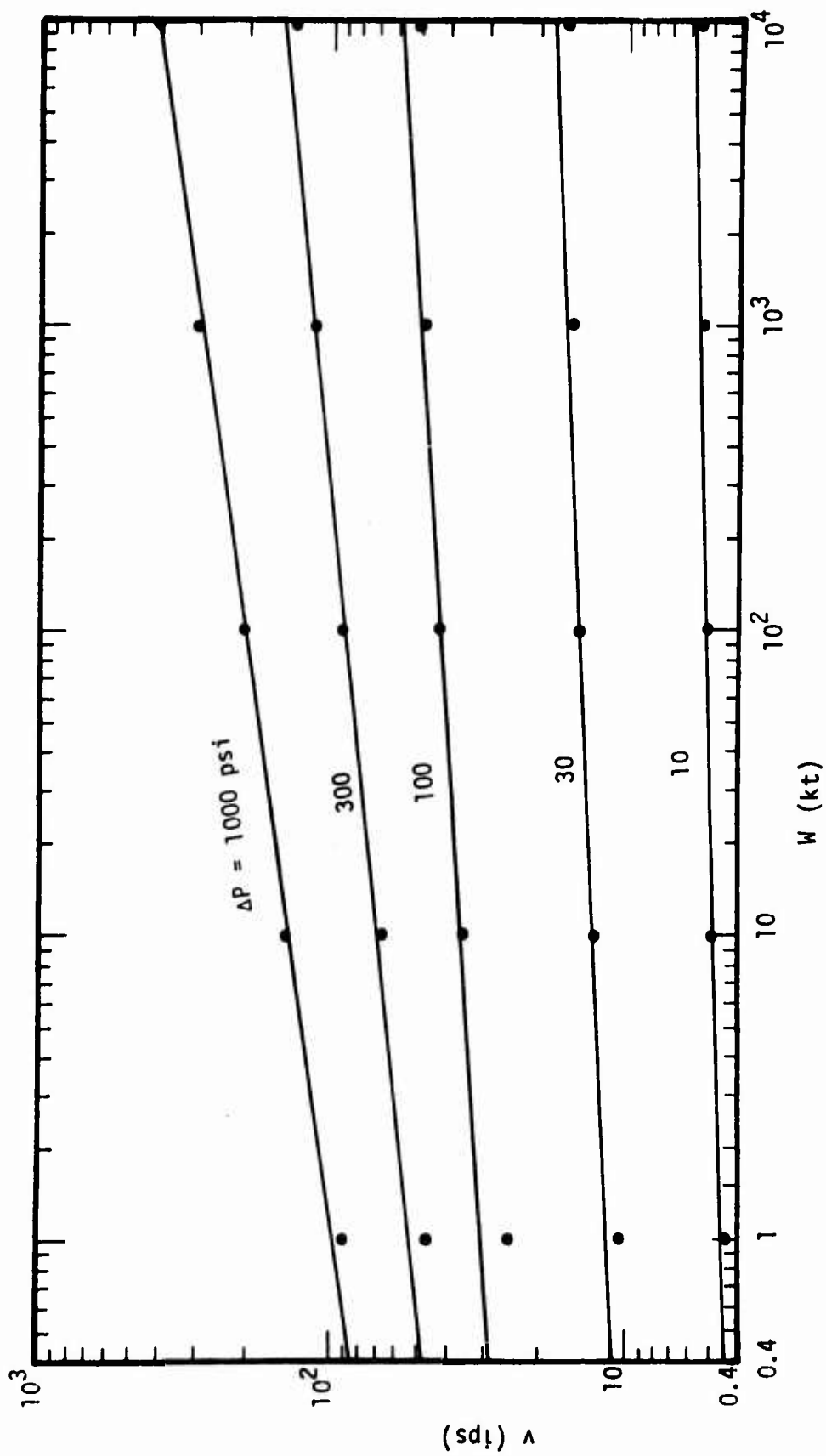


Figure 21. Peak Particle Velocity at 30 ft Depth in Frenchman
Flat as a Function of Yield

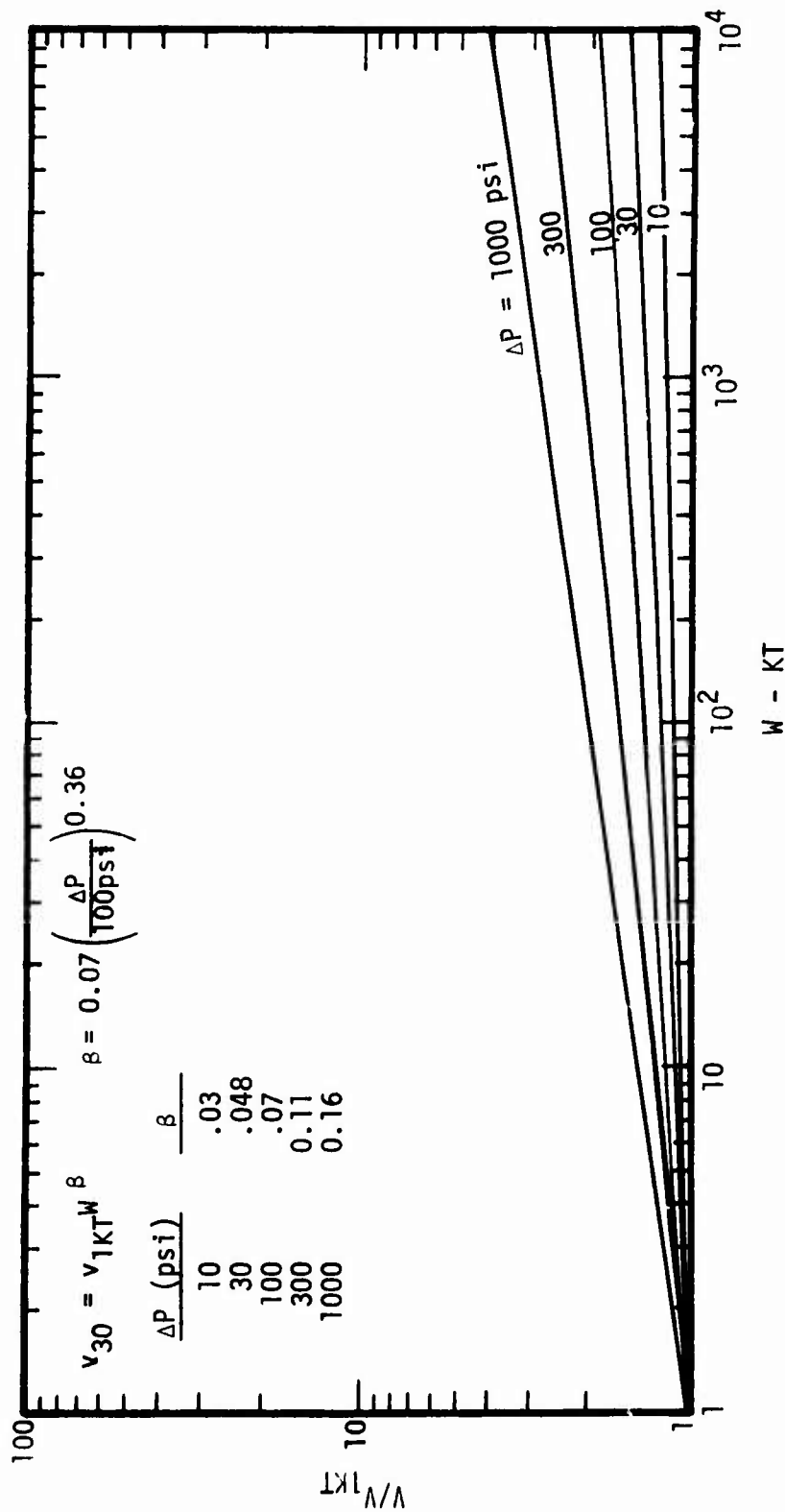


Figure 22. Normalized Peak Particle Velocity at 30 ft Depth as a Function of Yield (V_{1KT} = Peak Particle Velocity at 30 ft Depth and 1 KT)

The surface displacement (d_0) can be obtained from Figure 13 and from Eqs 2 - 4. Similarly, we can use Figures 21 and 22 to derive prediction formulae for the peak particle velocity at 30 ft depth; i.e.,

$$v_{30} = v_{1MT} \left(\frac{W}{1MT} \right)^\beta \quad (7)$$

where

$$\beta = 0.07 \left(\frac{\Delta P}{100 \text{ psi}} \right)^{0.36} ; \quad (8)$$

$$v_{1MT} = 50 \left(\frac{\Delta P}{100 \text{ psi}} \right)^{0.95} \text{ (IPS)} . \quad (9)$$

4. Summary

In the preceding analysis of results from a series of one-dimensional calculations, we developed graphical means of predicting vertical, airblast-induced velocities and displacements as a function of yield, peak overpressure and depth. Estimates of the graphical results that were developed to interpolate between the calculated results are summarized in Table II.

The systematic theoretical study of vertical ground motions in Frenchman Flat has led to the following observations that should be carefully considered in examining the nuclear test data:

- a. For a given yield, near-surface peak particle velocities and displacements are both strongly dependent on peak overpressure; e.g., at $z = 30$ ft, $v \propto \Delta P^{0.95}$ and $d \propto \Delta P^{0.78}$. Thus, uncertainties in predicting peak overpressure as a function of range are translated into nearly equivalent uncertainties in predicted near-surface peak vertical airblast-induced ground motions.
- b. For a given peak overpressure, near-surface peak particle velocities and displacements are weakly dependent on explosive yield; e.g., at

Table II

PREDICTION FORMULAE FOR NEAR-SURFACE VERTICAL AIRBLAST-INDUCED GROUND MOTIONS
FROM NEAR-SURFACE AIRBURSTS IN FRENCHMAN FLAT
(1 KT \leq W \leq 10 MT; 100 \leq ΔP \leq 1000 psi)

Peak Particle Velocity

$$V_{IPS} = 0.5 \Delta P \text{ at } z = 0$$

$$= 50 \left(\frac{\Delta P}{100 \text{ psi}} \right)^{0.95} \left(\frac{W}{1 \text{ MT}} \right)^{\beta} e^{-0.0085(z - 30)} \quad \text{for } 30 \leq z \leq 100 \text{ ft}$$

$$\text{where } \beta = 0.07 \left(\frac{\Delta P}{100 \text{ psi}} \right)^{0.36}$$

Peak Displacement

$$d_{IN} = 7 \left(\frac{\Delta P}{100 \text{ psi}} \right)^{0.78} \left(\frac{W}{1 \text{ MT}} \right)^{\alpha} e^{-0.0085z} \quad \text{for } 0 \leq z \leq 100 \text{ ft}$$

$$\text{where } \alpha = 0.15 \left(\frac{\Delta P}{100 \text{ psi}} \right)^{0.16}$$

$z = 30$ ft, $d \propto W^\alpha$ and $v \propto W^\beta$ where $0.15 \leq \alpha \leq 0.21$ and $0.07 \leq \beta \leq 0.16$ for $100 \leq \Delta P \leq 1000$ psi. Thus, uncertainties in specifying the explosive yield are only weakly translated into uncertainties in predicting the peak near-surface vertical ground motions.

- c. The calculations suggest that peak vertical displacements attenuate exponentially with depth at a rate that is relatively independent of yield and peak overpressure. Peak vertical particle velocities below about 30 ft also attenuate exponentially, but at a rate that is usually less rapid than at shallower depths. In general, the attenuation rates increase with increasing peak overpressure or decreasing yield.
- d. The response of the softer layers below about 30 ft leads to a downward acceleration of the surface such that a residual downward velocity remains, even after the overpressure positive phase is over for low yields. This downward motion is reversed by reflected compressional waves from either the 170 ft or 650 ft interface, depending on the yield and peak overpressure. Such downward coasting phenomena could easily be misinterpreted as a base line shift in the analysis of test data.

SECTION IV
COMPARISONS OF CALCULATIONS WITH TEST DATA FROM
FRENCHMAN FLAT

This section compares the ground motions predicted by the simplified model developed in the previous section with those measured on several nuclear events in Frenchman Flat. We emphasize the comparison with PRISCILLA data because they were the primary basis of empirical prediction procedures developed in the early 1960's and applied to develop criteria for many existing strategic systems (Ref. 7, 8). Comparisons with data from SMALL BOV will be presented in a separate report

1. In-Situ Impedance

Figure 23 compares the calculated in-situ "impedance" of the very near surface soils data from five nuclear tests in Frenchman Flat. Both the calculated and experimental data were derived by dividing the peak overpressure by the peak particle velocity at the indicated depths ($\rho c = \Delta P/v$). Thus, the term impedance strictly applies only for the free surface because peak particle velocity and stress attenuate with increasing depth. This attenuation, which is less significant at the low overpressures and high yields, is the cause of the variation between $\Delta P/v$ for 0 and 10 ft depths and for the yield variation between 1 and 100 kilotons.

Out-running conditions exist for peak overpressures less than about 25 psi in Frenchman Flat. Nevertheless, a jump in particle velocity is caused by the arrival of the airblast so that the low overpressure near-surface data in Figure 23 may be appropriate even though out-running conditions exist.

In any case, the calculated $\Delta P/v$ appears to be somewhat higher than the analogous nuclear test data from the upper 10 ft of soil in Frenchman Flat. This result implies that the loading stress-strain curve assumed for

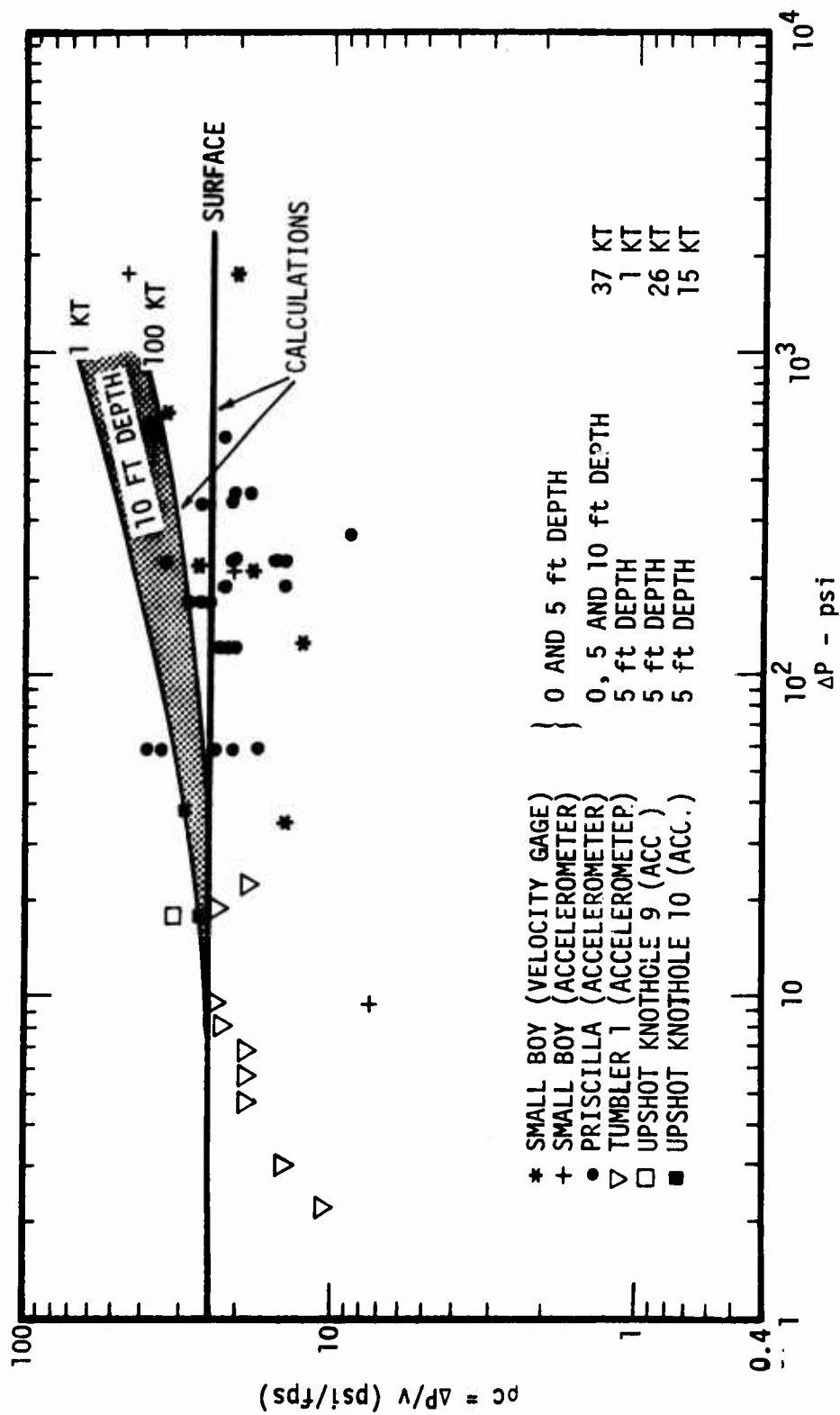


Figure 23. Comparison of Calculated and Measured $\Delta P/V$

the 0-10 ft layer of Frenchman Flat may have been too stiff. The experimental data suggest that $\Delta P/v \approx 20$ psi/fps as opposed to the calculated surface impedance of 24 psi/fps (or even larger values at 5 and 10 ft depths). Thus, the calculations would be more consistent with the experimental data if the modulus of the surface layer (for the peak pressures of concern) were reduced by about 30 to 50 percent; an alteration that would produce only a minor increase in the surface displacements and no change in displacements below 10 feet.

2. Comparison of Simplified Model with PRISCILLA Data

We shall now compare peak particle velocities and displacements predicted by the simplified theoretical model for a yield of 37 kilotons with the experimental data from PRISCILLA (Ref. 10, 11). Although the equations summarized in Table II could be used as a basis for comparison, we interpolated between the peak displacement and particle velocity attenuation curves in Figure 8 and Figures 15 through 18 to obtain Figure 24 for the case of a 37 KT near surface burst. These attenuation curves, in conjunction with the surface peak particle velocity and displacement given by Figure 12 and 13, define the ground motions in the upper 100 ft as a function of peak overpressure.

Figure 25 compares measured near-surface peak particle velocities and displacements with predictions from the simplified model. As noted previously, the theoretical model tends to underestimate the near-surface peak particle velocity experimental data. Peak displacements predicted by the simplified model lie more in the center of the data scatter.

Figures 26 through 29 compare peak particle velocity and displacement data at depth with predictions from the simplified model procedures. In cases where independent peak overpressure data were reported by Sandia and SRI, the simplified model is unfolded for both cases. It is difficult to evaluate the accuracy of the predicted attenuation characteristics from these plots because insufficient data exist at each range to define the

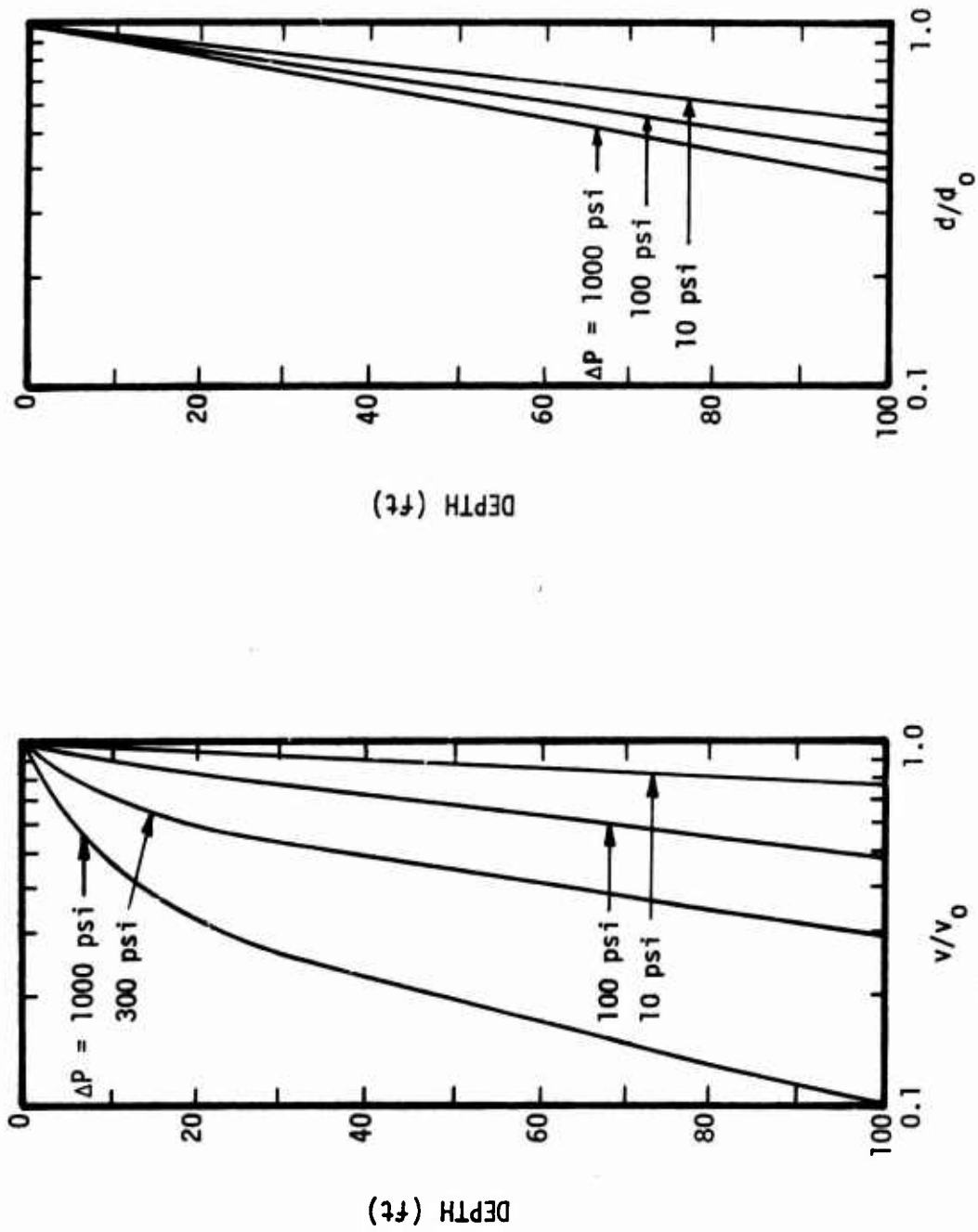


Figure 24. Peak Particle Velocity and Displacement Attenuation for a 37 MT Near-Surface Airburst over Frenchman Flat

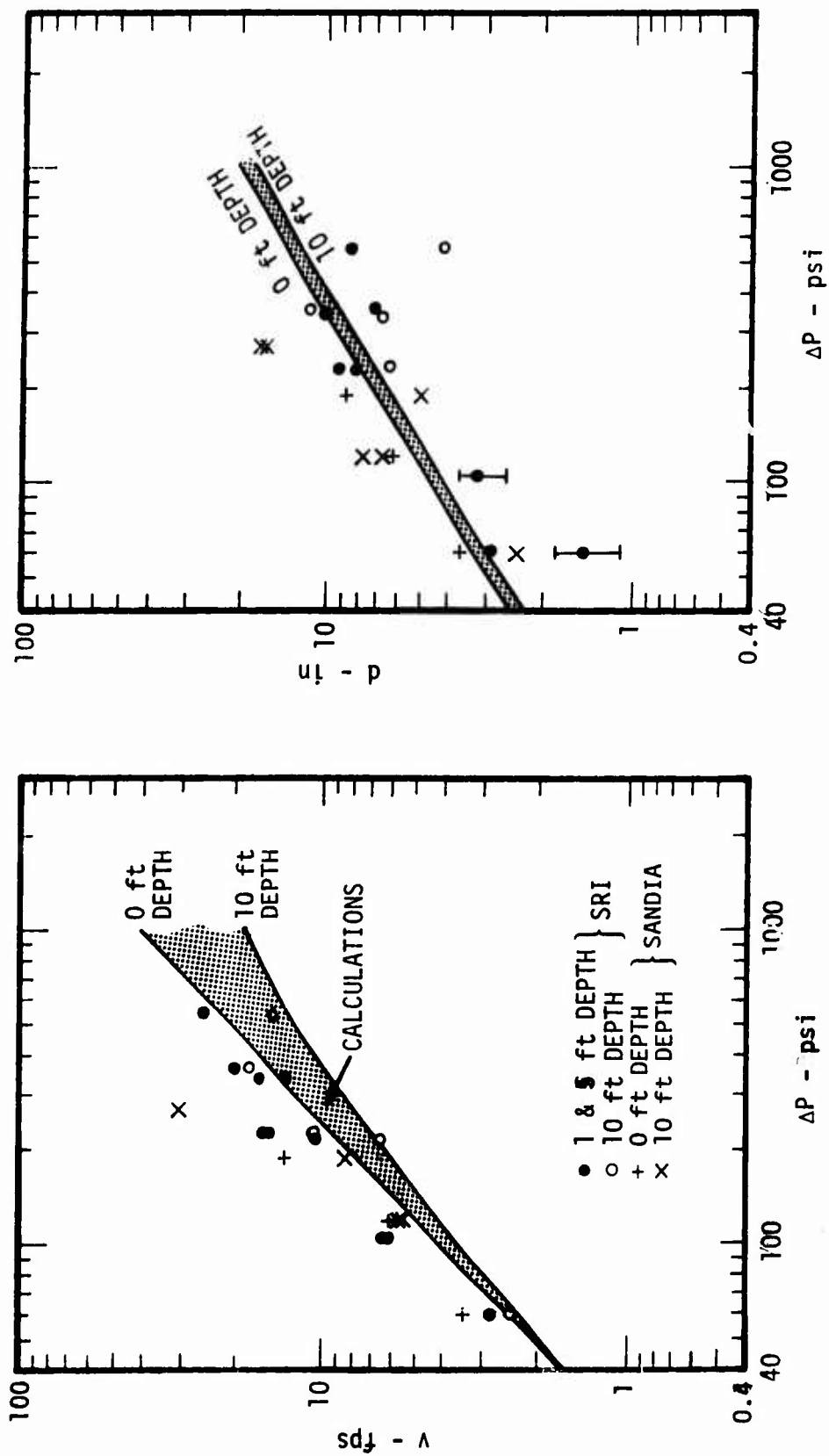
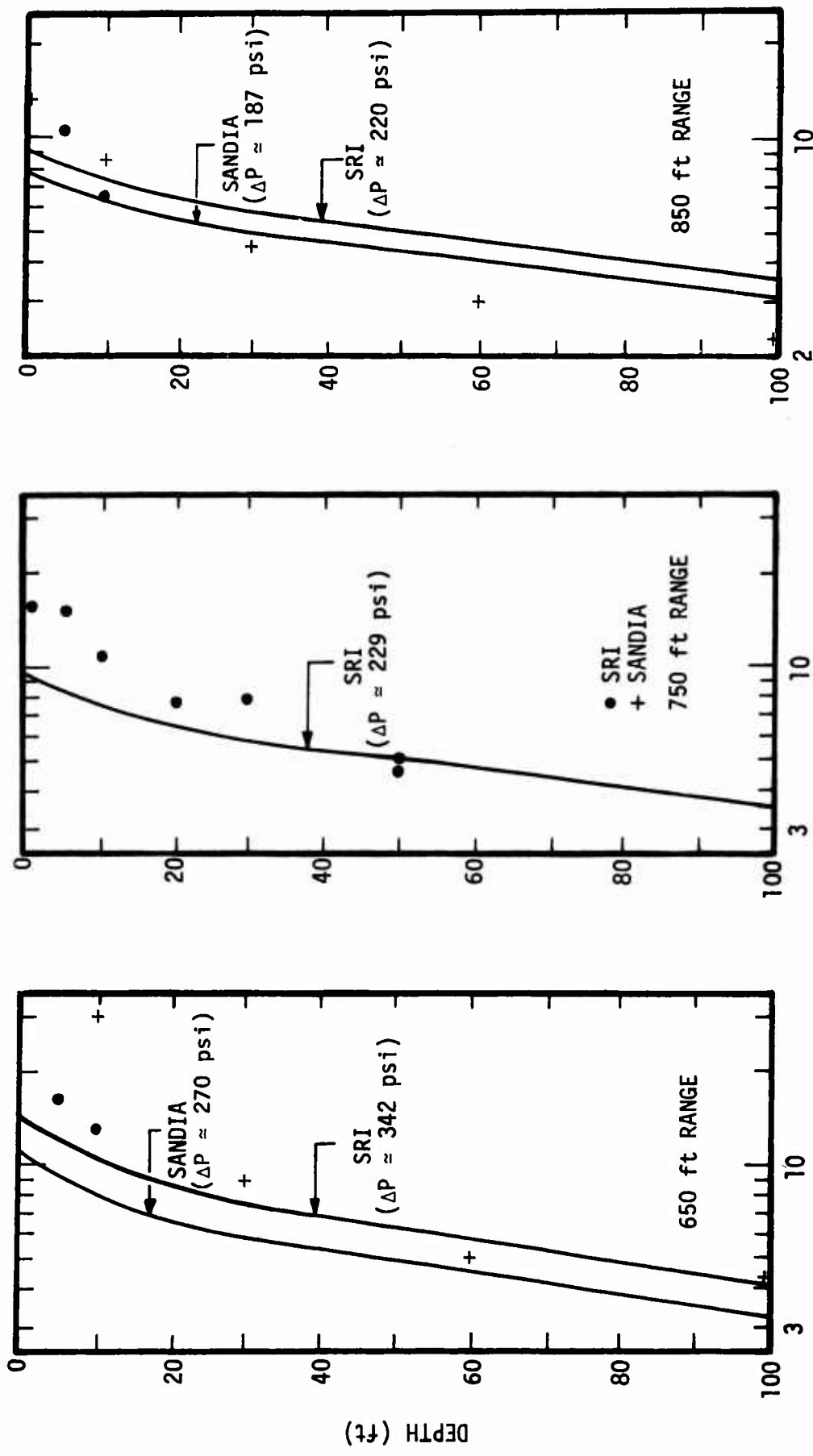


Figure 25. Comparison of Theoretical Model and Near-Surface Ground Motion Data from PRISCILLA



PEAK VERTICAL PARTICLE VELOCITY - fps

Figure 26. Comparison of Simplified Model with PRISCILLA Peak Particle Velocity Data

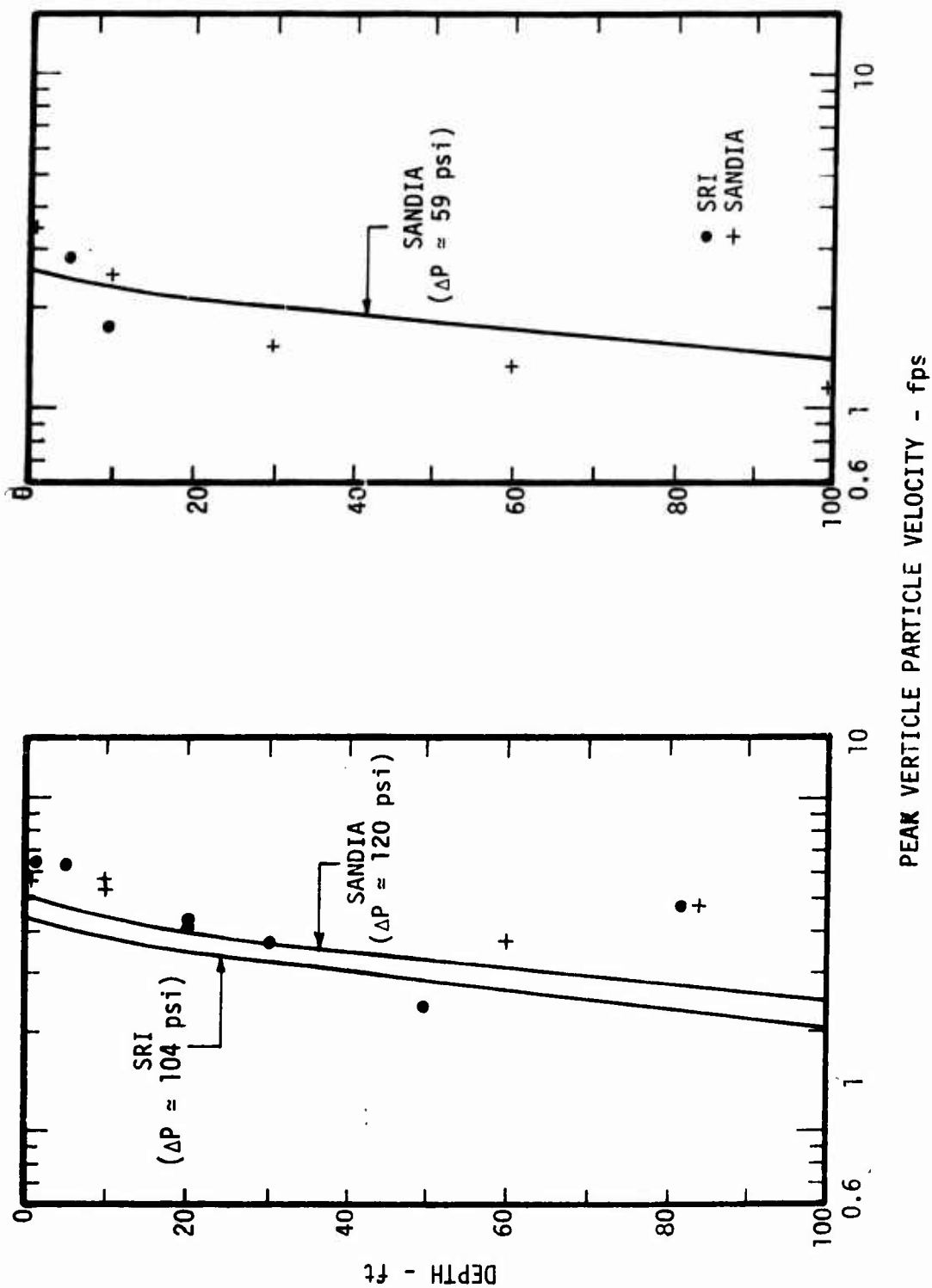


Figure 27. Comparison of Simplified Model with PRISCILLA Peak Particle Velocity Data

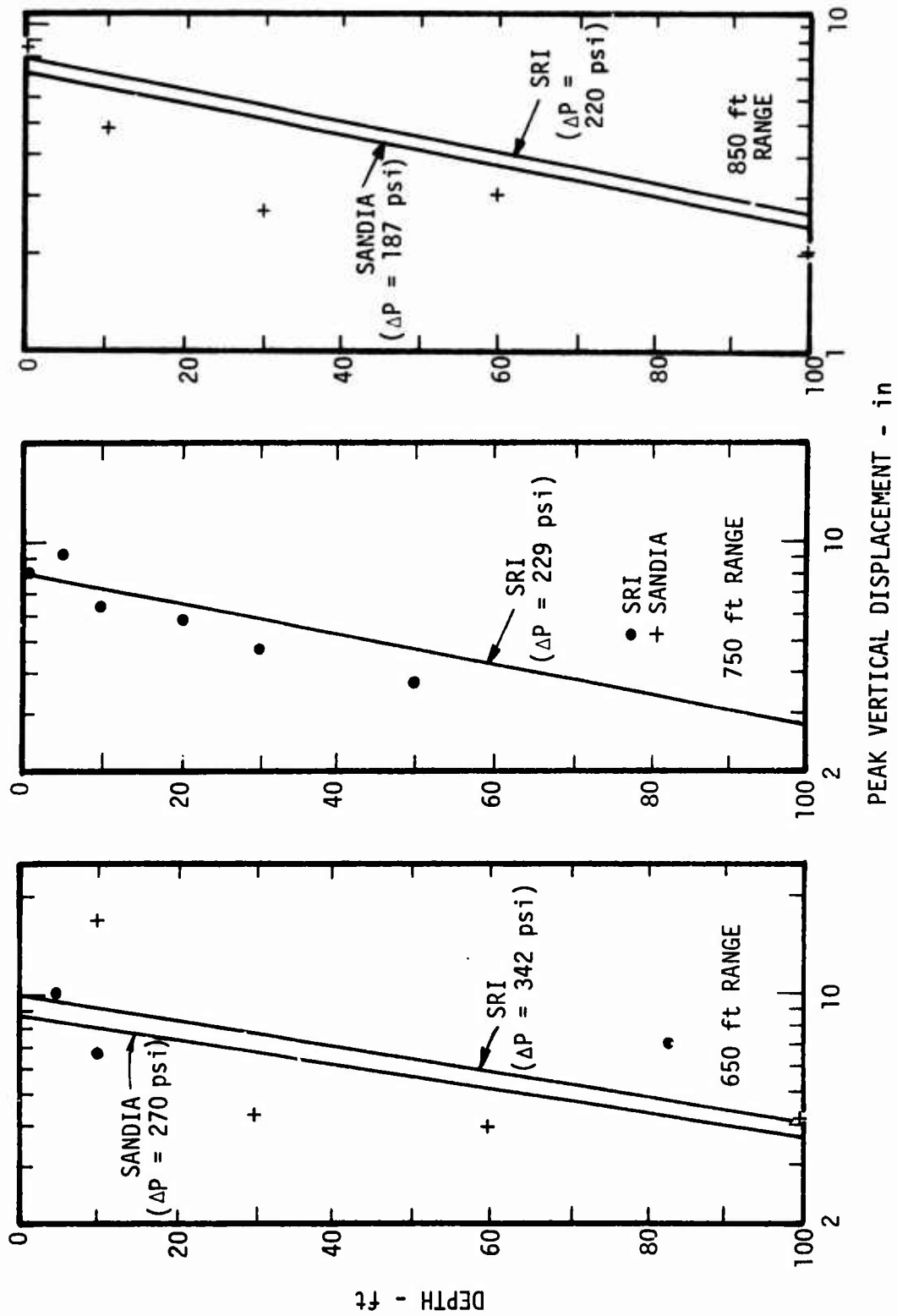


Figure 28. Comparison of Simplified Model with PRISCILLA Peak Displacement Data

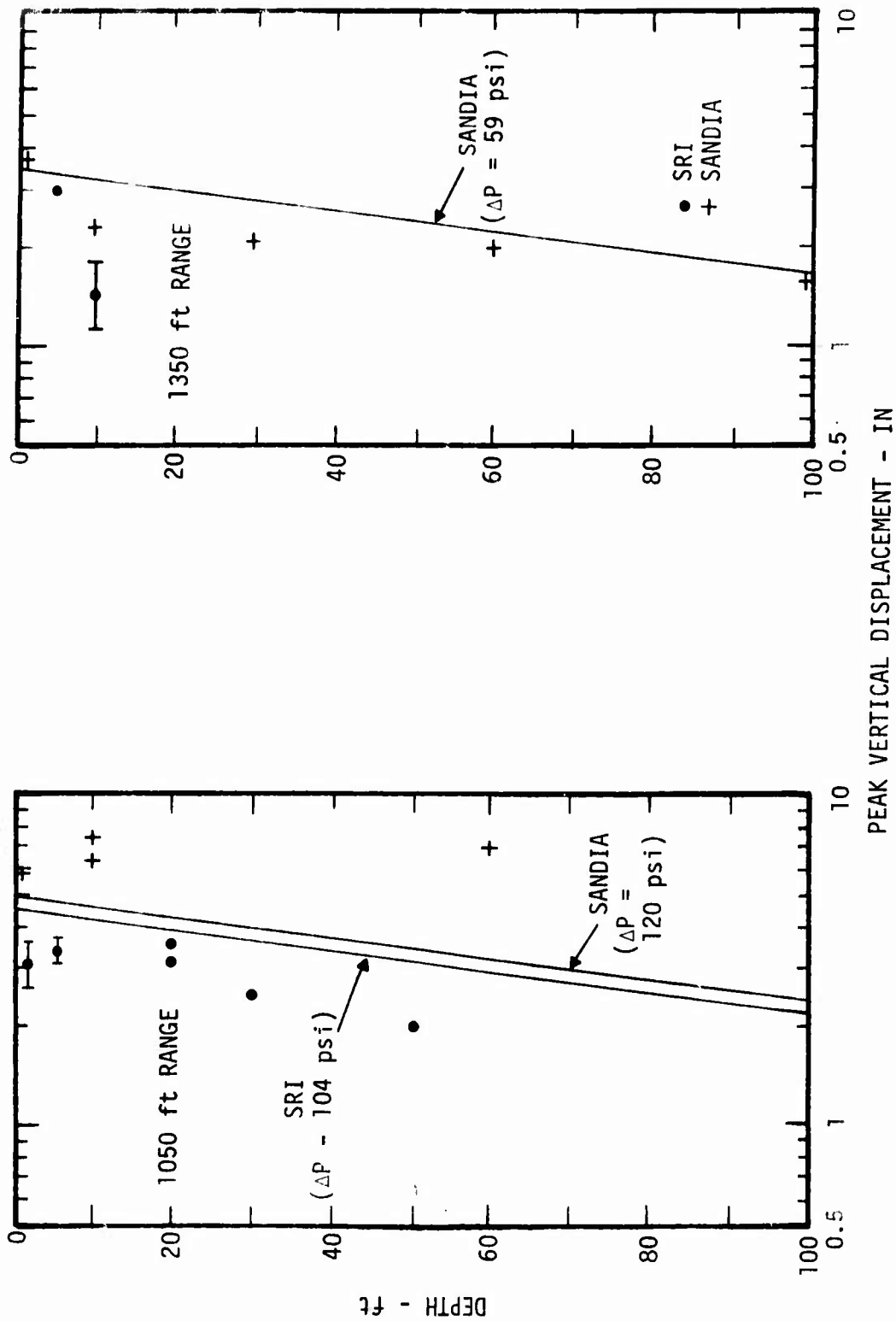


Figure 29. Comparison of Simplified Model with PRISCILLA Peak Displacement Data

inherent data scatter as a function of depth. To present the data in a form that allows a more representative comparison, the reported vertical motion data were normalized by the best estimate fit to the experimental surface data shown in Figure 30. Note that the estimate from the simplified model is an adequate fit for peak displacements but is about 20 percent lower than the peak particle velocity data. The normalized data are compared with the predicted attenuation of vertical peak particle velocity and displacement, as shown in Figure 31.

It is also instructive to compare calculated and measured arrival times. Figures 32 and 33 show measured arrival times obtained from the free field acceleration records. These data can be put on a useful differential time scale by subtracting the arrival time at the earth's surface, as shown in Figure 34. The calculated initial arrival times are earlier than measured at shallow depths and later than measured at depths greater than about 50 ft. The calculated peak particle velocity arrivals are more consistent with the experimental data, indicating that the theoretical material properties reasonably represented the in-situ confined moduli at overpressures of concern and shallow depths. Furthermore, Figure 35 shows that SMALL BOY time-of-arrival data (Refs. 12, 13) are consistent with the material property model of peak wave speeds down to 400 ft. The initial arrival times below 170 ft are also consistent with the 3600 fps seismic velocity that was the basis for the loading portion of the stress-strain curve for the 170 - 650 ft layer (Figure 4). However, there is a significant discrepancy between the calculated and measured wave speeds (based on initial arrival times) for the shallower depths - particularly between about 50 and 170 ft.

3. Calculations Using Measured Overpressure Boundary Condition

The simplified theoretical model was based on the overpressure boundary condition predicted for a surface burst, and prediction formulae were expressed in terms of peak overpressure. To reduce the possible ambiguity in interpreting discrepancies between the results of theoretical calcula-

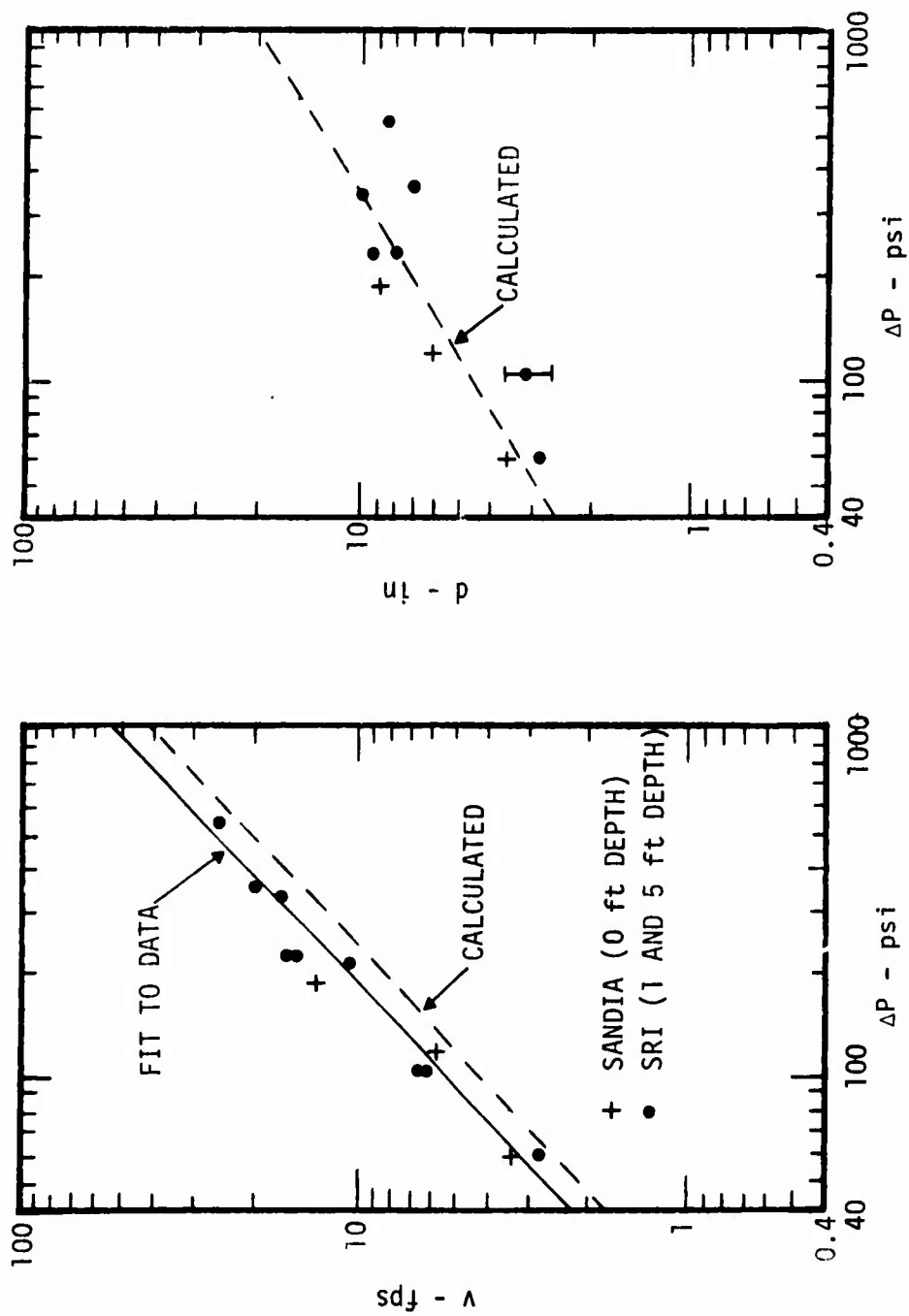


Figure 30. Best Estimate of Very Near-Surface Vertical Motion Data from PRISCILLA

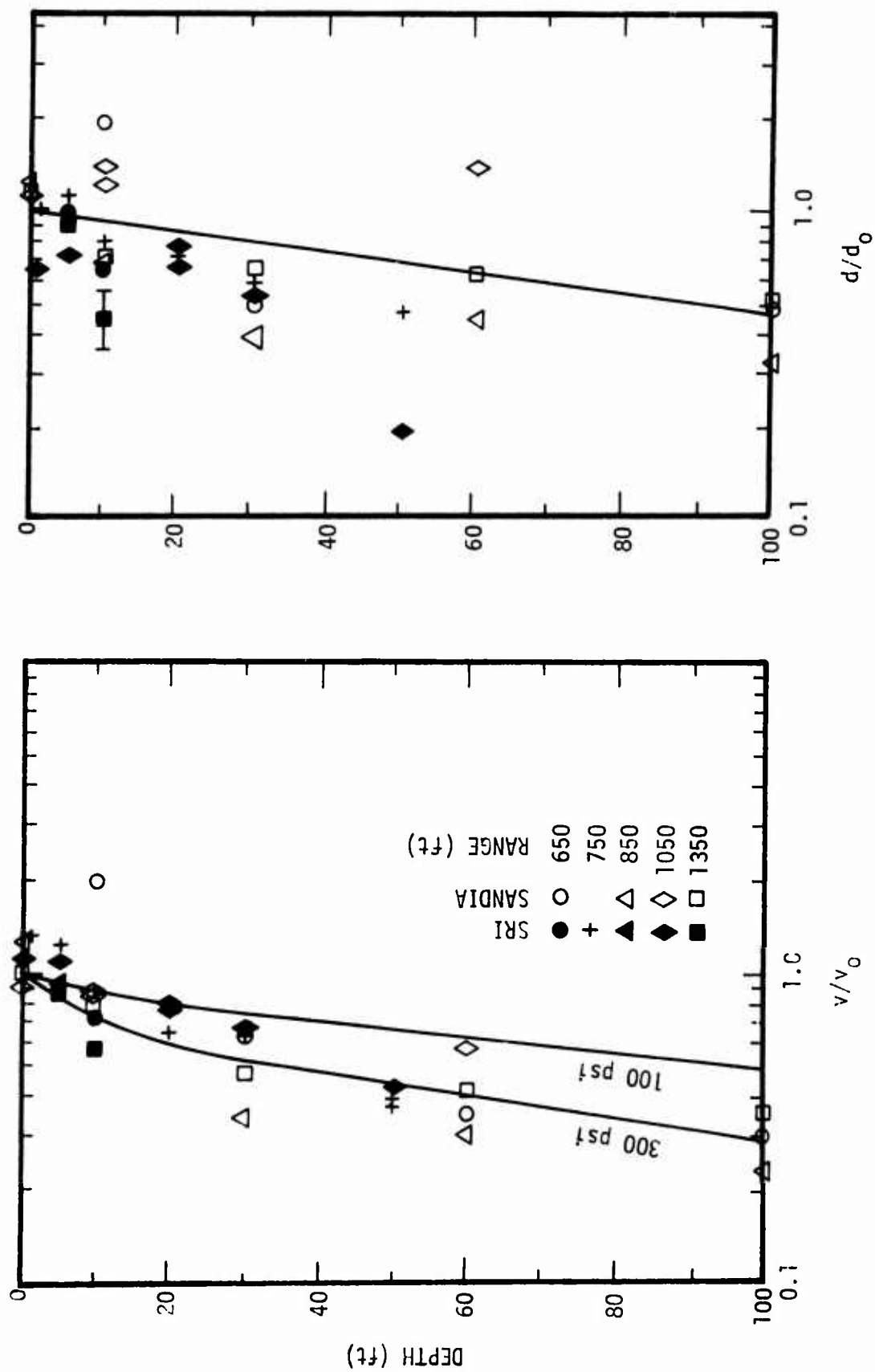


Figure 31. Comparison of Calculated Attenuation Rates with Normalized Peak Vertical Motion Data from PRISCILLA

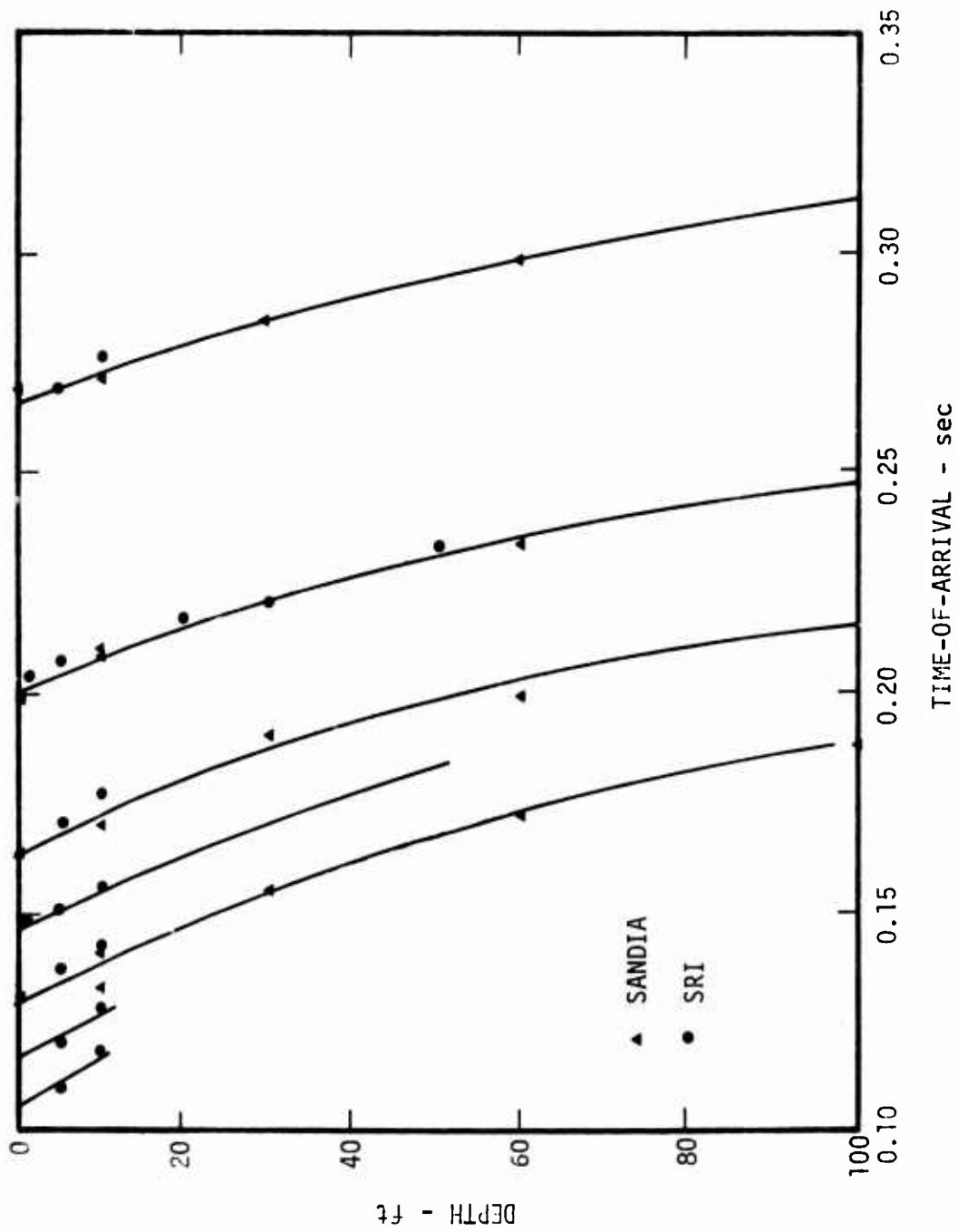


Figure 32. Vertical Motion Time-of-Arrival Data

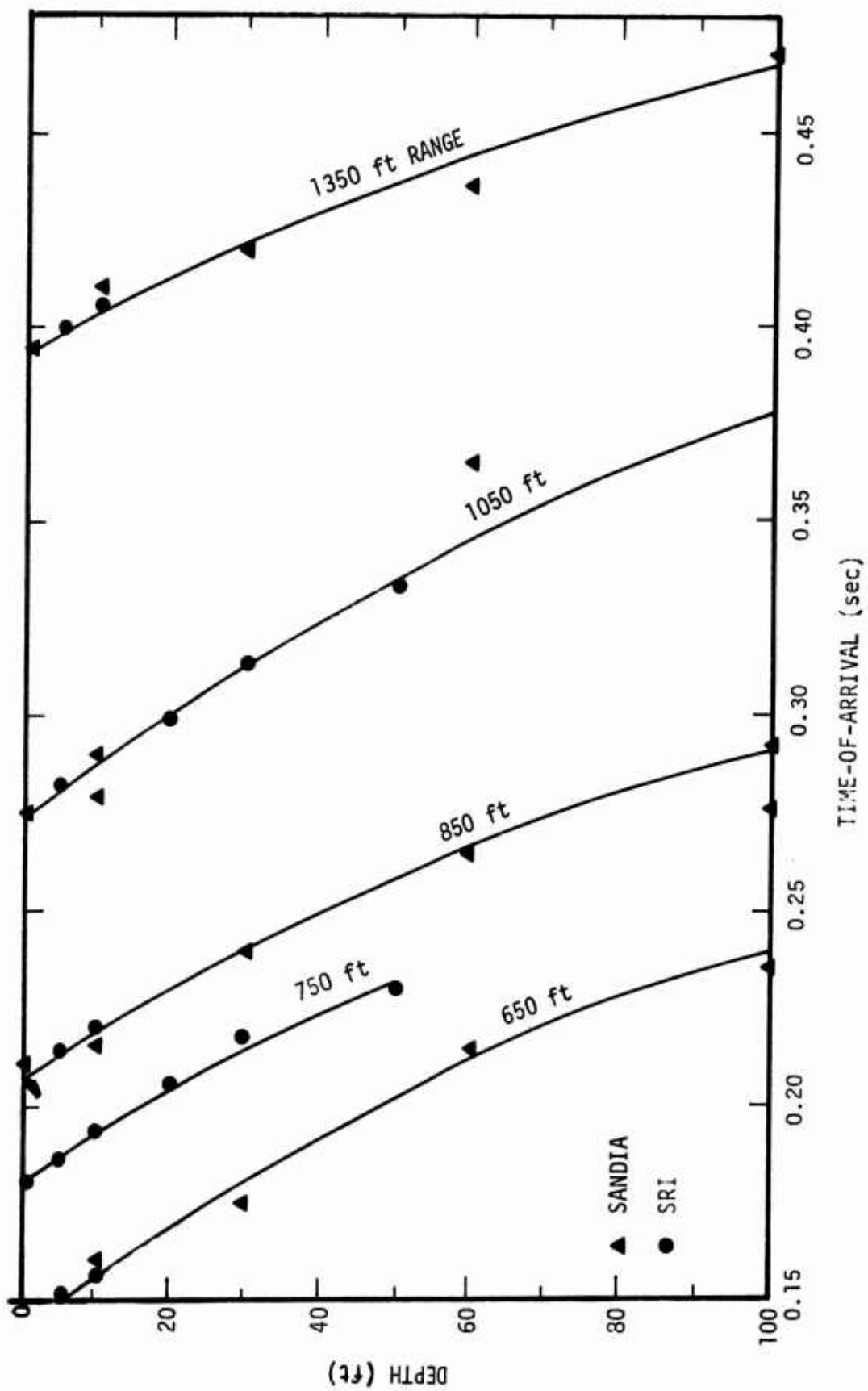


Figure 33. Peak Vertical Particle Velocity Time-of-Arrival

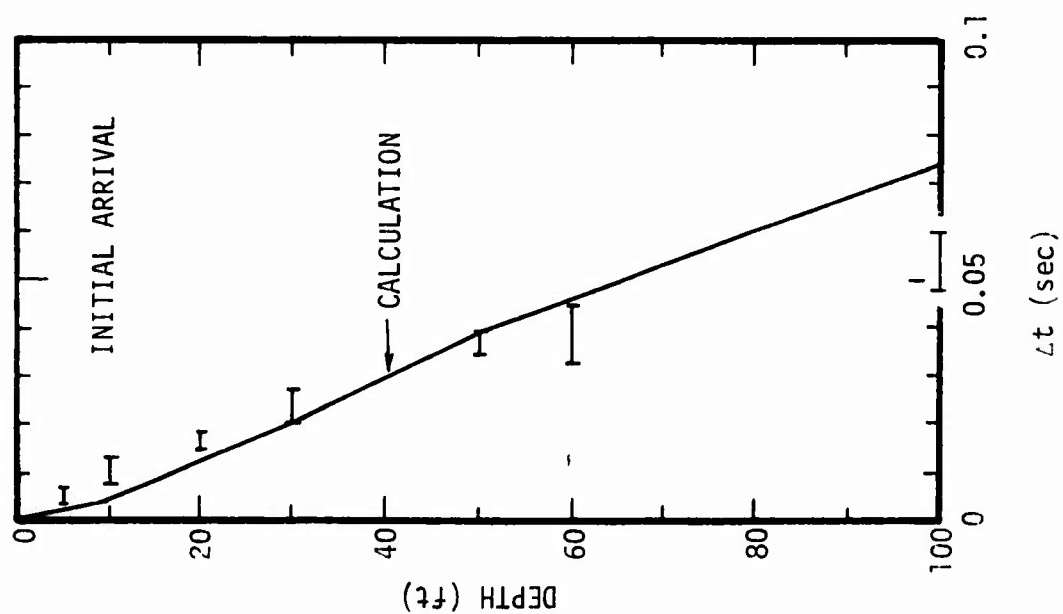
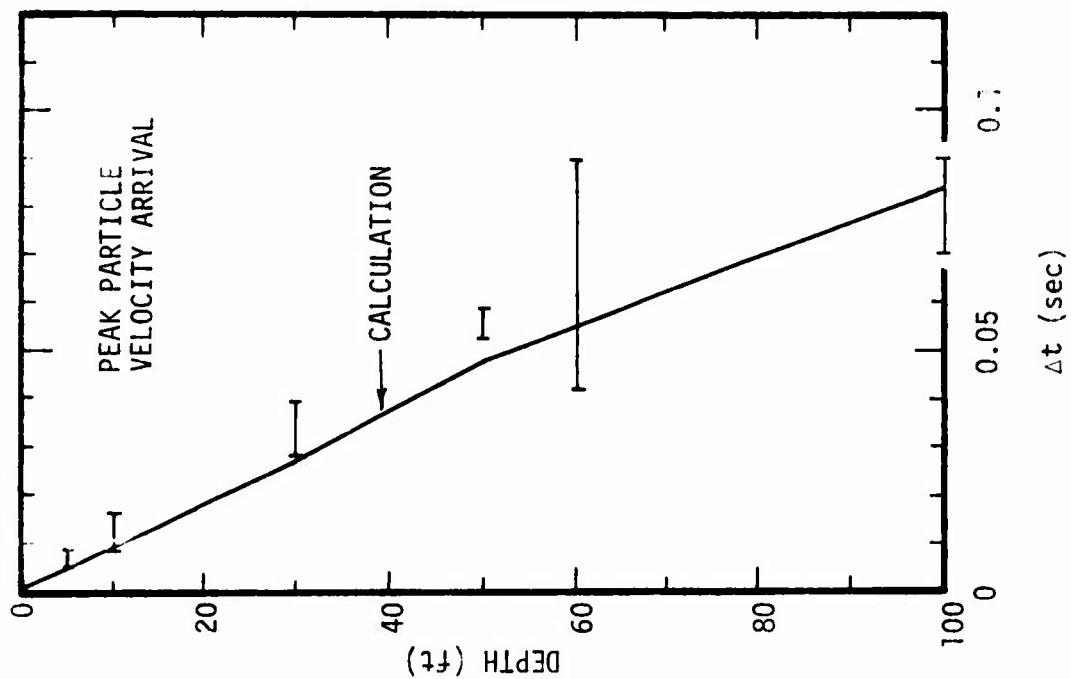


Figure 34. Comparison of Calculated and Measured Arrival Times for the PRISCILLA Event

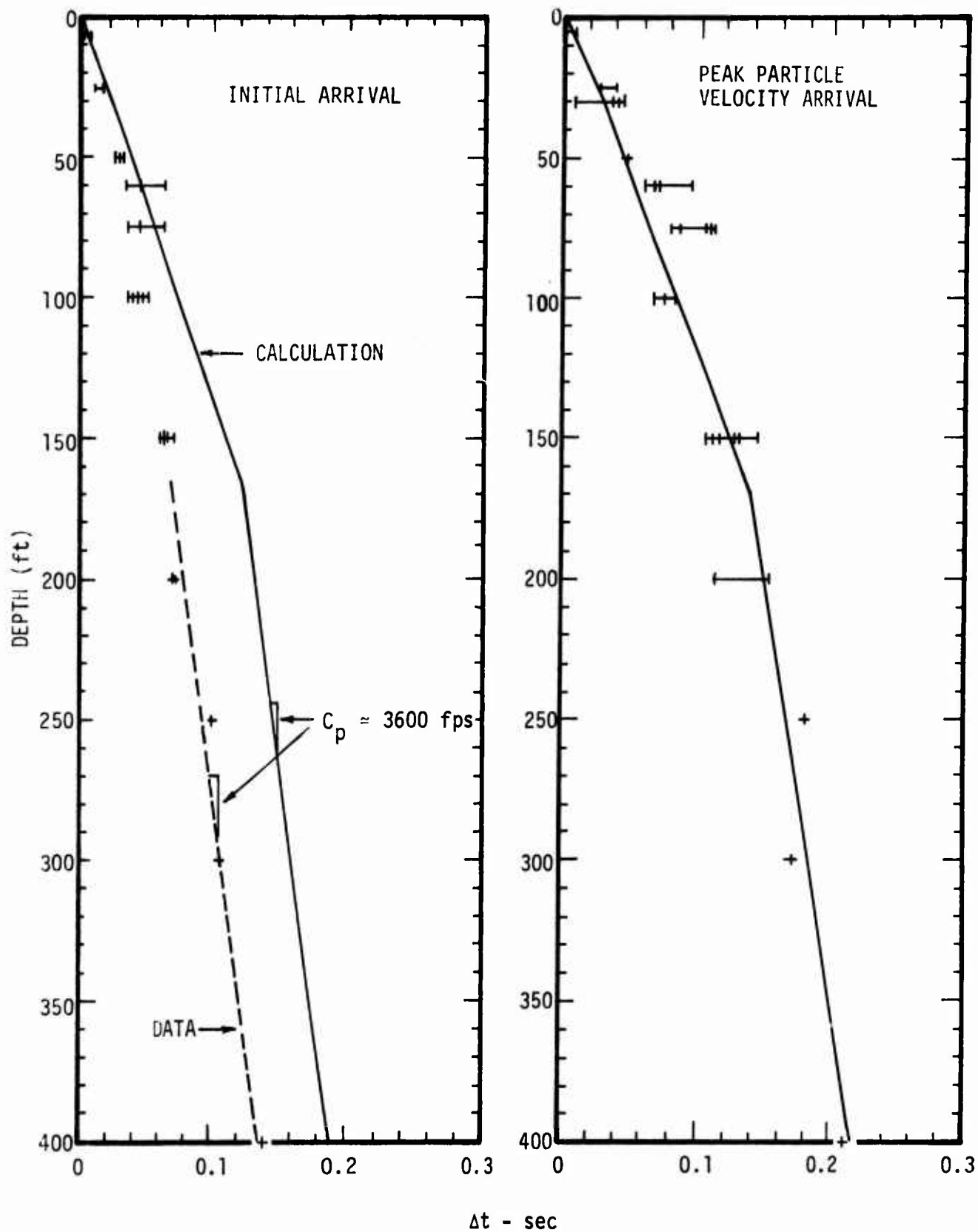


Figure 35. Comparison of Calculated and Measured Arrival Times for the SMALL BOY Event

tions and experimental data from other than surface bursts, we calculated the ground motions directly for the 650 ft and 1,050 ft ranges on PRISCILLA, utilizing fits to the measured overpressure as shown in Figure 36. Figures 37 and 38 compare calculated particle velocity time histories with measured particle velocity time-histories. The calculated particle velocity waveforms are qualitatively similar to those measured, but some quantitative discrepancies exist. As indicated previously, the calculations underestimate the near-surface peak particle velocity data. Perhaps of greater importance, the calculated positive phase durations are consistently longer than those reported by SRI (and sometimes significantly shorter than those reported by Sandia). Even so, the calculated and measured peak displacements in Figure 39 differ by at most a factor of 2, i.e., less than discrepancies between some of the SRI and Sandia data.

Figure 40 compares relative displacement data with calculated results for the 650 and 1,050 ft ranges (assuming the measured overpressure as a boundary condition). The calculated results underestimate the data at shallow depths suggesting that the surface layer may be more compressible than we assumed. On the other hand, the measured relative displacements between the surface and 50 ft depth and between the surface and 200 ft depth differ by significantly less than calculated, suggesting that our model for the soils between 50 and 200 ft may be too compressible. The reasonable comparison between calculated and measured peak wave speeds in Figure 35 suggests that this discrepancy in peak relative displacements results from differences between calculated and measured late-time phenomena rather than phenomena associated with the arrival of the particle velocity peak.

4. Peak Overpressure Uncertainties

As indicated by Eqs. 1 and 4, surface peak particle velocities and displacements are proportional to ΔP and $\Delta P^{0.78}$ respectively. Therefore, discrepancies between theoretical predictions of peak pressure and PRISCILLA airblast data cause comparable discrepancies between ground motion data and

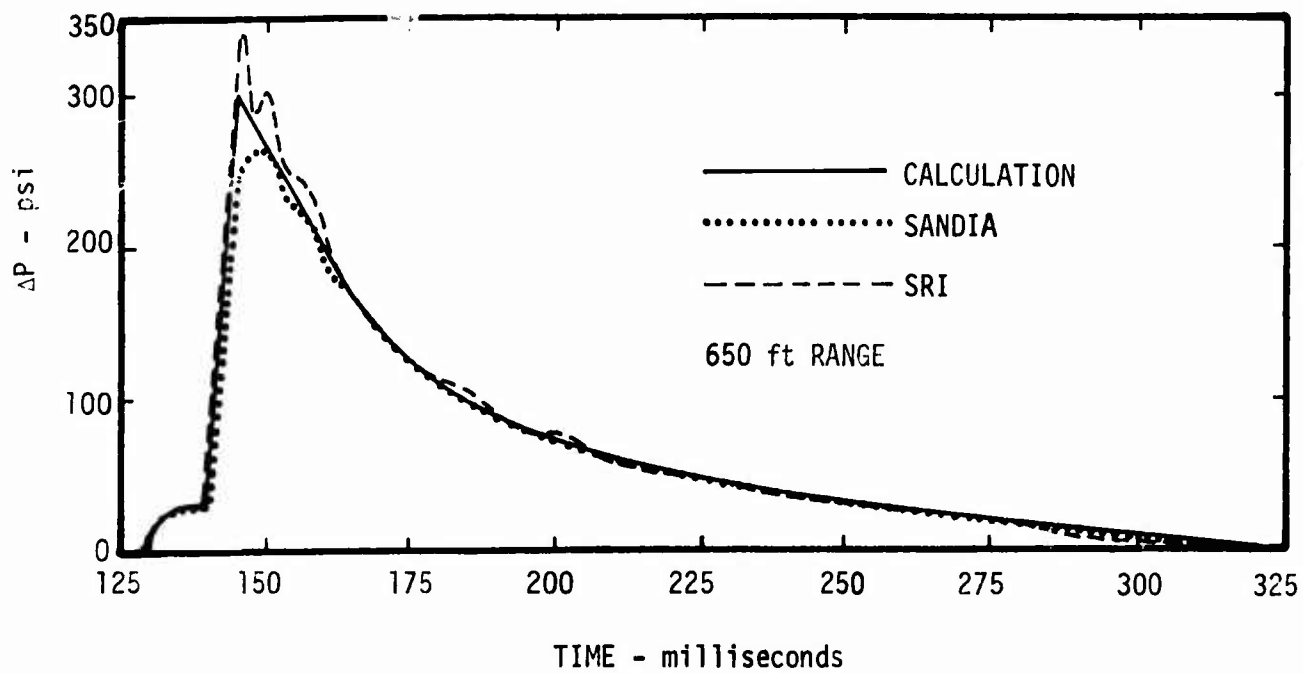
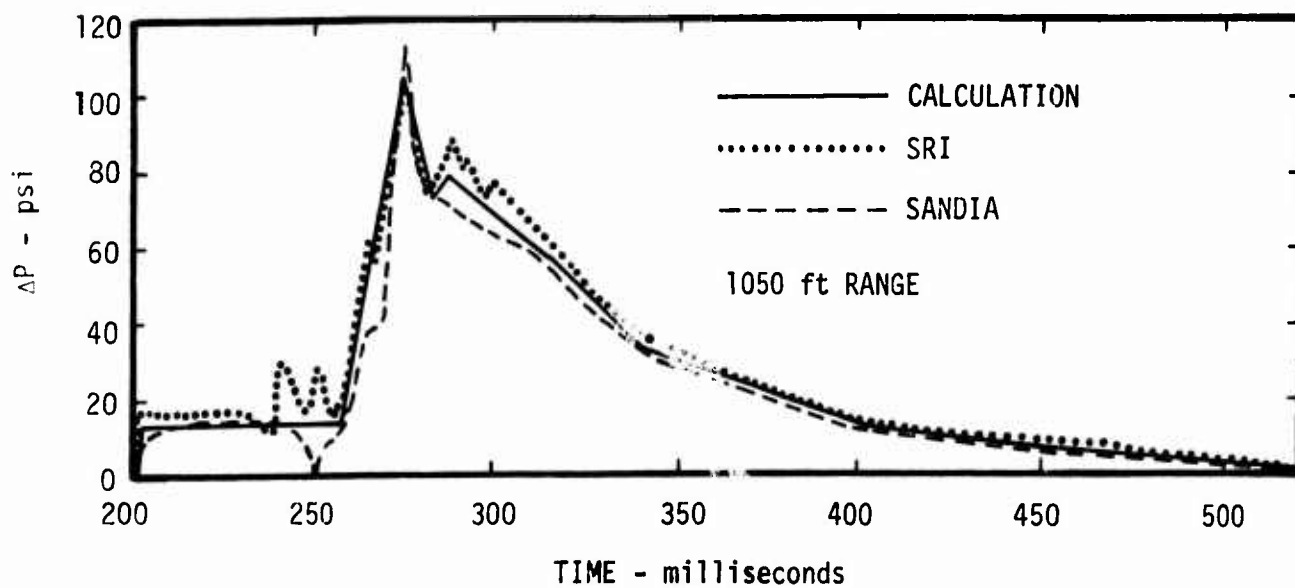


Figure 36. Comparison of Overpressure Boundary Condition with PRISCILLA Data

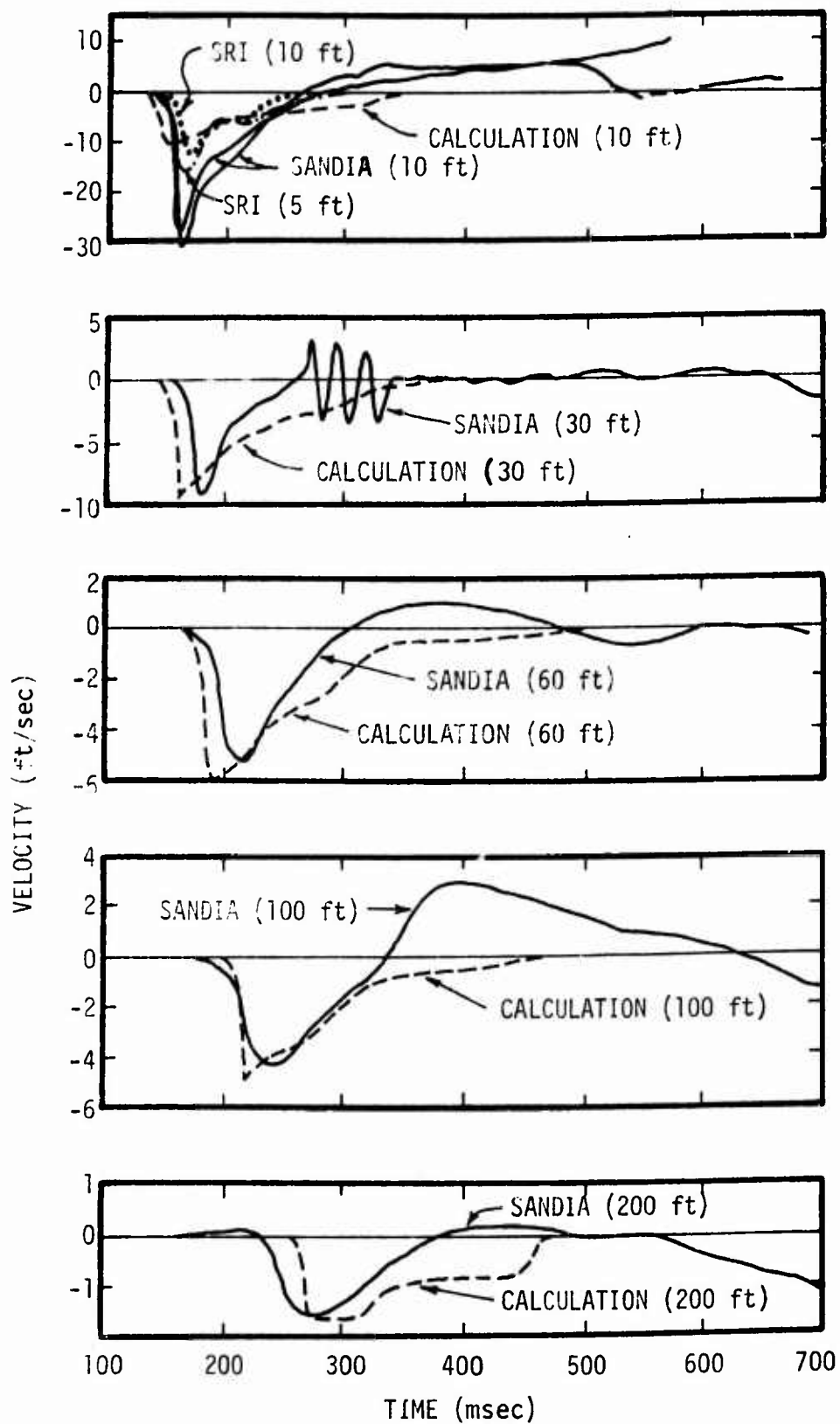


Figure 37. Comparison of Calculated and Measured Waveforms at 650 ft Range on PRISCILLA

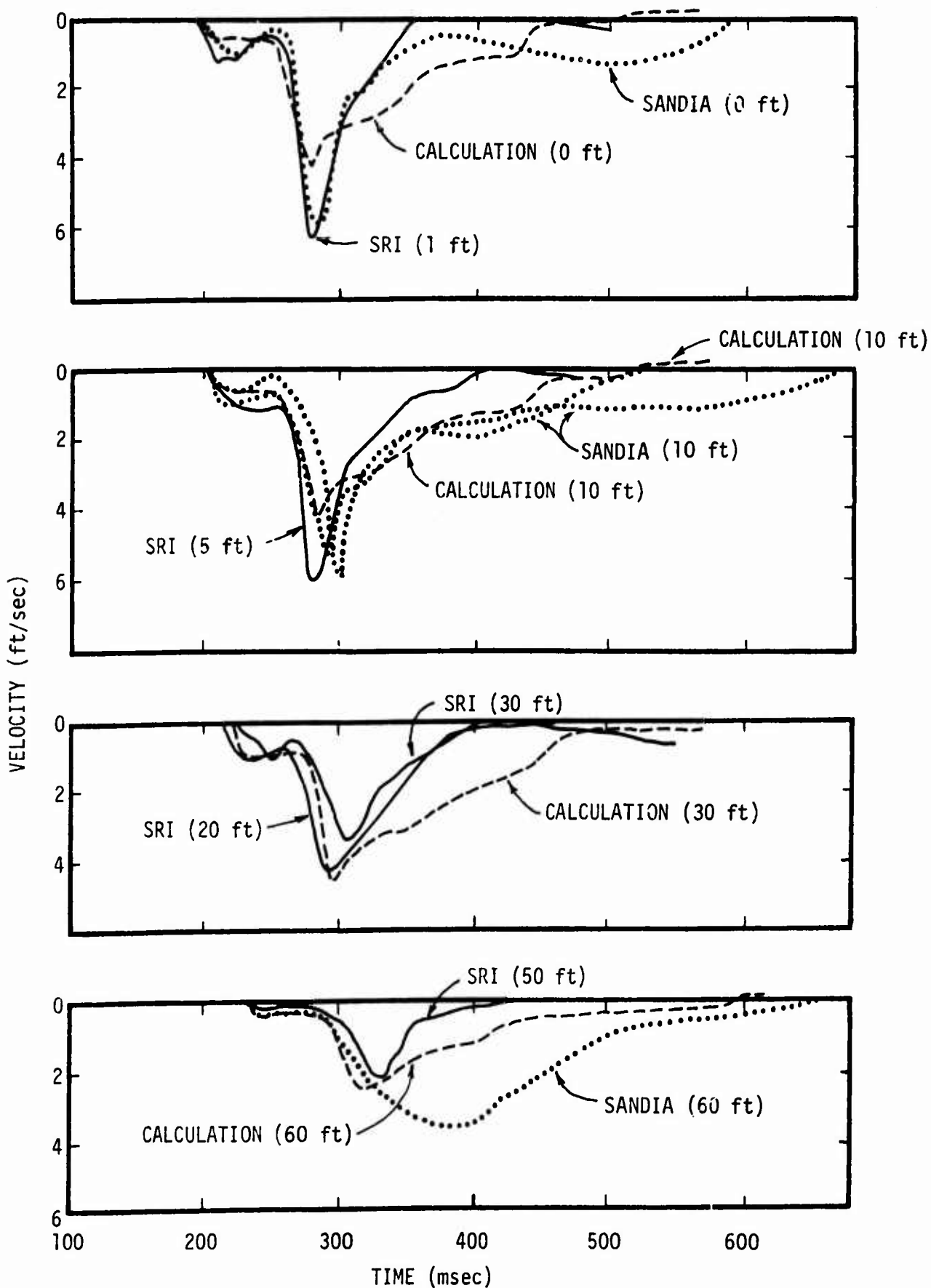


Figure 38. Comparison of Calculated and Measured Waveforms at 1050 ft Range on PRISCILLA

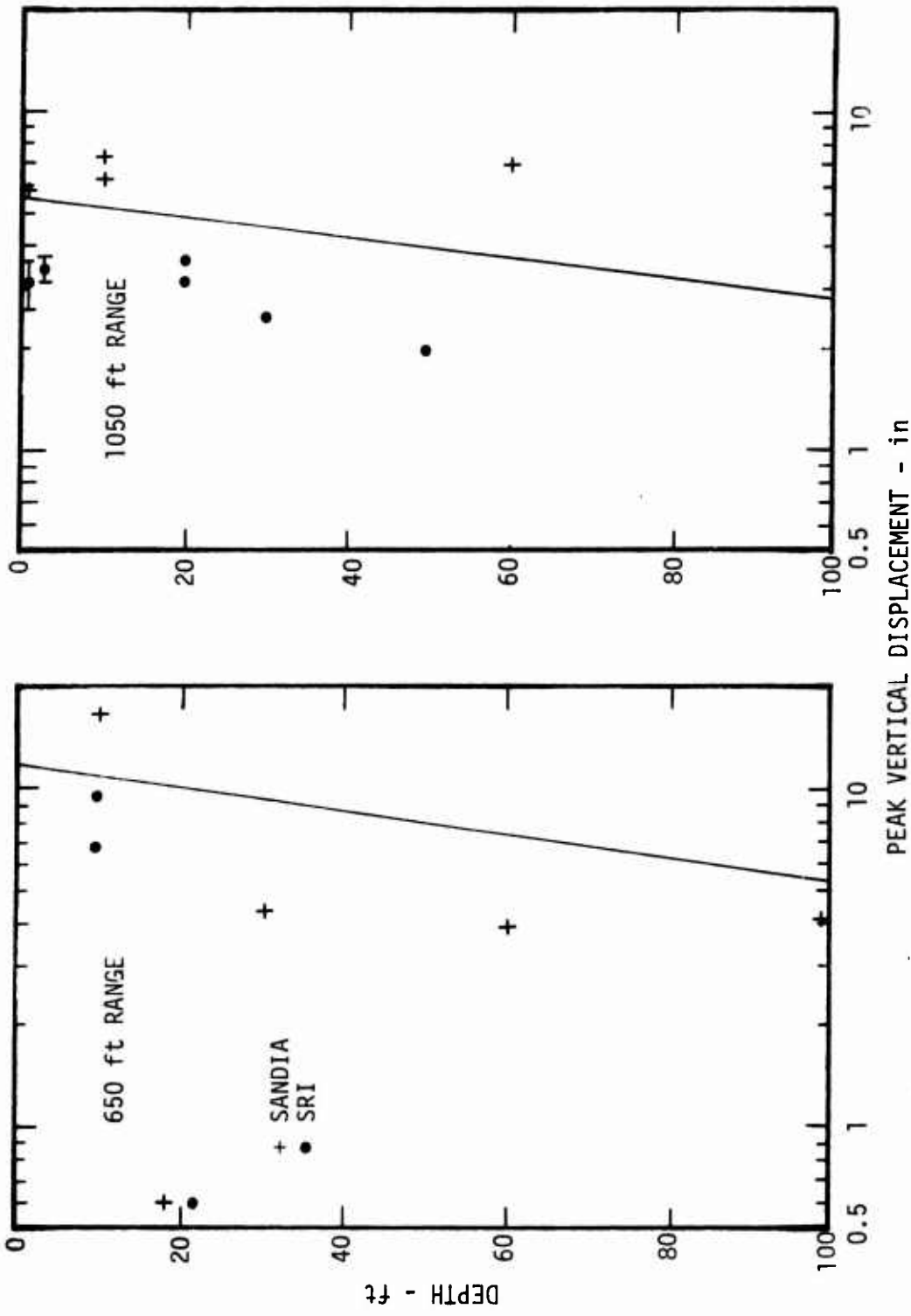


Figure 39. Comparison of Peak Vertical Displacements from PRISCILLA with Calculations Using Measured Air-blast Overpressure as a Boundary Condition

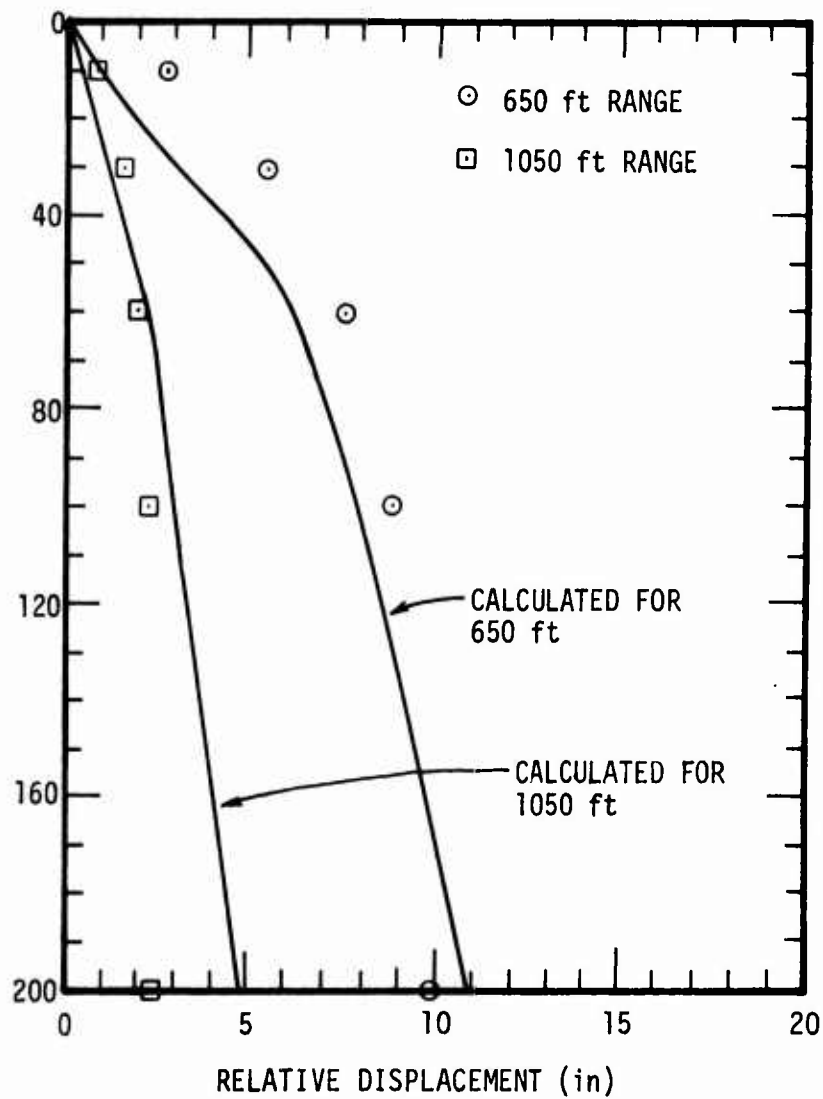


Figure 40. Comparison of Relative Displacement Data with Calculated Results Using Measured Overpressure as a Boundary Conditions

predictions using the simplified model.

The comparisons between the simplified model for Frenchman Flat and PRISCILLA data assumed that the overpressure was known at the range of interest. Thus, one must predict the overpressure as a function of range to apply the simplified prediction model in predicting ground motions at a given range from a given yield explosion. Hence, an evaluation of our overall predictive capabilities requires an assessment of the accuracy of theoretical predictions of both airblast and ground motion phenomena. Figure 41 shows that Brode's predictions (Ref. 5) for the peak pressure and impulse from a 700 ft height-of-burst, 37 kilotons event overestimate the PRISCILLA data at the close-in ranges. For overpressures less than about 200 psi, the PRISCILLA data and theoretical predictions are more consistent; perhaps with the peak impulse data falling somewhat above the theory.

Figure 42 shows that near-surface ground motions are consistently less than predicted on the basis of Brode's height-of-burst theoretical predictions of the PRISCILLA airblast. In other words, first principle calculations (starting with only the yield, height-of-burst, and our estimates of the soil properties for Frenchman Flat) would overestimate surface peak particle velocities and displacements measured at a given range on PRISCILLA. The largest portion of this discrepancy appears to result from the difference between predicted and measured blast overpressure; rather than discrepancies between predicted and measured ground motions once the blast overpressure boundary condition is known. One should not generalize this observation from the comparison with PRISCILLA to other cases because the source of the air blast discrepancy has not been evaluated; and therefore its reproducibility is not known.

5. Summary

Comparisons of experimental data from nuclear explosions in Frenchman Flat with theoretical estimates based on the calculations presented in

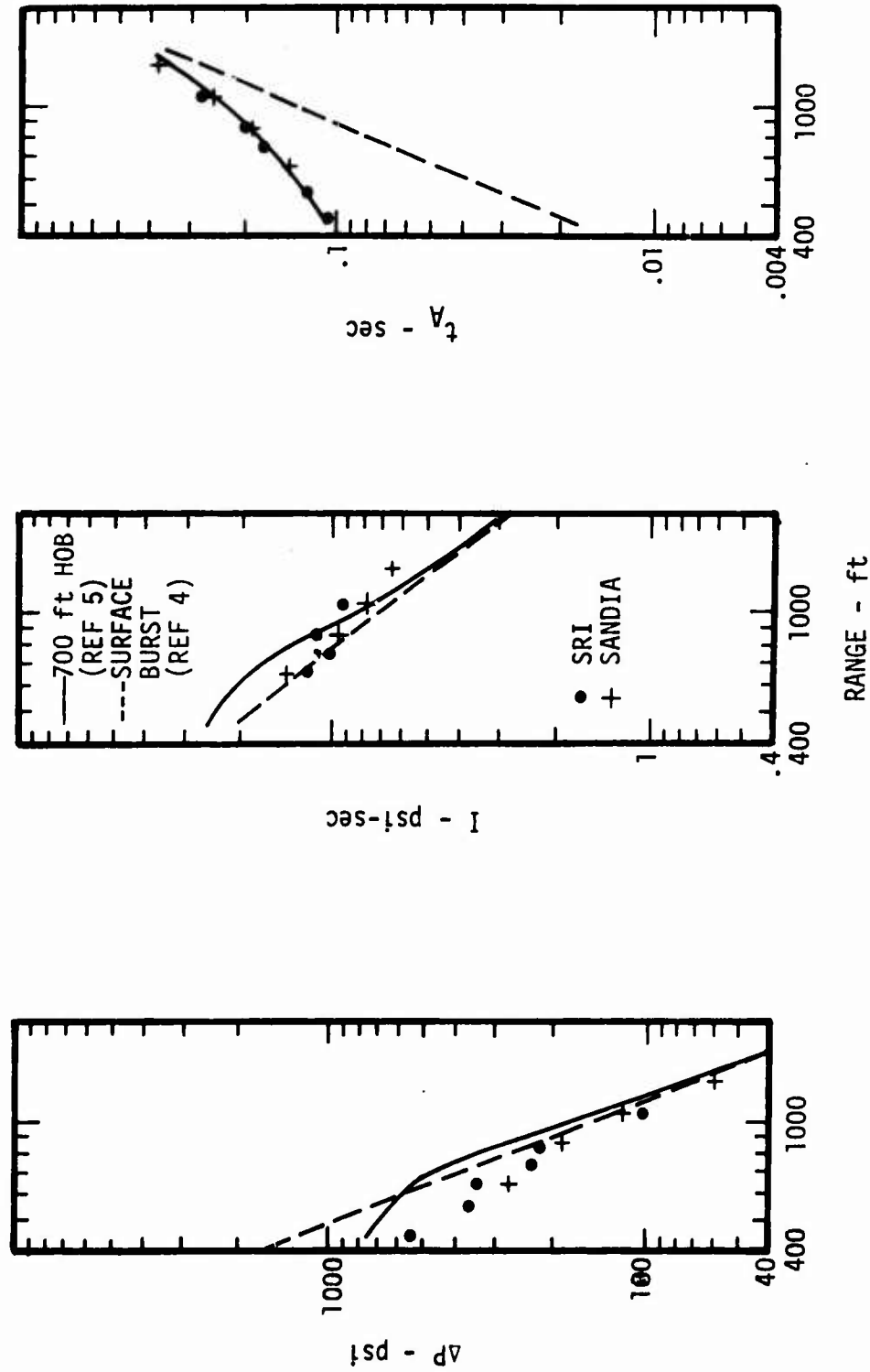


Figure 41. Comparison of Theoretical Airblast Results for $W = 37$ KT and PRISCILLA Data

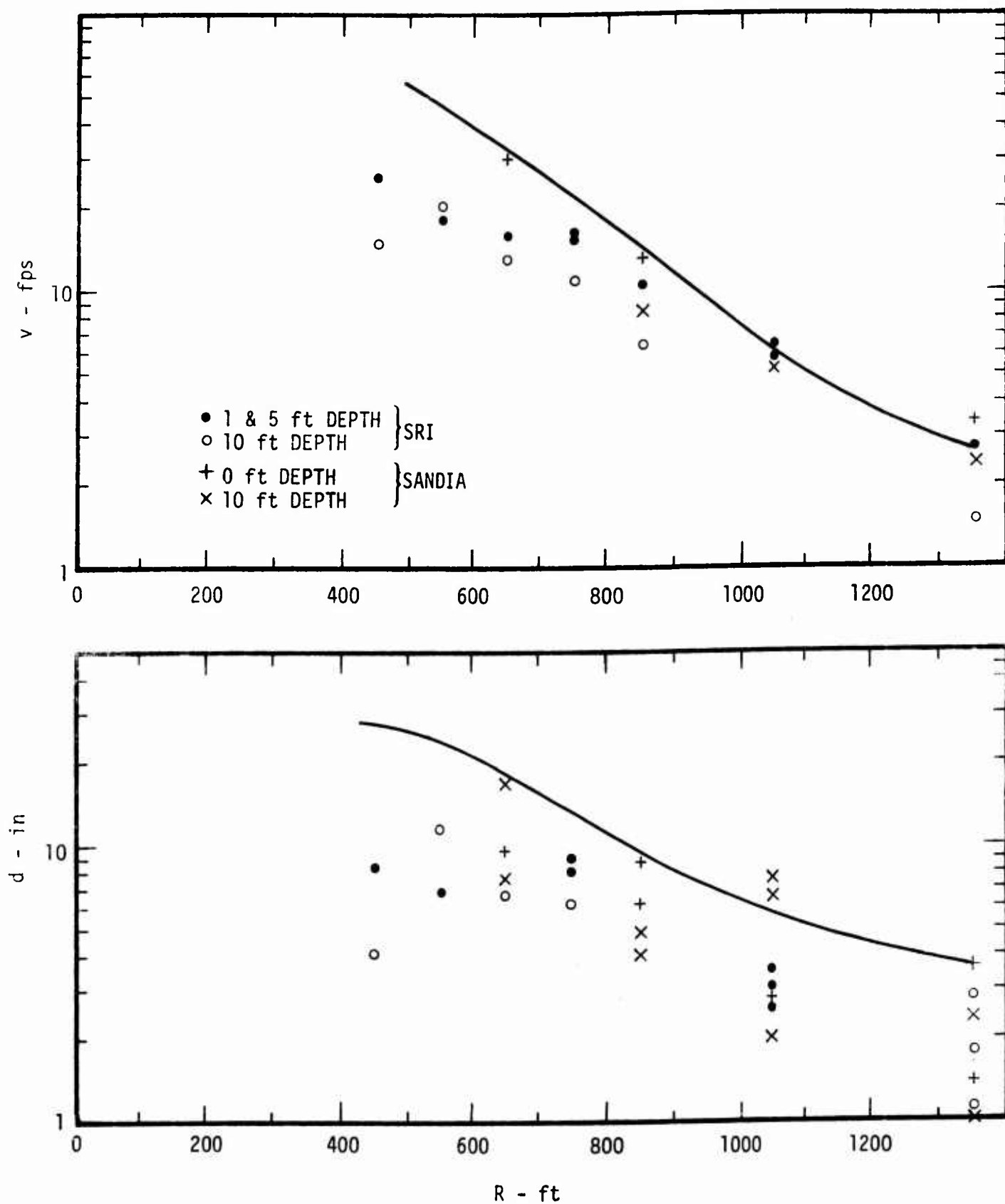


Figure 42. Comparison of PRISCILLA Data with Ground Motions Predicted Using Brode's Height-of-Burst Overpressure Model

Section III show good consistency in both qualitative and quantitative aspects. In general, there was much less than a factor of 2 discrepancy between calculated peak particle velocity or displacement and best estimates of the ground motions for a given overpressure derived from the experimental data. In fact, it is interesting that, in estimating ground motions from PRISCILLA as a function of range, a larger discrepancy resulted from uncertainties in predicting the overpressure as a function of range than from ground motion calculations once the overpressure was known.

The comparisons between calculations and data indicate some shortcomings in the theoretical material properties model, e.g., the surface layer is perhaps too stiff, and some layers deeper than about 50 ft are possibly too compressible. Calculated initial arrival times are consistent with the assumed seismic velocities.

Our premise that the assumed theoretical stress-strain curve for the surface layer was too stiff is based on observations that:

- (a) The calculated impedance of the surface soils was about 20 percent higher than indicated by the test data from all nuclear experiments in Frenchman Flat;
- (b) Calculated arrival times were early in the upper 10 ft, and
- (c) The calculated relative displacements at shallow depths were lower than measured.

The premise that the theoretical model may have underestimated the in-situ modulus of some of the deeper soils is based on the observations that:

- (a) Calculations underestimated the initial arrival times at depths greater than about 50-75 ft (although peak wave arrival times were reasonably modeled throughout); and
- (b) The rate of increase in calculated relative displacements

between the surface and 100 or 200 ft exceeded that observed on PRISCILLA.

On the other hand, some discrepancies between calculated and measured ground motions may result from incorrect judgments made by the early investigators when correcting baseline shifts of the integrated accelerometer data. For example, Swift, et al. (Ref. 11) state:

"The criterion for specification of the time that the velocity is zero was difficult to establish. After considerable study, it was decided that, for local air-blast induced effects only, the end of the overpressure positive phase would constitute a reasonable criterion for velocity equal to zero."

In our calculations, the positive phase duration of the particle velocity is determined by the arrival of compressional waves reflected from the 170 ft interface; i.e., there is no simple causal relationship between the positive duration of the overpressure pulse and the positive phase duration of the particle velocity. Thus, we recommend that the raw data from PRISCILLA be re-examined and reinterpreted in light of our current understanding of wave-propagation phenomena. Such a re-examination may lengthen the positive phase duration of the integrated accelerometer records and increase peak vertical displacements reported by SRI.

SECTION V
SUGGESTED MODIFICATIONS TO
THE MATERIAL PROPERTIES MODEL

Although the calculations based on the material properties model discussed in Section II agreed reasonably well with the PRISCILLA data, some improvement can be made by using the ground motion data from nuclear tests to iterate toward an "in-situ" model of the vertical uniaxial stress-strain curves for Frenchman Flat near-surface soils. The major suggested alterations are:

- a) a 30 to 50 percent reduction of the secant modulus (to stresses greater than several tens of psi) of surface layer to improve the comparison between calculated and measured near-surface peak particle velocities (figures 23 and 30);
- b) an increased initial modulus of the soils shallower than 170 ft to better reproduce the initial arrival data (figure 35).

As noted previously, some comparisons between calculated and measured ground motions suggested that the in-situ secant modulus of some soils below about 50 ft may be slightly greater than predicted by the theoretical model based on the laboratory properties. However, the calculated peak particle velocity arrival times were reasonably consistent with the data (figure 35) and the discrepancies between calculated and measured relative displacements (figure 40) may be reduced by the alterations a) and b) suggested above. Thus, no modification to the secant moduli of the deeper soils is suggested until the effects of the above alterations are evaluated.

Based upon our examination of the seismic data (in the Appendix) and the initial arrival time data from PRISCILLA and SMALL BOY, we suggest the initial moduli shown in figure 43. Also indicated in figure 43 (compare to figure 3) is a 50 percent reduction in the secant modulus (to 300 psi) of the surface layer. The alterations to the initial loading portion stress-strain curves (figure 4) are then indicated in figure 44. With the

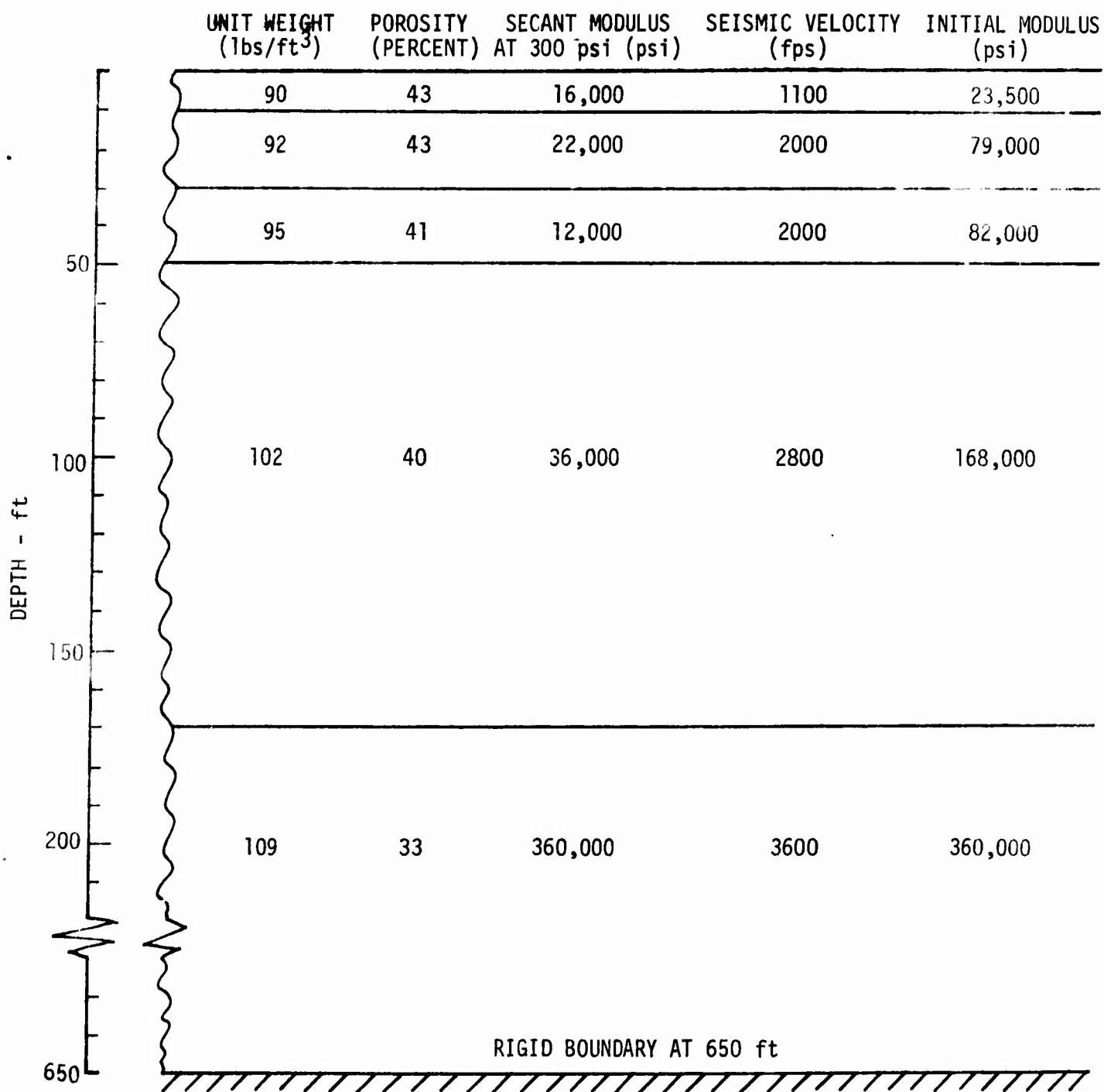


Figure 43. Suggested Improved Model for Frenchman Flat

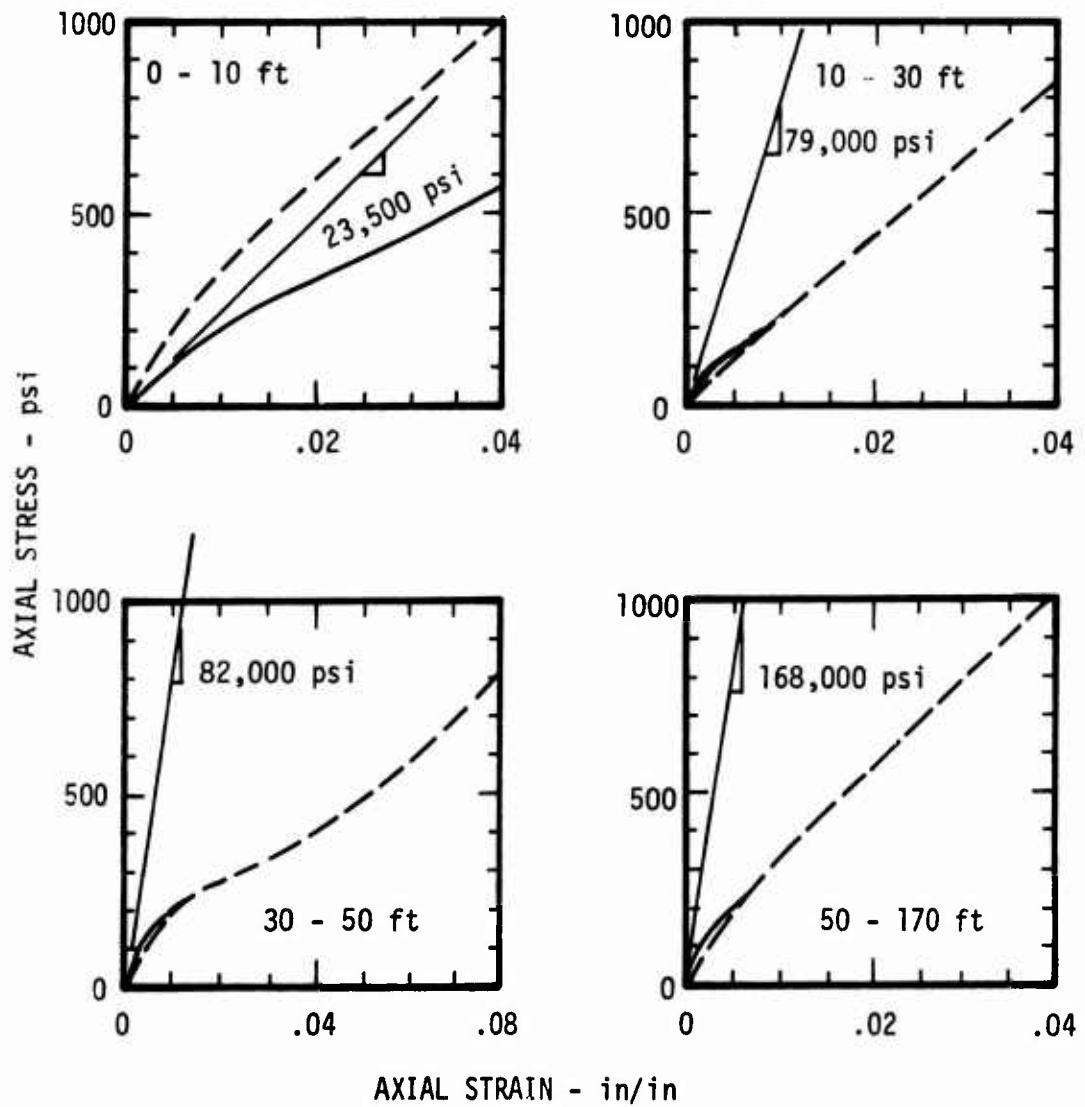


Figure 44. Suggested Alterations to the Low Stress Portion of the Laboratory Uniaxial Stress-Strain Curves (Dashed Line = Lab Data, Solid Line - Alteration)

exception of the surface layer, the modifications to the laboratory data appear to be minor on the scale of several thousand psi (which was the scale of the laboratory data). However, the impact of the changes could significantly alter the predictions of ground motions resulting from several hundred psi peak overpressures--generally in the direction of reducing peak displacements.

In this regard, it should be emphasized that the initial slopes of the altered stress-strain curves are based on arrival time data and are fairly objective. However, the manner in which the modulus of the assumed stress-strain curve departs from the initial modulus was somewhat arbitrarily chosen to force the suggested loading stress-strain curves into the laboratory data at a few hundred psi.

SECTION VI

DISCUSSION AND CONCLUSIONS

Our purpose in the research reported here was to obtain the best possible theoretical model (based on existing soil sampling and laboratory test information) for vertical airblast-induced ground motions in Frenchman Flat, and to compare predictions from that model with the available nuclear test data. Such a comparison allows an assessment of the current predictive state-of-the-art to the extent that the theoretical model is representative of the state-of-the-art. The calculational procedures were certainly representative of the state-of-the-art. However, the available dynamic material property data were limited to five data points for the upper 70 ft at a single location within Frenchman Flat (not in the immediate vicinity of the nuclear experiments); whereas state-of-the-art soil sampling and laboratory testing procedures would require a considerably larger data base at any given depth. Based on our current understanding of the pertinent wave propagation phenomena, the soils at greater depths also would be sampled and tested in developing a theoretical model.

In any case, the dynamic uniaxial strain test data from these five samples, in conjunction with relatively straightforward judgments derived from static test information and seismic surveys, were the basis for a theoretical model that was taken as a first order model of Frenchman Flat in the vicinity of the above-surface nuclear experiments. In view of the sparsity of the dynamic soil property data and the extrapolation from a single location to model Frenchman Flat, it is perhaps surprising that the comparison between calculated and measured ground motions was as good as indicated in Section IV. In fact, in this specific exercise, the discrepancies between predicted and measured airblast boundary conditions as a function of range (for PRISCILLA) were greater than the discrepancies between calculated and measured ground motion induced by the measured over-pressure boundary condition.

Based upon our analysis of the test data from Frenchman Flat, we conclude that the measured dynamic stress-strain curve taken to model the surface layer (between 0 and 10 ft depth) was too stiff. A 30 to 50 percent reduction in modulus (at stress levels of a few hundred psi) would considerably reduce the discrepancy between the calculated and measured near-surface particle velocities without significantly altering peak displacements. We also believe that our theoretical model for Frenchman Flat would be more representative of the in-situ properties if we assumed somewhat stiffer initial moduli (for stresses less than about 100 psi) for the soils between about 50 and 170 ft. This alteration would reduce somewhat the positive phase duration of the near-surface particle velocities, thereby providing greater consistency with the reported SRI data for PRISCILLA. Even transitional properties that gradually increase with depth below 50 ft would lead to shorter durations and smaller displacements near the earth's surface (Ref. 14). However, we point out that the SRI corrections to the raw accelerometer data were based upon an incorrect assumption; so that it would be fortuitous if their late time data are accurate as reported.

These altered stress-strain curves, based on analysis of nuclear test data are far more indicative of the in-situ response of Frenchman Flat than any of the sparse data available for our formulation of the theoretical model in Section II. In fact, it might be argued that the nuclear test data provide more information on the dynamic in-situ properties (in vertical compression) of Frenchman Flat than is available for any other geologic area of comparable size, i.e., geographic areas on the order of a square mile.

Although the previous section's modifications to the material properties are clearly improvements, sight should not be lost of the fact that reasonable consistency between the calculated and measured vertical ground motions was achieved with the initial model described in Section II. This result provides some degree of confidence that reasonable estimates

of the vertical airblast-induced ground motions can be made on the basis of limited laboratory dynamic soil test information and seismic data--at least for such dry, porous soils as exist in Frenchman Flat. In all cases, the discrepancies between a best fit to the experimental data and the calculated peak vertical particle velocities and displacements were no greater than a factor of 2, even including the effect of the largest single discrepancy that was discovered--that between predicted and measured blast overpressure conditions.

To reduce this discrepancy the airblast boundary condition must better account for the real surface effects that lead to precursors. A better theoretical treatment of the thermal and mechanical surface interaction is probably required to accomplish this goal. A simple extension of current state-of-the-art 2D blast calculations is unlikely to substantially improve the theoretical predictions.

SECTION VII

RECOMMENDATIONS

The comparison between calculated and measured vertical motions from nuclear explosions in Frenchman Flat provides new insight into the ground motion environment produced by several nuclear tests conducted during the late 1950's and the early 1960's. This improved understanding indicates that certain subjective decisions made during data reduction activities following the nuclear tests were incorrect. Thus, we recommend that the raw data from those experiments be re-examined and that a new data report be issued in the light of our improved understanding. A recommended course of action includes:

- (a) obtaining the raw data (accelerometer, velocity gages, and strong motion seismic data) from all nuclear experiments conducted in Frenchman Flat and subjecting them to modern data reduction procedures,

- (b) analysis of the raw data by a working group consisting of some members who are familiar with theoretical studies such as presented in this report, and other members who are well acquainted with instrumentation used in the nuclear experiments.

It is also recommended that theoretical studies be considered to complement the data analysis. Studies of two-dimensional motions produced by nuclear explosions in Frenchman Flat would be a natural extension to the work presented here. In particular, calculations of PRISCILLA and SMALL BOY may be beneficial. Those performing such theoretical studies should carefully consider previous one-dimensional studies such as presented here and in References 15 and 16 and previous two-dimensional calculations of ground motions that purport to model cratering and ground shock phenomena at the Nevada Test Site (e.g., Refs. 17, 18). A material property program, including some form of in-situ testing, is recommended to support the theoretical effort. This program should attempt to determine any anisotropy that might exist and evaluate this effect on calculated late-time ground motions.

Appendix
GEOLOGY AND MATERIAL PROPERTIES FOR FRENCHMAN FLAT

Knowledge of the in-situ uniaxial stress-strain curves for the near-surface soils is required to accomplish one-dimensional calculations to accurately model strongly superseismic vertical early time ground motions (from airbursts) over Frenchman Flat. Because the primary effect of the deeper, higher impedance soils is to reflect compressional waves that cause surface displacements to peak, knowledge of the location of interfaces that produce such reflections may be more important than detailed stress-strain characteristics of the underlying media. In any case, the following sections describe the basic data (existing when this study was initiated) that were considered in estimating densities and uniaxial stress-strain curves used in the calculations reported in the body of this report.

1. Site Geology

Frenchman Flat is at an elevation of about 3080 feet and is surrounded by mountains that rise to 4500 - 6000 feet about sea level. Materials eroded from high areas have been deposited in the low regions forming a large alluvial valley. Frenchman Flat is located at the lowest point in this valley where a small shallow lake exists for short periods after unusually large rains. Thus, fine particles deposited over a long period of time by this stagnant water comprise the major constituents of the near surface playa soil in Frenchman Flat. Cementation in the overburden soils make seismic reversals common and interpretation of deep refraction surveys difficult.

Because the geology of the Nevada Test Site is very complex (consisting of faults, unconformities, intensive and extrusive rock masses) extrapolation of geologic formations are speculative at best (Ref. 19). The best estimate of the geologic section through Frenchman Flat is shown in Figure (Ref. 20), and the location of this section is shown with the area geology

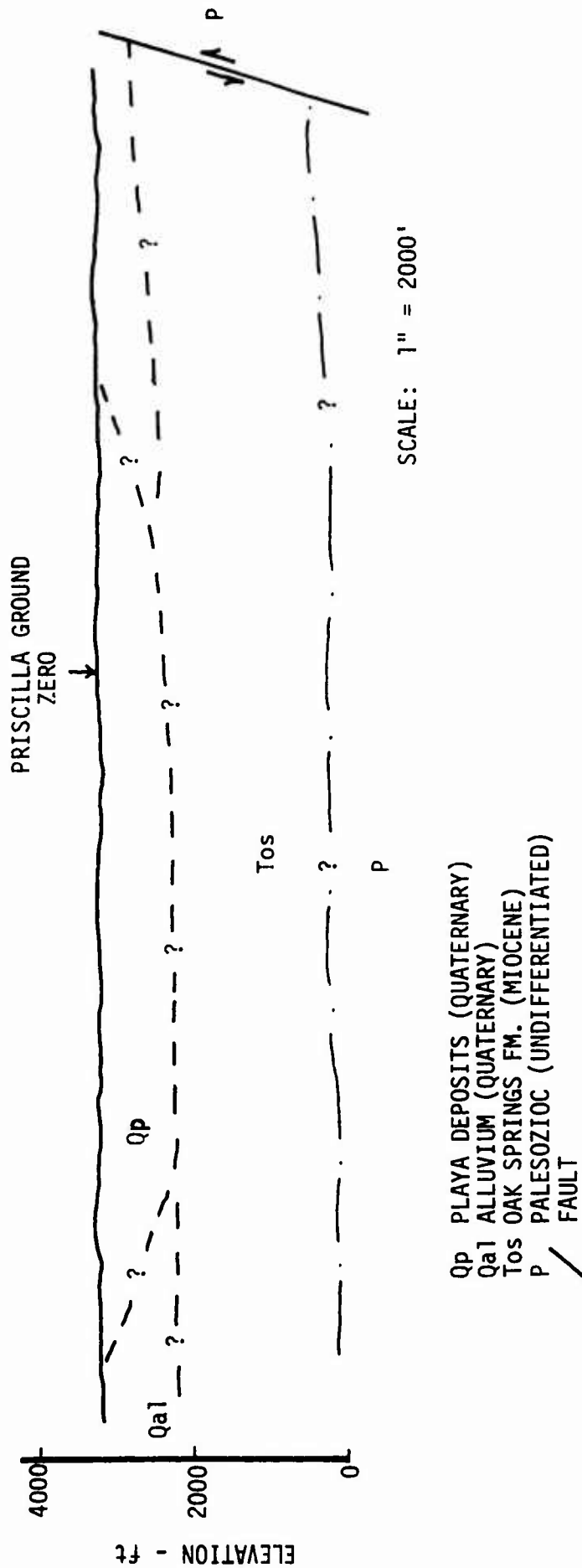


Figure 45. Geologic Cross Section

in Figure 46. Question marks indicate regions of major uncertainty in the profile.

2. Seismology

Previous seismic surveys of Frenchman Flat were conducted by Geo-Recon, Inc. (Ref. 20), the U. S. Army Engineer Waterways Experiment Station (Ref. 21), and U. S. Geological Survey (Ref. 22). Geo-Recon conducted both refraction and uphole tests; WES conducted near surface refraction and vibration tests; the USGS conducted a refraction survey. The reported compressional and shear wave velocities are shown in Figure 47. These independent investigations are reasonably consistent, but there are discrepancies in the estimated depths to some layers. Perhaps the most important inconsistency is the velocity reversal at about 36 feet suggested by Geo-Recon, Inc., but not by WES or the USGS. Such seismic reversals (which are not uncommon in such geology) cannot be detected with refraction surveys alone and can lead to erroneous interpretation of refraction data from deeper layers. The WES time-distance plots suggest an abnormality at about 30 ft depth which could be indicative of a velocity reversal, and no alternative explanation for the phenomena was given in reference A-3. The seismic reversal indicated by the Geo-Recon uphole survey is consistent with material property test results to be discussed in the next section.

The deep refraction survey conducted by Geo-Recon suggested that the compressional wave velocity increased from 2800 fps to 3600 fps at a depth between 160 and 190 feet. A second increase from about 3600 fps to 10,300 fps was estimated to occur at a depth between 720 and 860 feet. This 140 foot variation in depth to the 10,300 fps medium occurs 2000 feet from the PRISCILLA ground zero.

The U. S. Geological Survey data, summarized in Table IV, provided less detail near the surface than the Geo-Recon survey. As indicated above, the velocity reversal revealed by the Geo-Recon uphole survey was not recognized. If such a low velocity layer does exist, then their near

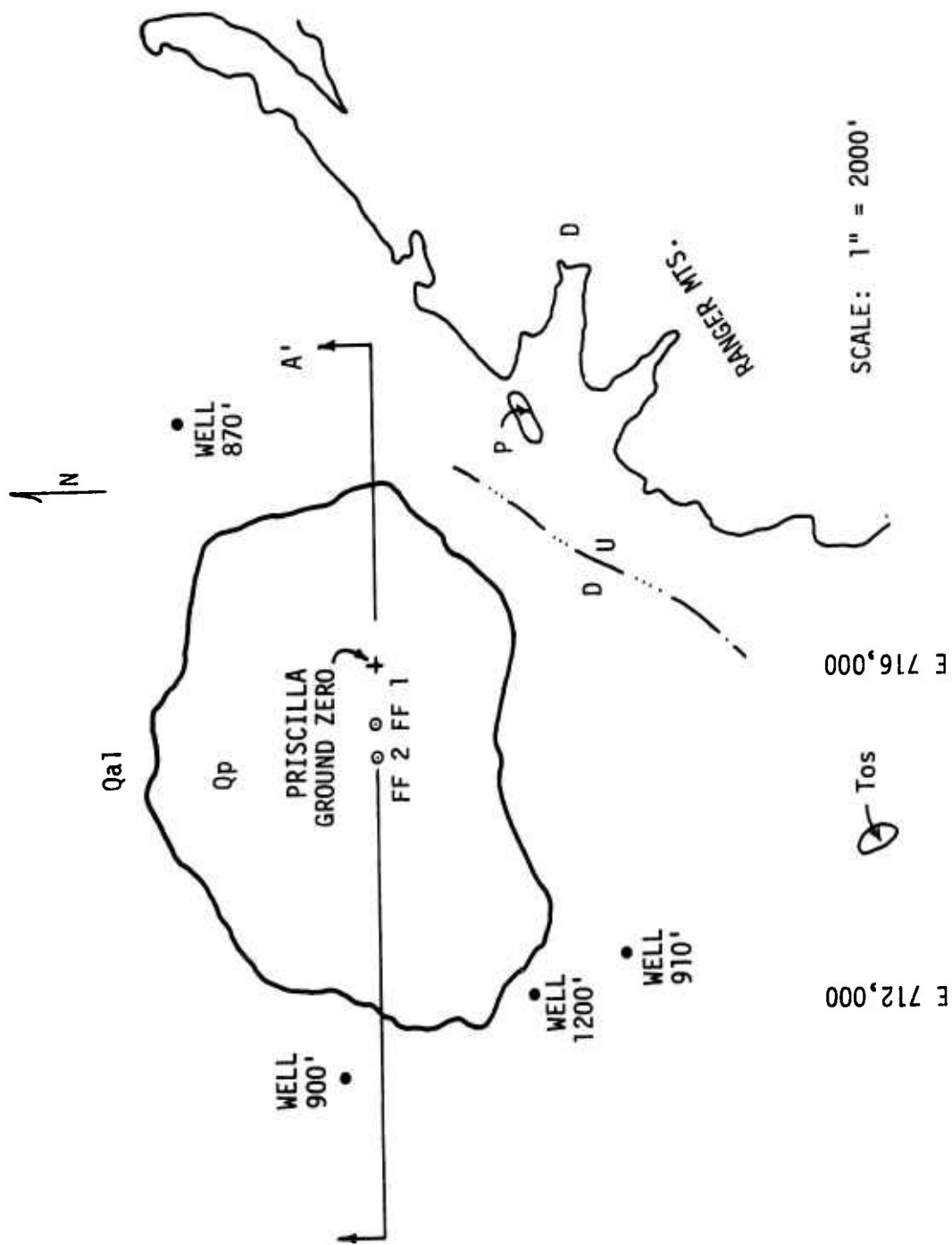


Figure 46. Aerial Geology

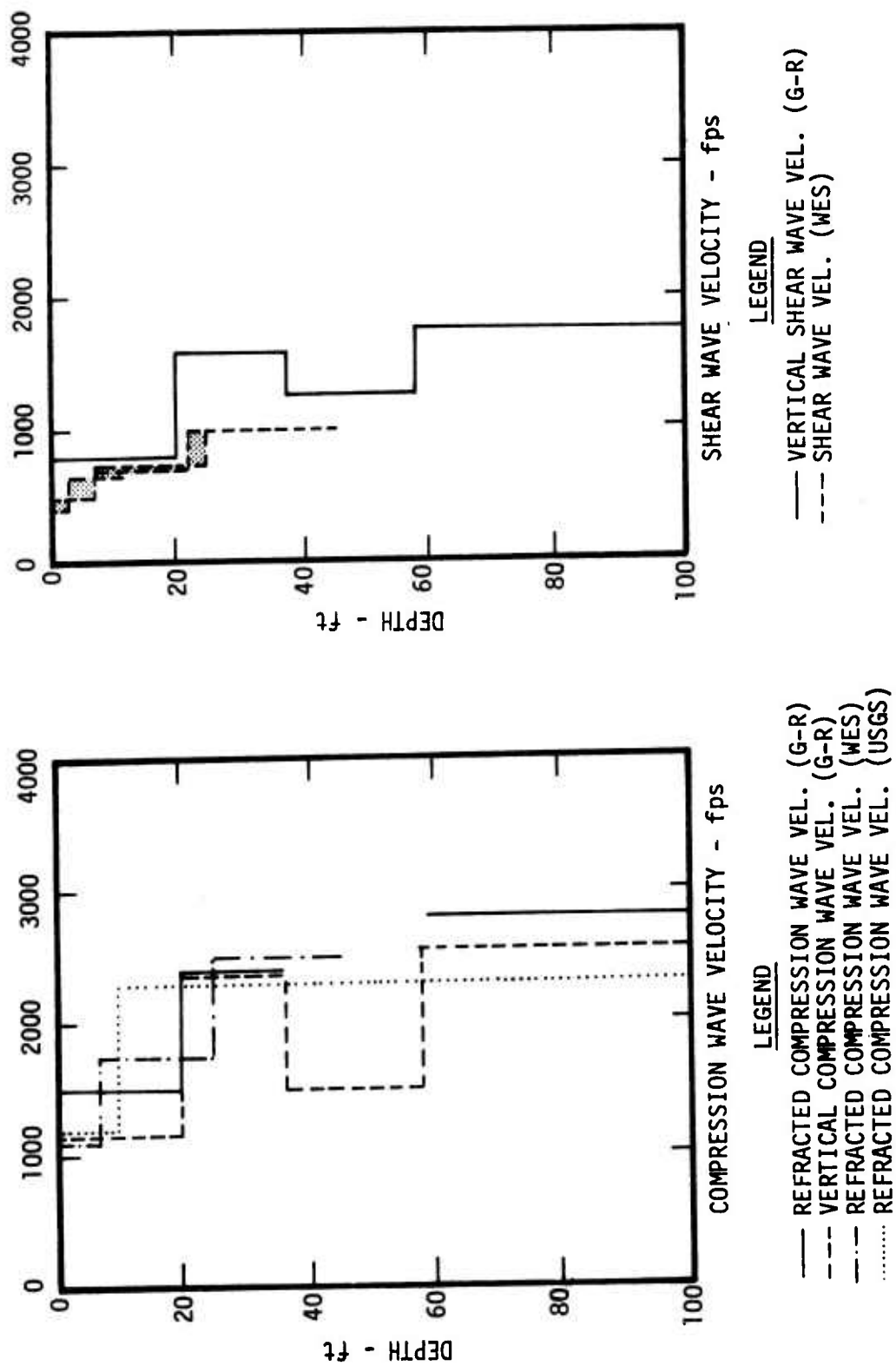


Figure 47. Seismic Profile

surface values are probably in error. However, the data from large depths should not be affected because the transient times to and from large depths are long with respect to the transient time across the low velocity layer.

TABLE III U. S. GEOLOGICAL SURVEY SEISMIC DATA

Depth (ft)	Velocities (fps)
0 - 10	1200
10 - 175	2600
175 - 650	3000
650	10,000

Based on our study of the data referenced above, we defined a "typical" Frenchman Flat seismic profile as summarized in Table IV. Variations of several feet in interface depths are clearly within the uncertainty of our knowledge of their precise depth at any given location in Frenchman Flat.

TABLE IV BEST ESTIMATE SEISMIC PROFILE

Depth (ft)	Cp - fps		C - fps	
	Recomm	Range	Recomm	Range
0 - 10	1,100	900 - 1350	500	290 - 770
10 - 20	1,500	1100 - 1750	700	620 - 900
20 - 36	2,400	1750 - 2750	1,200	800 - 1600
36 - 58	1,500	-	-	-
58 - 170	2,800	-	1,780	-
170 - 650	3,600	-	-	-
650 →	10,300	-	-	-

3. Soil Description

The soil in the upper 200 feet of Frenchman Flat is very uniform in appearance and composition; and is described as a hard, friable, tan silt or clayey silt with varying amounts of cementation (Ref. 23). The silt classifies as an ML (silt of low plasticity) according to the Unified Soil Classification System. No systematic bedding planes or layers were reported as being visually obvious during the drilling and sampling at the site, but playa deposits typically have a stratified nature and then zones of well-cemented material are known to exist in some areas of Frenchman Flat.

a. Moisture Density

Considerable variation in the moisture content and "in-situ" unit weight is indicated by scatter in test data taken at different times. Some systematic variation is probably related to different rainfall conditions immediately prior to soil sampling (several feet of water sometimes stands in the Frenchman Flat lake bed following heavy rainfall). For example, heavy rains fell between Flat Top II and III, and the moisture content from the borings near Flat Top II and Flat Top III ground zeros¹ increased by about 10 percent at most depths, and the wet unit weights increased accordingly. See Figure 48 (Ref. 24). As would be expected, dry unit weights show very little variation and no definite trend.

Figure 49 shows moisture-density data from soil samples taken by three different sampling methods from the PRISCILLA test area. The samples tested by CERF (Ref. 25) and Davisson (Ref. 23) were taken from a large (4 ft diameter) shaft, and the soil samples may have dried somewhat because they were exposed to the air for an extended period of time. The S&W boring (Ref. 20) were made with a Pitcher sampler using drilling mud to cool the bit and remove the cutting, a procedure that may have allowed some water to penetrate the samples. However, the fine grained silt is relatively

¹The soils at these locations were described as being lithologically the same at those at the PRISCILLA and SMALL BOY ground zeros.

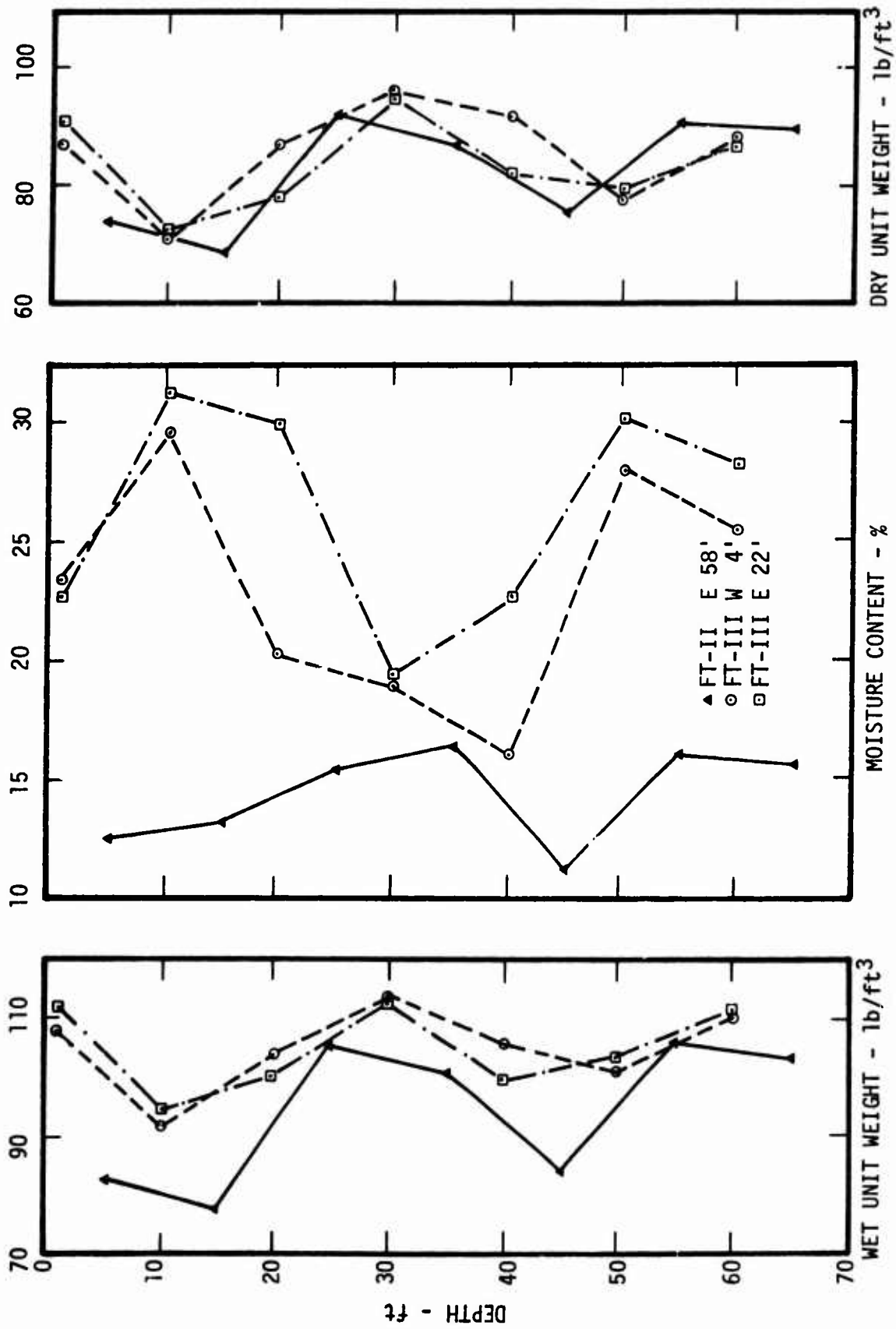


Figure 48. Soil Composition Data from the Vicinity of Flat Top II and III

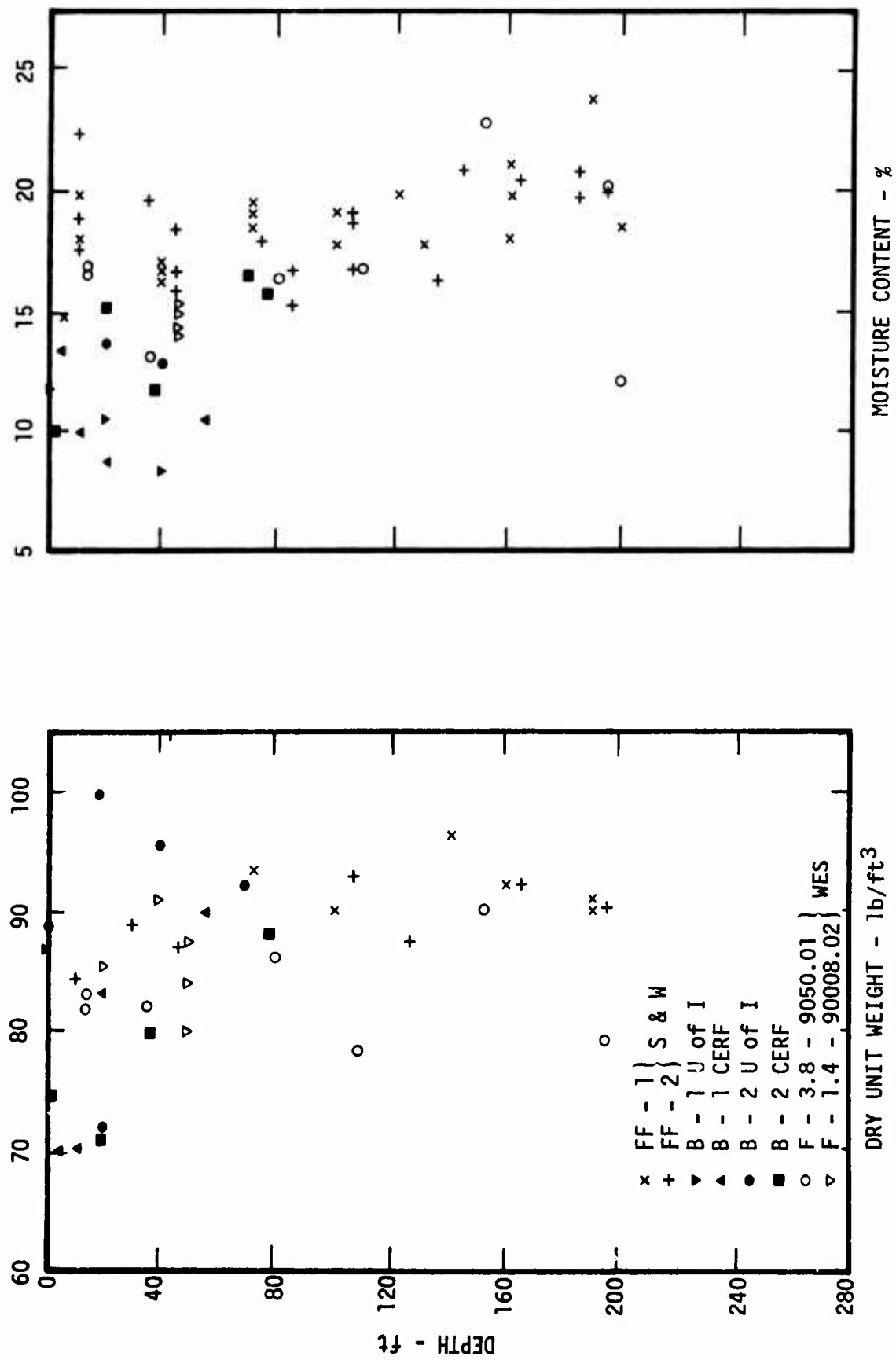


Figure 49. Frenchman Flat Soil Composition Data

impermeable. The WES sampling procedure (Refs. 26 and 27), used compressed air to cool the bit and remove the cuttings, and should have produced the best quality samples. In any case, the variation in moisture content derived from these three sampling techniques is smaller than that caused by the heavy rains between the Flat Top events. The dry unit weights from the three investigations are in good agreement; with the exception of several samples (tested by CERF) that were probably disturbed during shipment or handling.

The WES samples were taken in conjunction with the PRISCILLA event whereas the other samples were taken several years later. For this reason, the moisture content obtained from the WES samples are felt to be most representative of the PRISCILLA area at shot time. Because the hand carved samples from which the dynamic stress-strain curves were derived (see the following section) were drier, they were probably more compressible than the PRISCILLA site at shot time.

b. Stress-Strain Properties

The quantitative soil property input data for the one-dimensional calculations reported in Section III were derived from dynamic uniaxial-strain tests reported by M. T. Davisson, Foundation Engineer (Ref. 23). These were the only dynamic tests of Frenchman Flat soils available at the time this study was conducted. The tests were performed on hand carved samples taken from three four-foot diameter shafts at depths of 0, 20, 40 and 70 feet. Because only a very limited number of samples were available, only one dynamic test was run on the 0, 20 and 40 feet samples. Two dynamic tests were conducted on the 70 foot sample, but the resolution on the two tests was not comparable. Static and "rapid" tests were also run on samples from each depth to investigate strain rate effects. All of the tests were run to maximum stresses of several thousand psi; therefore, the resolution was relatively poor at a few hundred psi (the range of greatest interest in comparing calculated and measured ground motions).

The rise time to peak stress was several seconds, 100 - 150 msec and 2 - 3 msec for the static, rapid and dynamic tests respectively. Figures 50 through 53 show no appreciable difference in the stress-strain characteristics derived from the static and rapid tests. However, the stiffness from the dynamic tests is somewhat greater than for the static or rapid tests. The initial portion of all of these stress-strain curves is concave to the strain axis, an effect that probably results from an incremental breakdown of cementation. After the cementation is broken down, the curves become concave to the stress axis indicating an increase in stiffness with increasing compression, typical of uncemented sands.

The deposits that make up Frenchman Flat Playa are often stratified with numerous thin cemented zones referred to as caliche beds. This condition can lead to orthotropic material properties (normal and parallel to the natural bedding planes). Only two static tests were conducted on samples such that the loading was parallel to the bedding planes. Companion samples from the same boring and depth were tested with the load applied normal to the bedding planes. As shown in Figure 54, both tests show the material at low stresses is stiffer in a direction parallel to the bedding planes. The indicated orthotropic response of the shallow (14 ft deep) sample was not great, and disappeared for stresses above about 700 psi. On the other hand, a significant orthotropic response persisted throughout the test of the deeper sample (up to almost 1500 psi). Although this data is limited, it suggests that the soil may be significantly stiffer in the horizontal direction than in the vertical direction, an effect that should be considered if two-dimensional calculations of ground motions in Frenchman Flat are attempted.

4. Theoretical Model

Because a primary purpose of this effort was to compare one-dimensional calculations with vertical ground motions measured on nuclear tests, we attempted to minimize subjective judgments in selecting the soil properties. Thus, Davisson's dynamic uniaxial strain test data were used exactly as

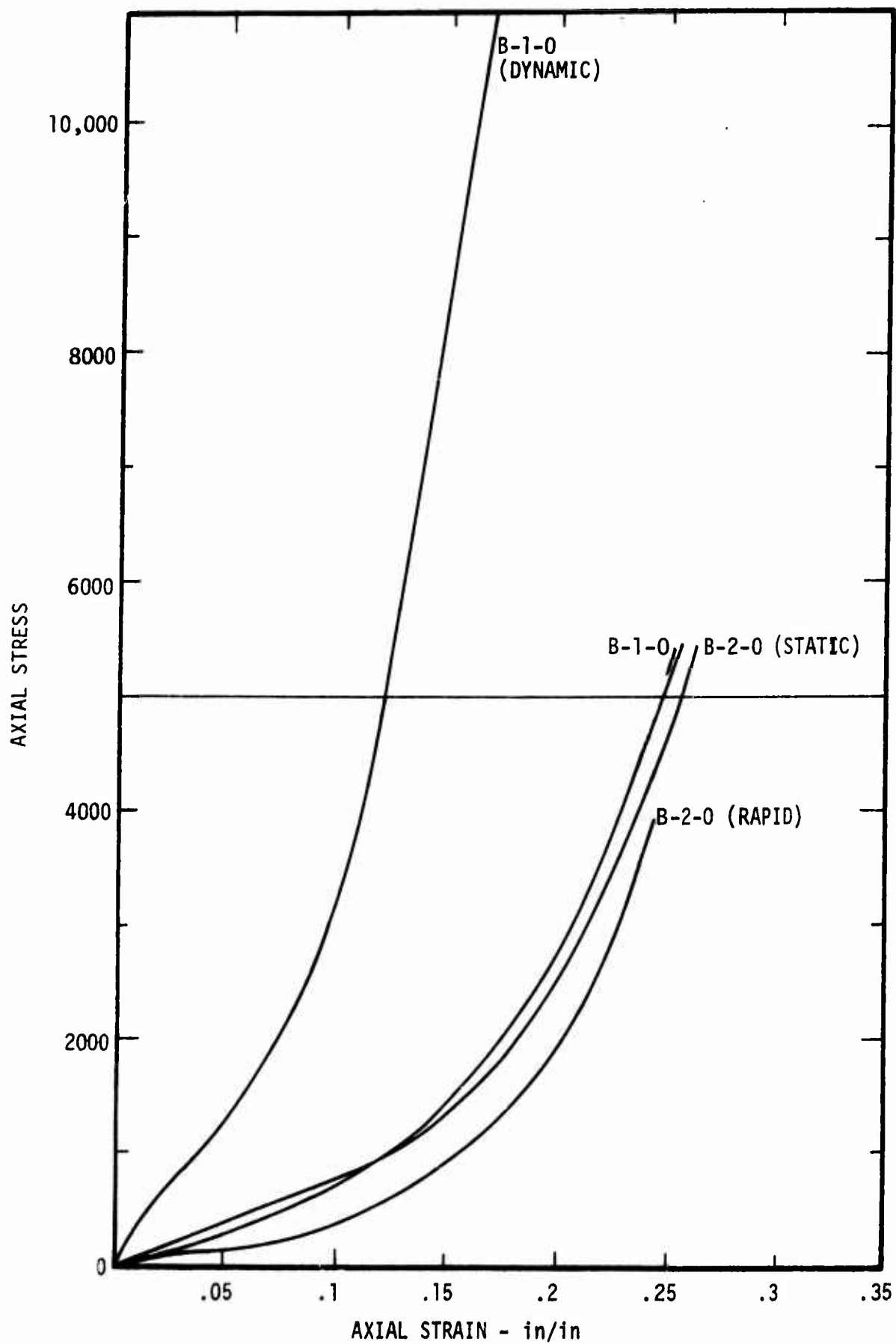


Figure 50. Uniaxial Stress-Strain Curves ($z = 0$)

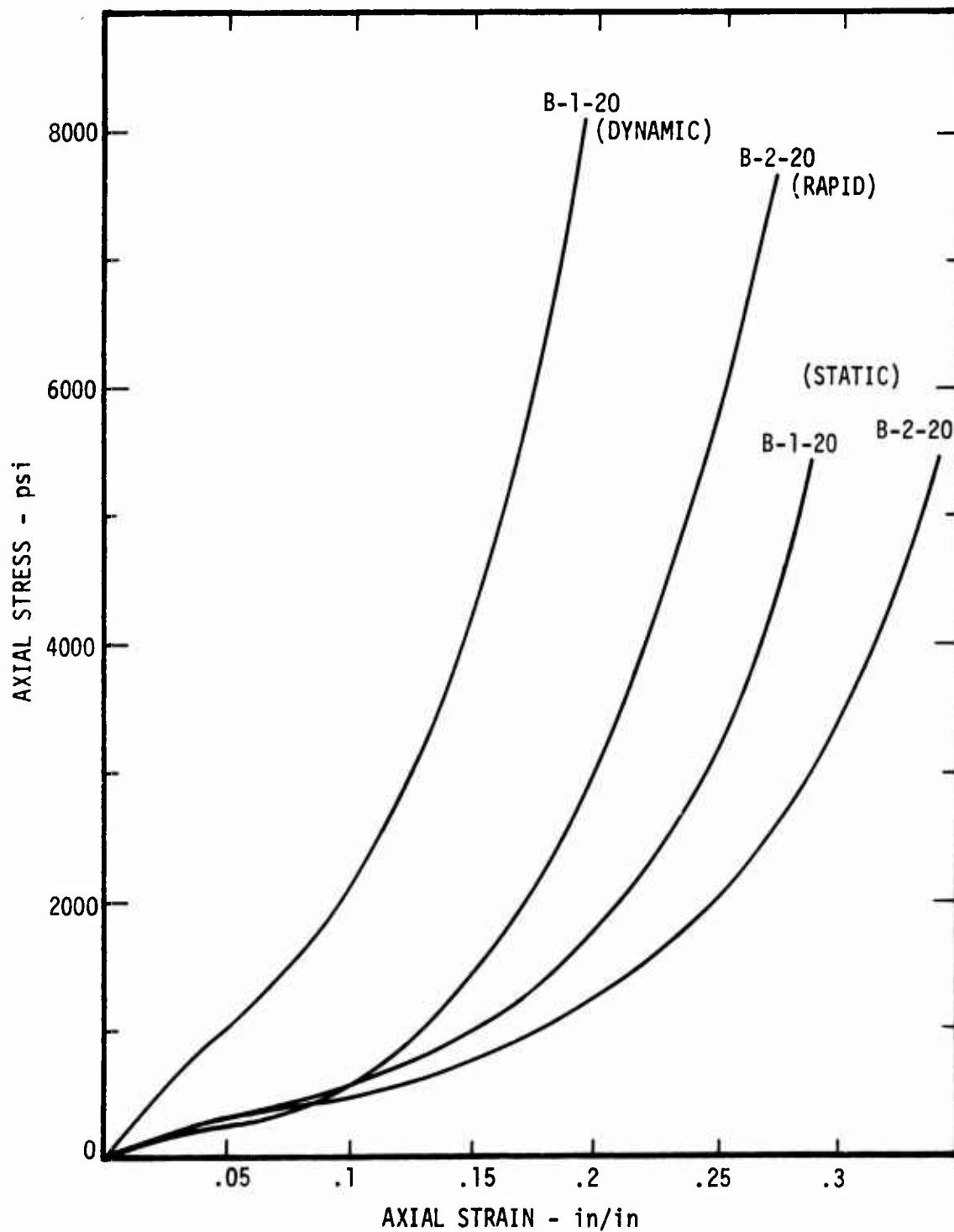


Figure 51. Uniaxial Stress-Strain Curves ($z = 20$ KT)

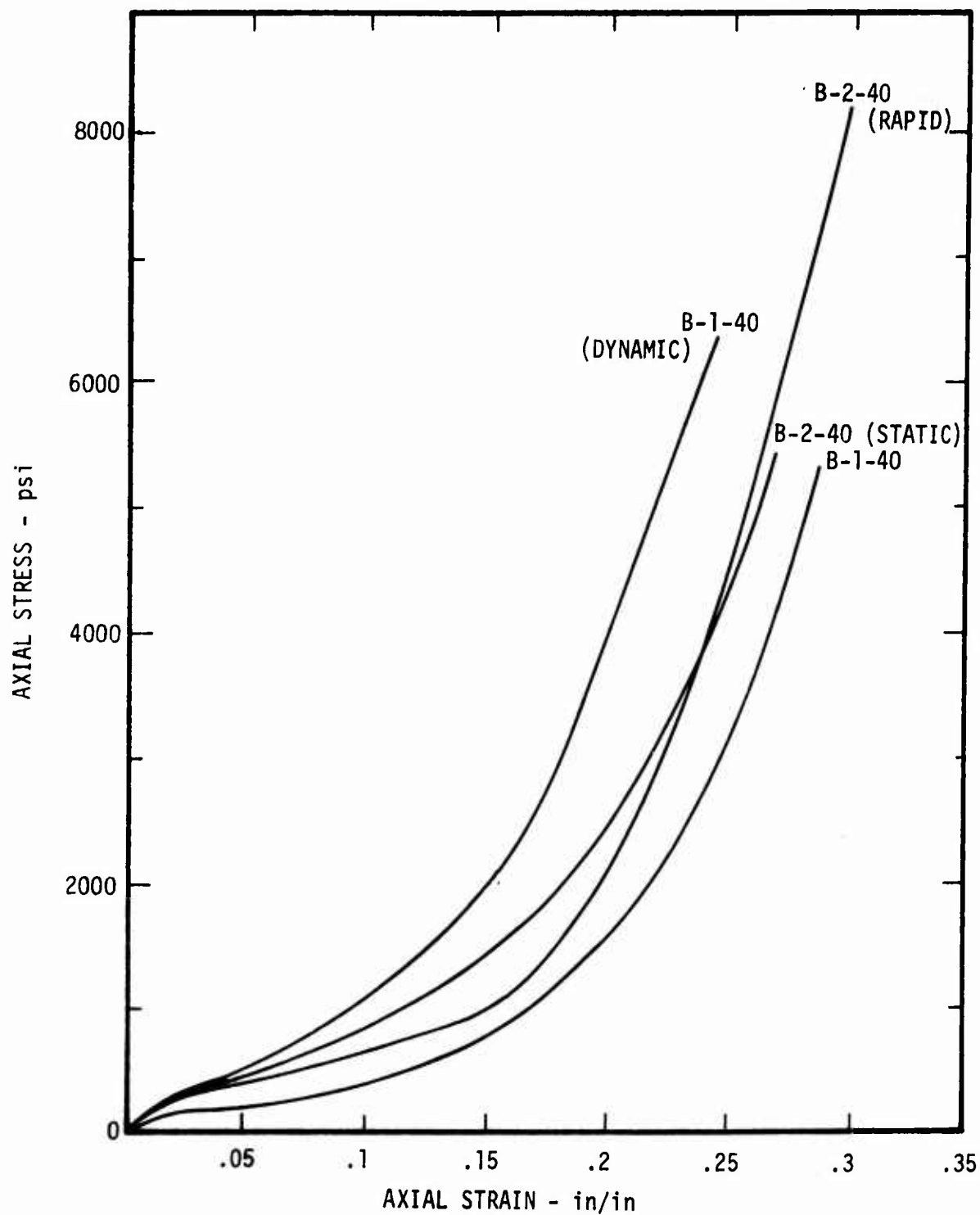


Figure 52. Uniaxial Stress-Strain Curves ($z = 40$ ft)

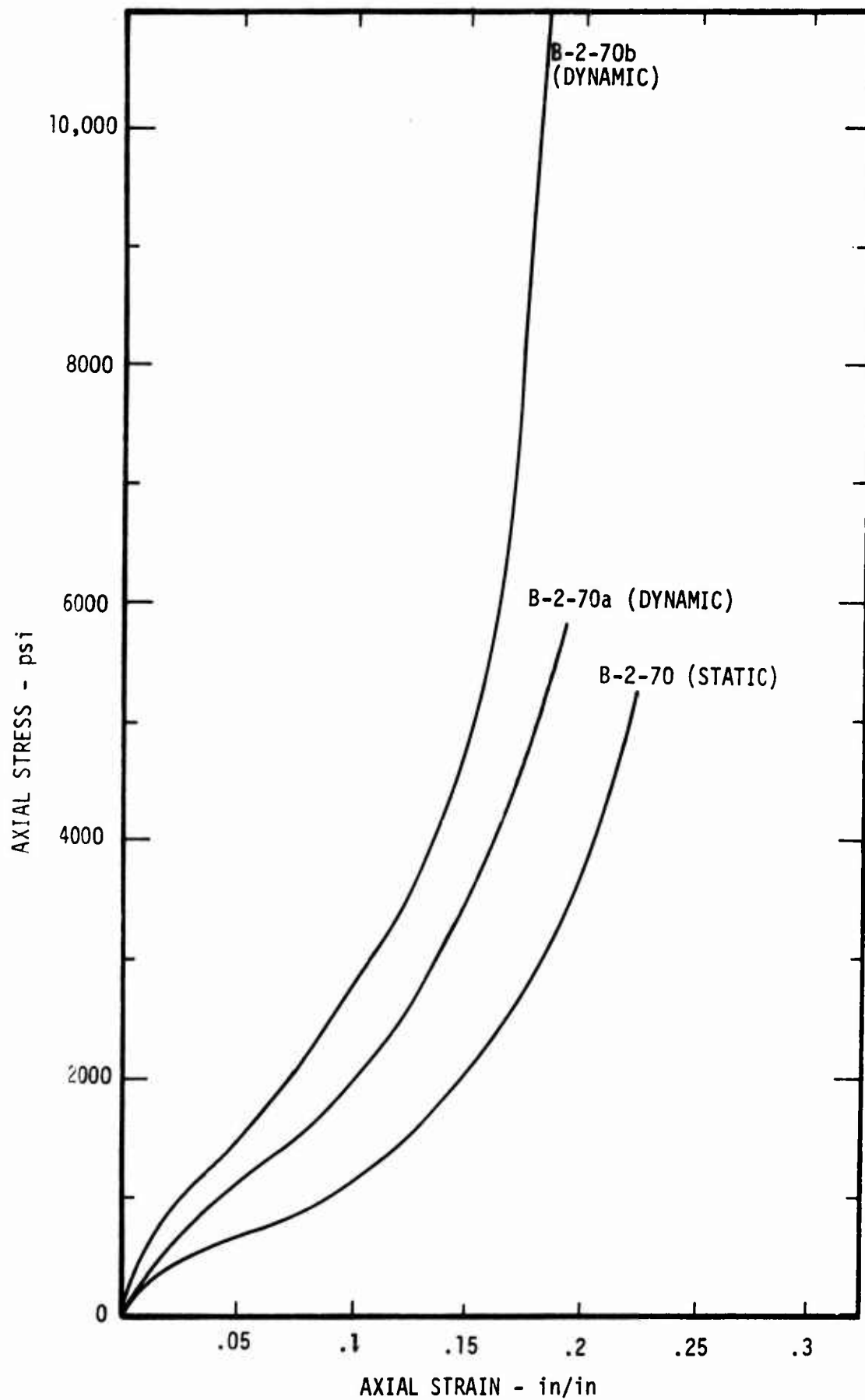


Figure 53. Uniaxial Stress-Strain Curves ($z = 70$ ft)

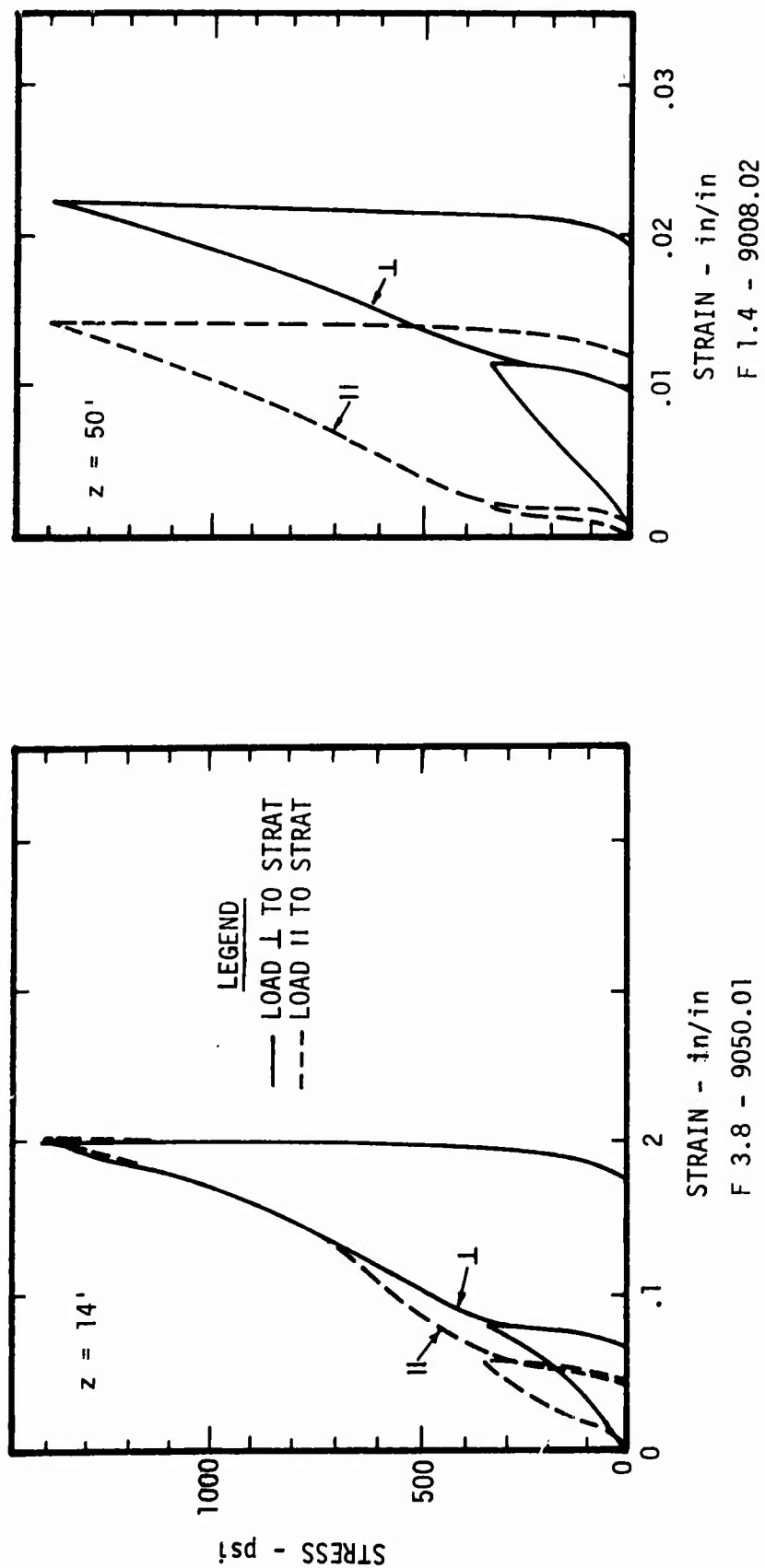


Figure 54: Static, Uniaxial Strain, Test Results that Suggest Possible Anisotropy in Frenchman Flat

reported to model the loading stress-strain curves, in spite of the fact that some systematic differences might be associated with known moisture content variations as discussed above.

The test device used in conducting the dynamic tests could not be unloaded immediately upon reaching peak stress so that in several instances significant creep and reloading took place. In order to synthesize unloading stress-strain curves, the unloading portion of all the test data (ignoring creep and reloading hysteresis) were normalized to the peak stress and strain reached on loading and plotted as shown in Figure 55. This figure shows that the normalized unloading curves from ten tests (for 3 loading rates and 4 depths) are very similar. Therefore, an average curve was drawn through this normalized plot and was used for all layers.

Examination of the seismic data suggested that the dynamic data, available at only four depths (0, 20, 40, and 70 ft) may be representative of four layers: 0 - 10 feet, 10 - 30 feet, 30 - 50 feet, and 50 - 170 feet. No stress-strain data were available for depths greater than 70 ft; so bilinear properties for the 170 - 650 ft layer were assumed such that the loading modulus was consistent with the seismic velocity and the unloading modulus was consistent with the modulus of the shallower soils. A rigid boundary was introduced at 650 ft depth to provide a reflected compressional wave, consistent with the appropriate physical effects of the high impedance soils estimated to exist below 650 ft.

These material properties show a rather unusual trend. Normally one expects a gradual increase in stiffness with depth when the soil type does not change. However, Figure 56 shows one of the stiffest samples to be from near the ground surface where the softest layer would normally be expected. Figure 47 shows this sample to be considerably more dense than any of the other samples in the upper 10 feet. This high density may be anomalous and could represent local effects of desiccation. As discussed above, the moisture content of the near-surface soils at the time of

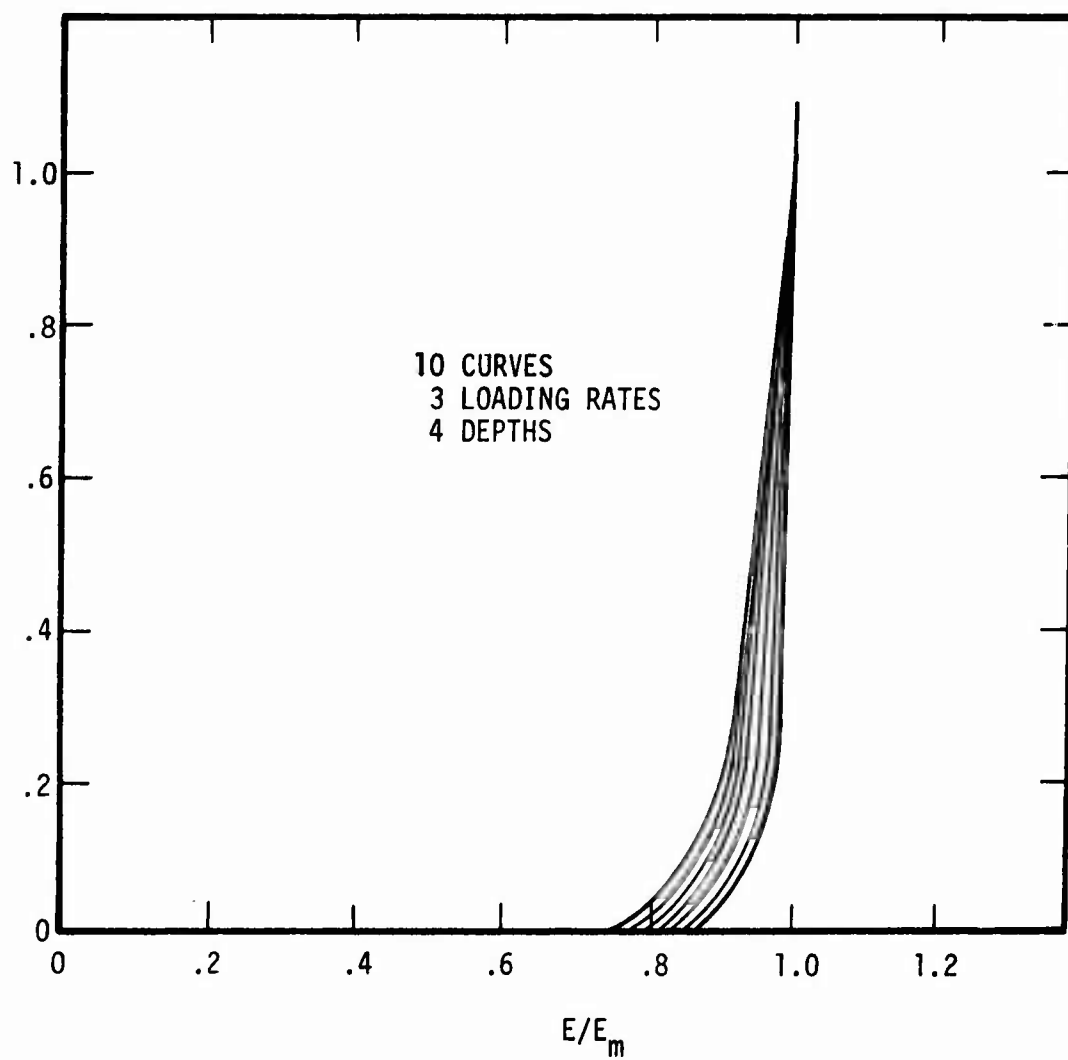


Figure 55. Normalized Unloading Curves

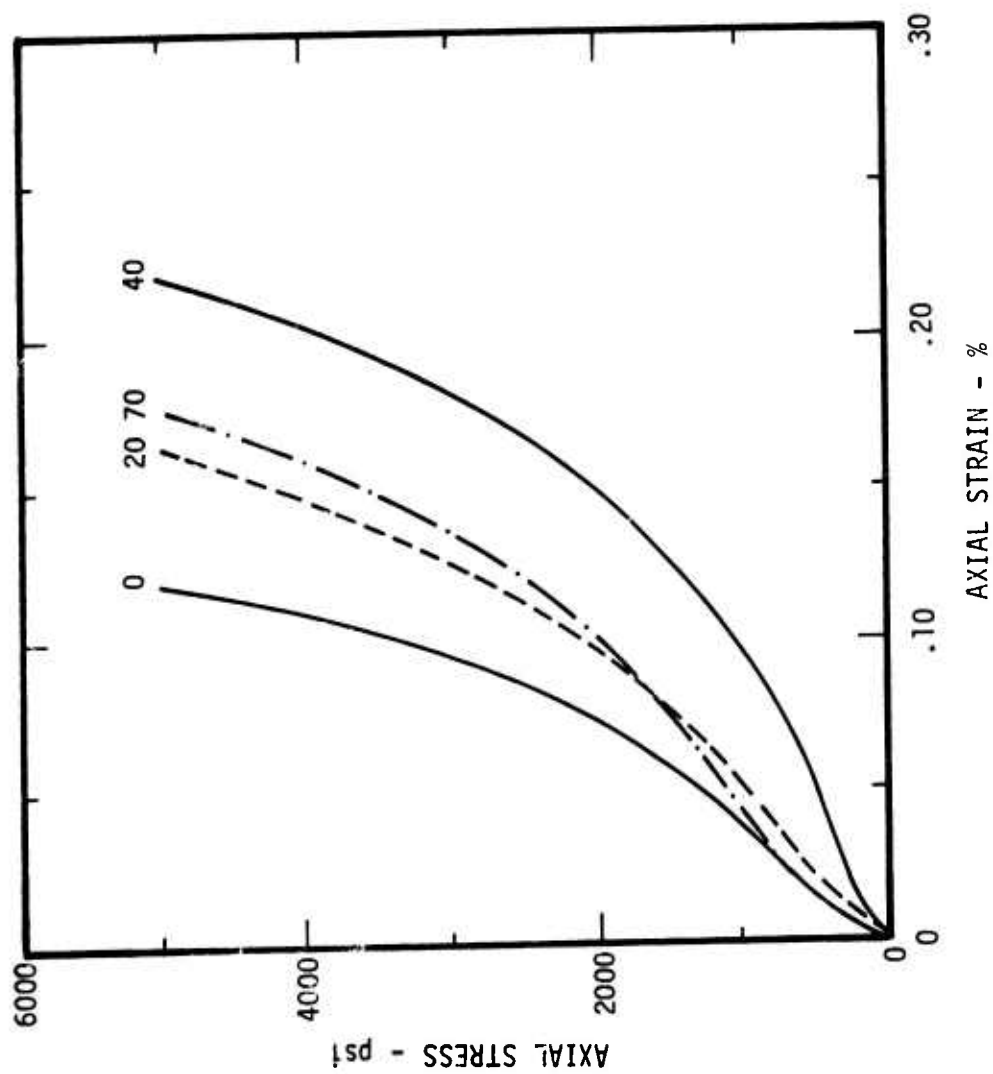


Figure 56. Comparison of Loading Curves from the Dynamic Uniaxial Strain Tests

PRISCILLA probably increased the "in-situ" density and stiffness. The most compressible soils sample was from the 40 foot depth, consistent with the Geo-Recon seismic investigation and the static compression test results.

In considering the test data from the two 70 foot samples (Figure 53), the stress-strain curve from sample B-2-70a was used to model the soils between 50 and 170 ft because it allowed better resolution at the stress levels less than 1000 psi. In addition, the proving ring capacity was exceeded during the tests of sample B-2-70b; casting some doubt on the results.

REFERENCES

1. Trulio, J. G. and Perl, N. K., "Limitations of Present Computational Models of Explosively-Induced Ground Motion: MIDDLE GUST Event III," Proceedings, MIDDLE GUST/MIXED COMPANY Combined Symposium 13 - 15 March 1973.
2. Port, R. J. and Gajewski, R., "Sensitivity of Uniaxial Stress-Strain Relations on Calculations of MIDDLE GUST III," Proceedings, MIDDLE GUST/MIXED COMPANY Combined Symposium, 13 - 15 March 1973.
3. Cooper, H. F. and Peterson, J., Estancia Layering Effects on Air-Induced Ground Motions, AFWL-TR-68-17, Air Force Weapons Laboratory, April 1968.
4. Brode, H. L., A Review of Nuclear Explosion Phenomena Pertinent to Protective Construction, The RAND Corporation, R-425, May 1964.
5. Brode, H. L., Height of Burst Effects at High Overpressures, The RAND Corporation, RM-6301-DASA, DASA 2506, July 1970.
6. Davissan, M. T., et al., Static and Dynamic Behavior of a Playa Silt in One-Dimensional Compression, RTD-TDR-63-3078, Air Force Weapons Laboratory, September 1963.
7. Newmark, N. M. and Halmiwanger, J. D., Air Force Design Manual, Principles and Practices for Design of Hardened Structures, AFSWC-TDR-62-1.8, December 1962.
8. Anderson, F. E., et al., Design of Structures to Resist Nuclear Weapons Effects, ASCE - Manual of Engineering Practice, No. 42, 1961.
9. Cooper, H. F. and Bratton, J. L., Calculations of Vertical Airblast-Induced Ground Motions on Event Small Boy (U), AFWL-TR to be published.
10. Perret, W. R., Ground Motion Studies at High Incident Overpressures, Operation Plumbob - Project 1.5, WT-1405, June 20, 1960.
11. Swift, L. M., Sachs, D. C. and Sauer, F. M., Ground Acceleration, Stress, and Strain at High Incident Overpressures; Operation Plumbob - Project 1.4, WT-1401, May 10, 1960.
12. Perret, W. R., Ground Motion Induced by a Near Surface Explosion, Operation Sun Beam, Shot Small Boy, WT-2205, October 14, 1964 (CFRD).
13. Swift, L. M., and Eisler, J. D., Close-In Earth Motion (U), Operation Sun Beam, Shot Small Boy, WT-2201, March 25, 1965 (CFRD).
14. Cooper, H. F., Abbott, P. A. and Mitchell, N. R., "Fundamental Studies in One-Dimensional Wave Propagation," Proceedings: Strategic Structures Vulnerability/Hardening Long Range Planning Meeting (U), DASA-2288-1, November 1969.

REFERENCES (cont.)

15. Hendron, A. J. and Auld, H. E., "The Effect of Soil Properties on the Attenuation of Airblast-Induced Ground Motions," Proceedings International Symposium on Wave Propagation and Dynamic Properties of Earth Materials, August 23 - 25, 1967, University of New Mexico Press, pp. 29 - 48.
16. Jackson, J. G., One-Dimensional Wave Propagation Calculations vs. Field Measurements: A Comparative Analysis of the 650 ft Ground Range of Shot PRISCILLA, WES report to be published.
17. Hadalla, P., Effect of Constitutive Properties of Earth Media on Out-running Ground Shock from Large Explosions, PhD thesis, University of Illinois, 1973. Also to be published as a WES-TR.
18. Maxwell, D. Reaugh, J. and Gerber, B., Johnie Boy Crater Calculations, Physics International, DNA 3048F, April 1973.
19. Johnson, M. S. and Hibbard, D. E., "A Geological Survey of the Atomic Energy Commission Area, Nye County, Nevada," WT-518, Armed Force Special Weapons Project, Washington, DC, March 1953.
20. "Subsurface Investigations and Ground Motions Studies at Nevada Test Site," Shannon and Wilson, Inc., January 1961.
21. "Dynamic Tests Frenchman Flat, Nevada Test Site, Mercury, Nevada, Misc Paper No. 4-645, U. S. Army Engineer Waterways Experiment Station, Vicksburg, Ms, April 1964.
22. Farnham, F. C., "Seismic Survey at Mercury, Nevada," U.S. Coast and Geodetic Survey, 1951.
23. Davisson, M. T., et al., "Static and Dynamic Behavior of a Playa Silt in One-Dimensional Compression," RTD-TDR-63-3078, Air Force Weapons Laboratory, Kirtland AFB, NM, September 1963.
24. Sauer, F. M., Vincent, C. T., "Earth Motion and Pressure Histories," WT-3002, Stanford Research Institute, Menlo Park, Ca, April 1967.
25. Calhoun, D. E., "Moisture-Density Determinations and Visual Examination of Soil Samples from the Vicinity of Ferris Wheel," AF Shock Tube Facility, Kirtland AFB, NM, May 1963.
26. Goode, T. B., et al., "Soil Survey and Backfill Control in Frenchman Flat," WT-1427, U. S. Army Engineer Waterways Experiment Station, Vicksburg, Ms, October 1959.
27. Goode, T. B., et al., "Soils Survey," WT-2207, U. S. Army Engineer Waterways Experiment Station, Vicksburg, Ms, October 1963.

DISTRIBUTION

No. of
Copies

	Hq USAF, Washington, DC 20330
1	(RDQPN, 1D425)
1	(RDQS)
	AFSC, Andrews AFB, Washington, DC 20331
1	(DLSP)
	AFLC, Wright-Patterson AFB, OH 45433
1	(DEE)
	ADC, Ent AFB, CO 80912
1	(DOA)
1	AUL (LDE), Maxwell AFB, AL 36112
1	AU (ED, Dir, Civ Eng), Maxwell AFB, AL 36112
	AFIT, Wright-Patterson AFB, OH 45433
1	(Tech Lib, Bldg 640, Area B)
1	(DAPD)
	FTD, Wright-Patterson AFB, OH 45433
1	Mr. Winston Dixon
	USAF Academy, CO 80840
1	(DFS LB)
1	(FJSRL, CC)
1	(DFCE)
1	ARL, Wright-Patterson AFB, OH 45433
	AFML, Wright-Patterson AFB, OH 45433
1	(Tech Lib)
	SAMSO, Norton AFB, CA 92409
1	(MNH) Capt Dick Guarino
1	Maj Mel Castillo
1	(DEN) Tex Culler
1	Maj Ton Anessi

DISTRIBUTION (Cont'd)

No. of Copies

	RADC, Griffiss AFB, NY 13440
1	(Doc Lib)
	AFSWC, Kirtland AFB, NM 87117
1	(HO)
1	SAC Res Rep (SACLO), AFSWC, Kirtland AFB, NM 87117
	AFWL, Kirtland AFB, NM 87117
5	(SUL)
1	(DE)
1	(DEV) Maj George Bulin
1	Mr. Bob Port
1	Capt Steve Melzer
1	Capt Bob Post
1	Capt Tom Edwards
3	Mr. J. L. Bratton
	RAND Corp, 1700 Main St, Santa Monica, CA 90401
1	(Dr. C. C. Mow)
1	Comdg Off, Diamond Lab (Lib), Washington, DC 20438
1	Dept Army NIKE-X Fld Ofc (AMCPM-NXE-FB), Bell Tel Lab, Whippany, NJ 07981
1	Chief of Eng (ENGMC-EM), Dept Army, Washington, DC 20315
	Dir, USA Eng WW Exp Sta, P. O. Box 631, Vicksburg, MS 39181
1	(WESRL)
1	(WESSS)
1	(Dr. J. Zelasko)
1	(Dr. J. G. Jackson, Jr.)
1	(Mr. Don Day)
1	(Mr. Leo Ingram)
1	(Tech Library)
1	(Mr. Paul Hadala)
1	(Mr. Ed Jackson)
1	Dept Army Ohio River Div Lab, Corps Eng (ORDLBVR), 5851 Mariemont Ave, Cincinnati, OH 45227

No. of
Copies

1	Ofc Chief, Nav Ops, Dept Navy, Wash, DC 20350
1	Ofc Nav Rsch, Depart Navy (Code 418), Washington, DC 20360
1	Dir, HRL (Code 2027), Washington, DC 20390
1	Comdr, NWC(Code 753), China Lake, CA 3557
1	Comdr, NOL (Code 730), White Oak, Silver Spring, MD 20910
1	Dir, Spec Proj Ofc, Dept Navy, Wash, DC 20360
	NCEL Port Hueneme, CA 93041
1	(Mr. Jay Algood)
	Dir, DNA, Washington, DC 20305
2	(APTL)
1	(SPSS) Mr. John Lewis
1	Mr. Cliff McFarland
1	Mr. Jud Leach
1	Mr. Kent Goering
2	(STAP)
	DDR&E, Washington, DC 20301
1	(Asst Dir, Strat Wpns)
1	(Mr. Don Walch)
	Dir, DIA, Washington, DC 20305
1	(Lt Col Paul Cavanaugh)
1	(DIAAP-8B)
1	(DIAST-3)
1	Dir, OSD, ARPA (NMR), 1400 Wilson Blvd, Arlington, VA 22209
1	(Col Ted Jones)
1	Comdr, FC DNA (FCSD-A4), Kirtland AFB, NM 87115
1	Dir, Wpn Sys Eval Gp (Doc Cont), Washington, DC 20305
1	Asst Scy Def, AE (Doc Cont), Washington, DC 20301
1	JSTPS (JLTW), Offutt AFB, NE 68113
1	(Maj Mike Baran)
2	DDC (TCA), Cameron Sta, Alexandria, VA 22314

DISTRIBUTION (Cont'd)

No. of
Copies

Sandia Lab, Kirtland AFB, NM 87115
1 (Info Dist Div)
1 (Dr. M. L. Merritt)
1 (Mr. Carter Broyles)
1 (Mr. Walt Herman)
1 (Mr. Wendel Weart)
1 Sandia Lab, P. O. Box 969, Livermore, CA 94550
Dir Ofc, LLL, P. O. Box 808, Livermore, CA 94550
1 (Barbara Crowley)
1 (Mr. Douglas Stephens)
1 (Dr. Robert Schock)
1 (Mark Wilkins)
1 (Ted Butcovich)
1 (Robert Terhune)
1 LLL (Lib), Bldg 50, Rm 134, Berkeley, CA 94720
Dir, LASL, P. O. Box 1663, Los Alamos, NM 87554
1 (Rpt Lib)
Aerospace Corp, P. O. Box 5866, San Bernardino, CA 92408
1 (Mr. Warren Pfefferle)
1 (Dr. Mason B. Watson)
Aerospace Corp, P. O. Box 92957, Los Angeles, CA 90009
1 (Dr. Prem Mather)
Agabian Associates, 8939 South Sepulveda Blvd, Los Angeles, CA 90045
1 (Dr. J. Isenberg)
1 (Document Control)
1 (Dr. Mike Agabian)
Analytic Services, Inc., 5613 Leesburg Pike, Falls Church, VA 22041
1 (George Hesselbacher)
Applied Theory, Inc., 1010 Westwood Blvd., Los Angeles, CA 90024
1 (Dr. J. Trulio)
1 (Neil Pearl)

DISTRIBUTION (Cont'd)

No. of Copies

	The Boeing Company, P. O. Box 3707, Seattle, WA 98124
1	(Mr. John Blaylock)
1	(Mr. R. Hager)
	California Institute of Technology, 1201 E. California Blvd, Pasadena, CA 91109
1	(Dr. Thomas J. Ahrens)
	Computer Sciences Corporation, P. O. Box 530, Falls Church, VA 22046
1	(Mr. O. A. Israelson)
	Environmental Research Corporation, 2769 South Highland Drive, Las Vegas, Nevada 89102
1	(Dr. W. W. Hays, Technical Director)
1	(Mr. Fred Power)
	General American Transportation Corporation, General American Research Division, 7449 N. Natchez Avenue, Niles, IL 60648
1	(Dr. G. L. Neidhardt, Manager of Engineering)
1	(Dr. Marion J. Balcerzak, Technical Director)
	IIT Research Institute, 10 West 35th Street, Chicago, IL 60616
1	(Tech Lib)
1	(Dr. Madan M. Singh, Manager)
	University of Illinois, 133 Davenport House, 807 South Wright Street, Champaign, Illinois 61820
1	(Dr. Nathan M. Newmark)
1	(Dr. Skip Hendron)
1	(Dr. Bill Hall)
	Institute for Defense Analyses, 400 Army-Navy Drive, Arlington, VA 22202
1	(Technical Information Office)
1	J. L. Merritt, Consulting and Special Engineering Services, Inc., P. O. Drawer 1206, Redlands, CA 92373
	Lockheed Missiles and Space Company, 3251 Hanover Street, Palo Alto, CA 94304
1	(Dr. Roland E. Meyerott, Dept 50-01, Bldg 201)
	Massachusetts Institute of Technology, 77 Massachusetts Avenue, Rm 24-120, Cambridge, MA 02139
1	(Prof. William F. Brace)

DISTRIBUTION (Cont'd)

No. of Copies

	University of New Mexico, Civil Engineering Research Facility, Albuquerque, NM 87106
1	(Mr. Del Calhoon)
	Physics International Company, 2700 Merced Street, San Leandro, CA 94577
1	(Document Control for Dr. Charles Godfrey)
1	(Document Control for Mr. Fred M. Sauer)
1	(Document Control for Dr. Robert Swift)
	Purdue University, Lafayette, IN 47907
1	(Mr. William R. Judd)
	R & D Associates, P. O. Box 3580, Santa Monica, CA 90403
1	(Dr. Albert Latter)
1	(Mr. Nick Kfourt)
5	(Dr. Henry Cooper)
1	(Mr. William B. Wright)
1	(Dr. Harold L. Brode)
1	(Mr. Bob Thompson)
1	(Mr. John Levesque)
1	(Mr. Shel Schuster)
	Research Analysis Corporation, McLean, VA 22101
1	(Documents Library)
	Science Applications, Inc., P. O. Box 2351, La Jolla, CA 92038
1	(Mr. Mike McKay)
	Science Applications, Inc., Suite 908 1701 North Fort Myer Drive, Arlington, VA 22209
1	(Bill Layson)
	Shock Hydrodynamics, Inc., A Division of Whittaker Corporation, 15010 Ventura Blvd., Sherman Oaks, CA 91403
1	(Mr. K. Kreyenhagen)
	Southwest Research Institute, P.O. Drawer 28510, San Antonio, TX 78284
1	(A. B. Wenzel)
	Stanford Research Institute, 333 Ravenswood Avenue, Menlo Park, CA 94025
1	(Dr. Carl Peterson)
1	(George Abrahamson)

DISTRIBUTION (Cont'd)

No. of Copies

Systems, Science and Software, Inc., P. O. Box 1620, La Jolla, CA 92037

- 1 (Mr. R. Bjork)
- 1 (Dr. Ted Cherry)
- 1 (Dr. Ronald R. Grine)
- 1 (Dr. D. Riney)
- 1 (Document Control)
- 1 (Dr. Thomas D. Riney)
- 1 (Mr. Bob Alken)

Terra Tek, Inc., 814 East Fourth South, Salt Lake City, UT 84102

- 1 (Dr. H. R. Pratt)

TRW Systems Group, One Space Park, Redondo Beach, CA 90278

- 1 (Mr. Norm Lipner)
- 1 (Dr. Peter K. Dai, R1/2178)
- 1 (Dr. Benjamin Sussholtz)
- 1 (Mr. Edgar Wong)

TRW Systems Group, San Bernardino Operations, P. O. Box 1310, San Bernardino, CA 92402

- 1 (Mr. Bing Fay)
- 1 (Mr. Fred Pieper)

URS Research Company, 155 Bovet Road, San Mateo, CA 94402

- 1 (Mr. Harold Mason)

Wiedlinger, Paul, Consulting Engineer, 110 East 59th Street, New York, NY 10022

- 1 (Dr. Melvin L. Baron)
- 1 (Ivan Nelson)

Civil Nuclear Systems Inc., 1200 University Blvd, NE, Albuquerque, NM 87106

- 1 (Dr. Robert Crawford)
- 1 (Mr. C. J. Higgins)

Shannon & Wilson Inc., 1105 North 38th Street, Seattle, WA 98103

- 1 (Mr. Earl Sibley)

University of Oklahoma, Dept of Information and Computing Sciences, 905 Asp, Norman Oklahoma 73069

- 1 (Dr. John Thompson)

DISTRIBUTION (Cont'd)

No. of
Copies

	Bureau of Mines, Twin Cities Research Center, P. O. Box 1660, Minneapolis, Minnesota 55111
1	(Dr. T. C. Atchison)
	Department of the Interior, Bureau of Mines, Bldg 20, Denver Federal Center, Denver, CO 80225
1	(Dr. Leonard A. Obert)
	Department of the Interior, U. S. Geological Survey, 345 Middlefield Road, Menlo Park, CA 94025
1	(Dr. Cecil B. Raleigh, Earthquake Res. Ctr.)
1	(Dr. John H. Healy)
	McDonald-Douglas, 5301 Bolsa Avenue, Huntington Beach, CA 92647
1	(Mr. Ken McClymonds)
1	(Dr. Joe Logan)
	Teledyne, Brown Engineering (SETAC), 300 Sparkman Dr. NW, Research Park, Huntsville, Alabama 35807
1	(Mr. Jack Cahoon)
1	(Mr. Manie Patel)
1	Official Record Copy to Mr. Bratton/DEV-F

UNCLASSIFIED

Security Classification

DOCUMENT CONTROL DATA - R & D		
(Security classification of title, body of abstract and indexing annotation must be entered when the overall report is classified)		
1. ORIGINATING ACTIVITY (Corporate author)		2a. REPORT SECURITY CLASSIFICATION
Air Force Weapons Laboratory (DEV) Kirtland Air Force Base, New Mexico 87117		UNCLASSIFIED
		2b. GROUP
3. REPORT TITLE		
CALCULATION OF VERTICAL AIRBLAST-INDUCED GROUND MOTIONS FROM NUCLEAR EXPLOSIONS IN FRENCHMAN FLAT		
4. DESCRIPTIVE NOTES (Type of report and inclusive dates)		
January 1972 through April 1973		
5. AUTHOR(S) (First name, middle initial, last name)		
Henry F. Cooper, Jr. Jimmie L. Bratton		
6. REPORT DATE	7a. TOTAL NO. OF PAGES	7b. NO. OF REFS
September 1973	114	27
8a. CONTRACT OR GRANT NO. F29601-72-C-0048 DNA001-72-C-0197		9a. ORIGINATOR'S REPORT NUMBER(S)
b. PROJECT NO. 133B1302 Task 13		AFWL-TR-73-111
c.		9b. OTHER REPORT NO(S) (Any other numbers that may be assigned this report)
d.		
10. DISTRIBUTION STATEMENT		
Distribution limited to US Government agencies only because of test and evaluation (Oct 73). Other requests for this document must be referred to AFWL (DEV), Kirtland Air Force Base, NM.		
11. SUPPLEMENTARY NOTES		12. SPONSORING MILITARY ACTIVITY
		AFWL (DEV) Kirtland AFB, NM 87117
13. ABSTRACT (Distribution Limitation Statement B)		
<p>This report discusses vertical airblast-induced ground motions produced by nuclear explosions over a dry soil medium taken to model Frenchman Flat of the Nevada Test Site (NTS). Material properties for use in first principle calculations were synthesized from very limited dynamic laboratory stress-strain data, various soil index characteristics, and seismic data. Parametric calculations with a one-dimensional, plane-strain finite difference code were used to define a "theoretical" simplified model that expresses peak vertical particle velocities and displacements as a function of yield, peak overpressure and depth. Ground motions predicted by this model were then compared to ground motion data from nuclear explosions in Frenchman Flat. In particular, predictions of the simplified model were reasonably consistent with PRISCILLA data which were a primary basis of empirical prediction procedures widely used in the design and analysis of strategic structures during the past ten years. The theoretical model could be altered (where little or no dynamic soil property data exist) to provide even better agreement between calculated and measured ground motions. Conversely, study of qualitative features of the theoretical results provide insight into the basic wave propagation phenomena in Frenchman Flat that could improve the interpretation of the experimental data such that a more consistent comparison between theory and experiment may result.</p>		

UNCLASSIFIED

Security Classification

14 KEY WORDS	LINK A		LINK B		LINK C	
	ROLE	WT	ROLE	WT	ROLE	WT
Wave Propagation Nuclear Weapons Effects Free Field Ground Motions PRISCILLA Ground Motion Calculations Frenchman Flat Soil Dynamics						

UNCLASSIFIED

Security Classification

THIS REPORT HAS BEEN DELIMITED
AND CLEARED FOR PUBLIC RELEASE
UNDER DOD DIRECTIVE 5200.20 AND
NO RESTRICTIONS ARE IMPOSED UPON
ITS USE AND DISCLOSURE.

DISTRIBUTION STATEMENT A

APPROVED FOR PUBLIC RELEASE,
DISTRIBUTION UNLIMITED.